

UNIVERSIDADE FEDERAL DE SANTA MARIA
CENTRO DE TECNOLOGIA
PROGRAMA DE PÓS-GRADUAÇÃO EM ENGENHARIA QUÍMICA

Henrique Gasparetto

**EXTRAÇÃO DE ÓLEO DE SOJA UTILIZANDO SOLVENTES
VERDES: CINÉTICA, TERMODINÂMICA E TRANSFERÊNCIA DE
MASSA**

Santa Maria, RS
2022

Gasparetto, Henrique
Extração de óleo de soja utilizando solventes verdes:
cinética, termodinâmica e transferência de massa /
Henrique Gasparetto.- 2022.
151 p.; 30 cm

Orientadora: Nina Paula Gonçalves Salau
Coorientadora: Fernanda de Castilhos
Dissertação (mestrado) - Universidade Federal de Santa
Maria, Centro de Tecnologia, Programa de Pós-Graduação em
Engenharia Química, RS, 2022

1. Acetato de etila 2. 1-Butanol 3. p-Cimeno 4. COSMO
SAC I. Salau, Nina Paula Gonçalves II. de Castilhos,
Fernanda III. Título.

Sistema de geração automática de ficha catalográfica da UFSM. Dados fornecidos pelo autor(a). Sob supervisão da Direção da Divisão de Processos Técnicos da Biblioteca Central. Bibliotecária responsável Paula Schoenfeldt Patta CRB 10/1728.

Declaro, HENRIQUE GASPARETTO, para os devidos fins e sob as penas da lei, que a pesquisa constante neste trabalho de conclusão de curso (Dissertação) foi por mim elaborada e que as informações necessárias objeto de consulta em literatura e outras fontes estão devidamente referenciadas. Declaro, ainda, que este trabalho ou parte dele não foi apresentado anteriormente para obtenção de qualquer outro grau acadêmico, estando ciente de que a inveracidade da presente declaração poderá resultar na anulação da titulação pela Universidade, entre outras consequências legais.

Henrique Gasparetto

**EXTRAÇÃO DE ÓLEO DE SOJA UTILIZANDO SOLVENTES VERDES:
CINÉTICA, TERMODINÂMICA E TRANSFERÊNCIA DE MASSA**

Dissertação apresentada ao Curso de Pós-Graduação em Engenharia Química (PPGEQ) da Universidade Federal de Santa Maria (UFSM) como requisito parcial para obtenção do título de **Mestre em Engenharia Química**.

Orientadora: Profa. Dra. Nina Paula Gonçalves Salau
Coorientadora: Profa. Dra. Fernanda de Castilhos

Santa Maria, RS
2022

Henrique Gasparetto

**EXTRAÇÃO DE ÓLEO DE SOJA UTILIZANDO SOLVENTES VERDES:
CINÉTICA, TERMODINÂMICA E TRANSFERÊNCIA DE MASSA**

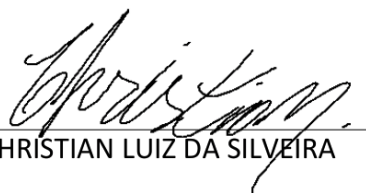
Dissertação apresentada ao Curso de Pós-Graduação em Engenharia Química (PPGEQ) da Universidade Federal de Santa Maria (UFSM) como requisito parcial para obtenção do título de **Mestre em Engenharia Química**.

Aprovado em 02 de setembro de 2022:



NINA PAULA GONCALVES SALAU

(UFSM, Orientadora)



CHRISTIAN LUIZ DA SILVEIRA

(UFSM)



CHRISTIANNE ELISABETE DA COSTA
RODRIGUES

(USP, Videoconferência)

Santa Maria, RS
2022

AGRADECIMENTOS

À minha família, obrigado por confiarem em mim, sem vocês a realização deste sonho não seria possível.

À minha orientadora, Dra. Nina Paula Gonçalves Salau, obrigado pelos ensinamentos, correções, sugestões, disponibilidade e por servir de inspiração. Sou imensamente grato pela sua orientação.

À minha coorientadora, Dra. Fernanda de Castilhos, obrigado pelo auxílio e pelas contribuições.

À Granol por ceder a soja laminada utilizada na realização desta pesquisa.

À Ana Nedel por extrair óleo de soja comigo.

Aos colegas do Laboratório de Biocombustíveis, em especial, à Ana Luiza por compartilhar seus conhecimentos em cromatografia gasosa.

Aos colegas do Laboratório de Engenharia de Processos Assistida por Computador, em especial, à Carol pelas trocas de conhecimento.

Aos amigos fora do PPGEQ.

À UFSM e ao PPGEQ pela estrutura física disponibilizada.

Ao PRH 52.1 e à ANP pela bolsa de estudos concedida.

A todos que de alguma forma contribuíram para a realização deste trabalho.

Muito obrigado.

*Research is to see what everybody else sees,
and to think what nobody else has thought.*

Albert Szent-Györgyi

RESUMO

EXTRAÇÃO DE ÓLEO DE SOJA UTILIZANDO SOLVENTES VERDES: CINÉTICA, TERMODINÂMICA E TRANSFERÊNCIA DE MASSA

AUTOR: Henrique Gasparetto
ORIENTADORA: Nina Paula Gonçalves Salau
COORIENTADORA: Fernanda de Castilhos

O estudo cinético, termodinâmico e de transferência de massa sobre a aplicação de solventes verdes na extração de óleo de soja é foco de avaliação desta dissertação. No primeiro trabalho, é abordada a aplicação dos solventes acetato de etila e 1-butanol. As variáveis temperatura e razão solvente-sólido foram otimizadas utilizando a metodologia de superfície de resposta. A cinética da extração foi avaliada utilizando o modelo *washing-diffusion* de So e Macdonald e o modelo cinético de transferência de massa. Apesar de ambos os solventes não apresentarem melhores resultados que o n-hexano, o estudo mostra que o acetato de etila é o melhor candidato para a substituição direta do hexano em nível industrial, ainda que o 1-butanol possua melhor capacidade de solubilização dos triacilgliceróis. O segundo estudo avaliou a aplicação do terpeno p-cimeno na extração de óleo de soja. As variáveis temperatura e razão solvente-sólido também foram otimizadas e uma abordagem estatística aprofundada foi utilizada para comparar modelos cinéticos para descrever a cinética de extração. O modelo cinético de So e Macdonald foi determinado como o melhor modelo para descrever o processo de extração, sendo então associado ao procedimento de redução de viés por reamostragem *bootstrap*. Melhores resultados que os obtidos com o uso de n-hexano como solvente a 55 °C foram obtidos para o p-cimeno. A teoria COSMO-SAC foi capaz de prever o comportamento dos solventes supracitados através do coeficiente de atividade em diluição infinita em comparação aos parâmetros de solubilidade de Hansen. O último trabalho desta dissertação utilizou dados experimentais da literatura e os obtidos experimentalmente para o acetato de etila, 1-butanol e p-cimeno, a fim de avaliar a aplicação de um modelo de ordem de potência de derivada fracionária generalizada. Melhores resultados estatísticos foram obtidos em comparação ao modelo de derivada de ordem inteira através da análise do coeficiente de determinação, raiz do erro quadrático médio, distribuição chi-quadrada, critério de informação Akaike e teste exato de Fisher. Para todos os solventes, a análise termodinâmica indicou processos endotérmicos, irreversíveis e espontâneos e o perfil dos ácidos graxos e espectro do infravermelho do óleo extraído está de acordo com o que é apresentado pela literatura.

Palavras-chave: Acetato de etila. 1-Butanol. p-Cimeno. COSMO-SAC.

ABSTRACT

SOYBEAN OIL EXTRACTION USING GREEN SOLVENTS: KINETIC, THERMODYNAMIC AND MASS TRANSFER

AUTHOR: Henrique Gasparetto
ADVISOR: Nina Paula Gonçalves Salau
COADVISOR: Fernanda de Castilhos

This dissertation focuses on the kinetic, thermodynamic, and mass transfer study on applying green solvents in soybean oil extraction. The first work discusses ethyl acetate and 1-butanol solvents application. Temperature and solvent-to-solid mass ratio variables were optimized using the response surface methodology. The So and Macdonald and the mass transfer kinetic models were applied for modeling extraction kinetics. This study shows that ethyl acetate is the best candidate for directly replacing hexane at an industrial level, even though 1-butanol is better for the solubilization of the triacylglycerols. However, both solvents did not present better results than n-hexane. The second study evaluated the application of p-cymene in soybean oil extraction. Temperature and solvent-to-solid mass ratio variables were also optimized, and an in-depth statistical approach was used to compare kinetic models to describe vegetable oil extraction. So and Macdonald's kinetic model was considered the best in describing the extraction process, which was further associated with bootstrap resampling to reduce the bias of the estimators. P-cymene resulted in better extraction yields than n-hexane at 55°C. The COSMO-SAC theory could predict the behavior of the solvents mentioned above through the activity coefficient at infinite dilution compared to the Hansen solubility parameters. The last work used experimental data from the literature and those obtained experimentally for ethyl acetate, 1-butanol, and p-cymene, to evaluate the application of a generalized fractional derivative power order model. Better statistical results were obtained compared to the integer order derivative model through the analysis of the coefficient of determination, root-mean-square error, chi-square distribution, Akaike information criterion, and Fisher's exact test. For all solvents, the thermodynamic assessment indicated endothermic, irreversible, and spontaneous processes; the extracted oil's fatty acid profile and infrared spectrum agree with what the literature present.

Keywords: Ethyl acetate. 1-Butanol. P-Cymene. COSMO-SAC.

LISTA DE FIGURAS

CAPÍTULO 2

Figura 2. 1 - Solubilidade do óleo de soja em etanol em função da temperatura.....	25
Figura 2. 2 - Curva típica de extração em batelada utilizando solvente.....	27

CAPÍTULO 4

Figure 4. 1 - Sigma profiles obtained from JCOSMO using COSMO-SAC (MOPAC) theory for (a) the triacylglycerols and (b) the solvents.....	52
Figure 4. 2 - FTIR spectra of soybean oil extracted with hexane, ethyl acetate, and 1-butanol in the region of 4500 to 500 1/cm.	55
Figure 4. 3 - Observed vs. Predicted values for the extraction of soybean oil using ethyl acetate (●) and 1-butanol (▲).	58
Figure 4. 4 - (a) Perspective and (b) contour plot for the yield of extraction using ethyl acetate.	59
Figure 4. 5 - (a) Perspective and (b) contour plot for the yield of extraction using 1-butanol.	60
Figure 4. 6 - Experimental and predicted yields of extraction for the mass transfer kinetic model (dash-dotted line) and the So and Macdonald model (continuous line) for (a) ethyl acetate and (b) 1-butanol at a solvent-to-soybean ratio of 7 and different temperatures.	63
Figure 4. 7 - Experimental and predicted yields of extraction for ethyl acetate, 1-butanol, ethanol, and hexane at 328.15 K using the solvent-to-solid ratio of 7.	64
Figure 4. 8 - Rate of extraction at the beginning of the process at 328.15 K for each solvent using the solvent-to-solid ratio of 7.	65
Figure S. 1 - Experimental apparatus.	74
Figure S. 2 - Parameters stability for ethyl acetate as function of the number of terms of the mass transfer kinetic model for (a) C_{∞} , and (b) D/L^2	75
Figure S. 3 - Parameters stability for 1-butanol as function of the number of terms of the mass transfer kinetic model for (a) C_{∞} , and (b) D/L^2	76

CAPÍTULO 5

Figure 5. 1 - Sigma-profile of different triacylglycerols (dotted lines) in comparison with p-cymene (dashed line) and hexane (continuous line).....	90
Figure 5. 2 - Fourier-transform infrared spectra of the soybean oil extracted with p-cymene in different temperatures.....	93
Figure 5. 3 - The perspective plot of soybean oil extraction using p-cymene.....	96
Figure 5. 4 - Average between the experimental data and the bootstrap samples and simulation of soybean oil extraction using p-cymene (continuous line) and hexane (dashed line).	101

CAPÍTULO 6

Figure 6. 1 - Experimental and predicted yields of extraction for FOKM (continuous line) and FOM (dash-dotted) at (●) 298 K, (■) 313 K, and (▲) 328 K using ethanol anhydrous and (◆) ethanol 96% at 298 K [11].....	127
Figure 6. 2 - Experimental and predicted yields of extraction for FOKM (continuous line) and FOM (dash-dotted) at (●) 298 K, (■) 313 K, and (▲) 328 K using ethanol with 5% of biodiesel [11].	128

Figure 6. 3 - Experimental and predicted yields of extraction for FOKM (continuous line) and FOM (dash-dotted) at (●) 298 K, (■) 313 K, and (▲) 328 K using ethanol with 10% of biodiesel [11].	128
Figure 6. 4 - Experimental and predicted yields of extraction for FOKM (continuous line) and FOM (dash-dotted) at (●) 313 K, (■) 323 K, and (▲) 333 K using ethanol anhydrous [13].	129
Figure 6. 5 - Experimental and predicted yields of extraction for FOKM (continuous line) and FOM (dash-dotted) at (●) 313 K, (■) 323 K, and (▲) 333 K using ethanol 94.02% [13].	129
Figure 6. 6 - Experimental and predicted yields of extraction for FOKM (continuous line) and FOM (dash-dotted) at (●) 298 K, (■) 313 K, and (▲) 328 K using ethanol with 5% of ethyl acetate [14].	130
Figure 6. 7 - Experimental and predicted yields of extraction for FOKM (continuous line) and FOM (dash-dotted) at (●) 298 K, (■) 313 K, and (▲) 328 K using ethanol with 10% of ethyl acetate [14].	130
Figure 6. 8 - Experimental and predicted yields of extraction for FOKM (continuous line) and FOM (dash-dotted) at 328 K for (●) n-hexane (■) 2-MeTHF, and (▲) 2-MeTHF 95.5% [10].	131
Figure 6. 9 - Experimental and predicted yields of extraction for FOKM (continuous line) and FOM (dash-dotted) at (●) 298 K, (■) 313 K, and (▲) 328 K using ethyl acetate (This work).	131
Figure 6. 10 - Experimental and predicted yields of extraction for FOKM (continuous line) and FOM (dash-dotted) at (●) 298 K, (■) 313 K, and (▲) 328 K using 1-butanol (This work).	132
Figure 6. 11 - Experimental and predicted yields of extraction for FOKM (continuous line) and FOM (dash-dotted) at (●) 298 K, (■) 313 K, (▲) 328 K, and (◆) 443 K using p-cymene (This work).	132

APÊNDICE A

Figura A 1 - Cromatograma para determinação de FFA, MAG, DAG e TAG.	151
---	-----

LISTA DE TABELAS

CAPÍTULO 2

Tabela 2. 1 - Composição típica do óleo de soja bruto e refinado.	21
Tabela 2. 2 - Aplicação de diferentes solventes verdes na extração de óleo de soja.....	24

CAPÍTULO 3

Tabela 3. 1 - Matriz de planejamento experimental.	33
Tabela 3. 2 - Rotinas disponíveis no software MatLab®.	38

CAPÍTULO 4

Table 4. 1 - RED and ln(IDAC) calculations for hexane, ethyl acetate, and 1-butanol.	53
Table 4. 2 - Extraction yields and fatty acids profile of the soybean oil extracted with hexane, ethyl acetate, and 1-butanol.	54
Table 4. 3 - Summary of the experiment design at equilibrium condition (120 minutes).....	56
Table 4. 4 - ANOVA for the yield of extraction using ethyl acetate.....	56
Table 4. 5 - Analysis of variance for the yield of extraction using 1-butanol.	57
Table 4. 6 - Estimated parameters for the mass transfer kinetic model.....	61
Table 4. 7 - Estimated parameters for the So and Macdonald model.....	62
Table 4. 8 - Diffusivity coefficients and mass transfer parameters for So and Macdonald model for soybean extraction reported by several authors.	67
Table 4. 9 - Thermodynamic assessment for the soybean oil extraction using ethyl acetate and 1-butanol.....	67

CAPÍTULO 5

Table 5. 1 - Fatty acid profile of the soybean oil extracted with p-cymene.	92
Table 5. 2 - Mean composition of the soybean oil extracted with p-cymene at each temperature.	92
Table 5. 3 - The extracted oil's prominent FTIR spectra peaks and their assignments.	93
Table 5. 4 - Factors and responses for soybean oil extraction using p-cymene.	94
Table 5. 5 - ANOVA for the yield of soybean oil extraction using p-cymene.....	95
Table 5. 6 - Mass transfer coefficients and concentrations at equilibrium with the likelihood confidence interval and its statistical metrics for the first-order model (FOM).....	97
Table 5. 7 - Mass transfer coefficients and concentrations at equilibrium with the likelihood confidence interval and statistical metrics for the second-order model (SOM).....	97
Table 5. 8 - Mass transfer coefficients and concentrations at equilibrium with the likelihood confidence interval and its statistical metrics for MTKM.....	97
Table 5. 9 - Mass transfer coefficients and concentrations at equilibrium with the likelihood confidence interval and its statistical metrics for SMM.....	98
Table 5. 10 - Comparison of the models.	99
Table 5. 11 - F calculated for the models with two parameters compared to the So and Macdonald model in which $F_{crit}(2,7)_{0.05} = 4.734$	99
Table 5. 12 - Mass transfer coefficients and concentrations at equilibrium condition with bootstrap resampling and the likelihood confidence interval for p-cymene and hexane.	100
Table 5. 13 - Thermodynamic assessment with and without bootstrap resampling (BS).	102

CAPÍTULO 6

Table 6. 1 - Parameters obtained for the first-order model and their statistical metrics for different solvents and temperatures.....	121
Table 6. 2 - Parameters obtained for the fractional-order kinetic model and its statistical metrics for different solvents and temperatures.	123
Table 6. 3 - Statistical comparison of the models for different solvents and temperatures....	125
Table 6. 3 - Statistical comparison of the models for different solvents and temperatures....	126
Table 6. 4 - Shapiro-Wilk normality test applied for both models.....	134

LISTA DE ABREVIATURAS E SIGLAS

ANOVA	Análise de variância
COSMO	<i>COnductor-like Screening MOdel</i>
C16:0	Ácido graxo palmítico
C18:0	Ácido graxo esteárico
C18:1	Ácido graxo oleico
C18:2	Ácido graxo linoleico
C18:3	Ácido graxo linolênico
DM	Massa seca (<i>Dry Mass</i>)
FAMEs	Éster Metílico de Ácido Graxo (<i>Fatty Acid Methyl Esters</i>)
FFA	Ácidos graxos livres (<i>Free fatty acid</i>)
FID	Detector por Ionização de Chama (<i>Flame Ionization Detector</i>)
FTIR	Espectroscopia por infravermelho com transformada de Fourier (<i>Fourier-transform infrared spectroscopy</i>)
GC	Cromatografia Gasosa (<i>Gas chromatography</i>)
MOPAC	Pacotes de orbital molecular (<i>Molecular orbital packages</i>)
MTKM	Modelo cinético de transferência de massa (<i>Mass transfer kinetic model</i>)
PSO	Otimização por enxame de partículas (<i>Particle swarm optimization</i>)
SAC	<i>Segment activity coefficient</i>

LISTA DE SÍMBOLOS

a_p	Área interfacial da partícula
AIC	Critério de informação Akaike (<i>Akaike information criterion</i>)
B_i	Matriz de sensibilidade das respostas do modelo
C	Concentração de óleo extraído
C_0	Concentração inicial de óleo nas lâminas de soja
C_∞	Concentração de óleo extraído no equilíbrio
C_∞^d	Concentração de óleo extraído no equilíbrio para o período de difusão
C_∞^w	Concentração de óleo extraído no equilíbrio para o período de dissolução
C_i	Valores observados
\bar{C}_i	Média dos valores observados
\hat{C}_i	Valores preditos
D_{AB}	Difusão molecular
D_{eff}	Difusão efetiva
E	Esperança
h	Espessura da lâmina de soja
H	Matriz Hessiana
J	Matriz Jacobiana
k	Constante de taxa de extração
k_d	Constante de extração no período de difusão
k_F	Coefficiente externo de transferência de massa
k_w	Constante de extração no período de dissolução
m	Ordem do modelo de potência
n	Número de pontos experimentais
p	Número de parâmetros estimados
R	Raio da partícula
R_0	Raio de solubilidade do soluto
R^2	Coefficiente de determinação
R_{adj}^2	Coefficiente de determinação ajustado
RED	Diferença relativa de energia (<i>Relative energy distance</i>)
RMSE	Raiz do erro quadrático médio (<i>Root mean square error</i>)
S	Função objetivo
s^2	Variância das observações experimentais
t	Tempo
$t_{n-p}^{1-\alpha/2}$	Valor t-Student para $n - p$ graus de liberdade e nível de confiança $(1 - \alpha/2)$
V_θ	Matriz de covariância
v_{ij}, v_{ii} e v_{jj}	Elementos da matriz de covariância
γ_i^∞	Coefficiente de atividade do componente i em diluição infinita
ρ_{ij}	Correlação entre os parâmetros i e j
θ	Vetor de parâmetros estimados
χ^2	Distribuição qui-quadrada
ε	Vetor de erro do modelo
λ	Autovalores
Γ	Função gama
α	Ordem da derivada
δ_d	Parâmetro de solubilidade de Hansen de energia dispersiva
δ_h	Parâmetro de solubilidade de Hansen de energia de pontes de hidrogênio
δ_p	Parâmetro de solubilidade de Hansen de energia polar

SUMÁRIO

1 INTRODUÇÃO	17
1.1 MOTIVAÇÃO E JUSTIFICATIVA	17
1.2 OBJETIVOS	19
1.2.1 Objetivos específicos	19
1.3 ESTRUTURA DA DISSERTAÇÃO	19
2 REVISÃO BIBLIOGRÁFICA	21
2.1 A SOJA E O ÓLEO DE SOJA	21
2.2 MÉTODOS DE EXTRAÇÃO DO ÓLEO BRUTO DE SOJA	22
2.2.1 Uso de solventes verdes	22
2.3 SELEÇÃO DE SOLVENTES	26
2.4 MODELAGEM CINÉTICA E DE TRANSFERÊNCIA DE MASSA NA EXTRAÇÃO DE ÓLEO DE SOJA	27
2.4.1 Modelos empíricos	28
2.4.2 Modelo cinético de transferência de massa	29
2.5 COMENTÁRIOS FINAIS	32
3 METODOLOGIA	33
3.1 PLANEJAMENTO DE EXPERIMENTOS	33
3.2 METODOLOGIA EXPERIMENTAL	33
3.3 ESTIMAÇÃO DE PARÂMETROS.....	35
4 SOYBEAN OIL EXTRACTION USING ETHYL ACETATE AND 1-BUTANOL: FROM SOLVENT SELECTION TO THERMODYNAMIC ASSESSMENT	41
ABSTRACT	41
NOMENCLATURE	42
4.1 INTRODUCTION	43
4.2 MATERIALS AND METHODS	45
4.2.1 Material	45
4.2.2 Methods	45
4.2.2.1 Feedstock Characterization	45
4.2.2.2 Screening of Solvent.....	46
4.2.2.3 Experimental Procedure	46
4.2.2.3.1 <i>Extraction of Soybean Oil</i>	46
4.2.2.3.2 <i>Determination of Fatty Acid Composition</i>	47
4.2.2.3.3 <i>Component Analysis</i>	48
4.2.2.4 Modeling and Simulation	48
4.2.2.4.1 <i>Response Surface Methodology</i>	48
4.2.2.4.2 <i>Kinetic and Thermodynamic Modeling</i>	48

4.2.2.5 Model Evaluation	50
4.3 RESULTS AND DISCUSSION.....	51
4.3.1 Screening of Solvents.....	51
4.3.2 Soybean and Soybean Oil Characterization	53
4.3.3 RSM Results.....	56
4.3.4 Kinetic Modeling and Mass Transfer Analysis.....	61
4.3.5 Thermodynamic Analysis	67
4.4 CONCLUSIONS	68
CONFLICT OF INTERESTS	68
ACKNOWLEDGMENT	68
REFERENCES	69
SUPPLEMENTARY MATERIAL	74
5 THEORETICAL AND EXPERIMENTAL STUDIES ON TECHNICAL VIABILITY OF SOYBEAN OIL EXTRACTION WITH P-CYMENE.....	77
ABSTRACT	77
NOMENCLATURE	78
5.1 INTRODUCTION	80
5.2 MATERIALS AND METHODS	82
5.2.1 Material	82
5.2.2 Methods	83
5.2.2.1 Experimental procedures	83
5.2.2.2 Modeling and simulation	84
5.2.2.2.1 <i>Solvent selection</i>	84
5.2.2.2.2 <i>Response surface methodology</i>	85
5.2.2.2.3 <i>Kinetic and thermodynamic</i>	85
5.2.2.2.4 <i>Uncertainties evaluation and parameters estimation</i>	87
5.2.2.3 Statistical evaluation.....	88
5.3 RESULTS AND DISCUSSION.....	89
5.3.1 Insights on solvent selection.....	89
5.3.2 Soybean and soybean oil characterization	90
5.3.3 Response surface methodology results	94
5.3.4 Kinetic and thermodynamic analysis.....	96
5.4 CONCLUSIONS	102
CONFLICT OF INTERESTS	103
ACKNOWLEDGMENT	103
REFERENCES	103
6 A NOVEL APPLICATION OF THE FRACTIONAL-ORDER MODEL TO GREEN SOYBEAN OIL EXTRACTION	112

ABSTRACT	112
NOMENCLATURE	113
6.1 INTRODUCTION	113
6.2 MATERIALS AND METHODS	115
6.2.1 Experimental data	115
6.2.2 Kinetic Modeling and Parameter Estimation	116
6.2.3 Statistical Evaluation.....	117
6.3 RESULTS AND DISCUSSION.....	120
6.4 CONCLUSIONS	135
CONFLICT OF INTERESTS	135
ACKNOWLEDGMENT	135
REFERENCES	135
7 DISCUSSÃO DOS RESULTADOS	139
8 CONCLUSÕES E SUGESTÕES DE TRABALHOS FUTUROS	142
8.1 CONCLUSÕES	142
8.2 SUGESTÕES DE TRABALHOS FUTUROS	142
REFERÊNCIAS	143
APÊNDICE A – CROMATOGRAMA	151

1 INTRODUÇÃO

Neste capítulo, apresenta-se a motivação para o estudo sobre a aplicação de solventes verdes na extração de óleo de soja, compreendendo desde uma investigação teórica sobre seleção de solventes até o estudo cinético, termodinâmico e de transferência de massa aplicando acetato de etila, 1-butanol e p-cimeno em comparação com o n-hexano, o solvente industrialmente utilizado, e o etanol, um solvente verde em potencial. Em sequência, apresenta-se a motivação para a realização do trabalho, os objetivos e a estrutura da dissertação.

1.1 MOTIVAÇÃO E JUSTIFICATIVA

Por sua versatilidade de aplicações e facilidade de cultivo, a soja é uma das leguminosas mais cultivadas no mundo. Segundo o departamento de agricultura dos Estados Unidos (USDA, 2020), o Brasil é líder na produção mundial de soja. A proteína da soja tem vasta aplicação na alimentação humana (QIN; WANG; LUO, 2022) e animal (QIN; WANG; LUO, 2022) enquanto a porção de lipídios pode ser direcionada para a produção de biocombustíveis (COLOMBO et al., 2019; SCALDAFERRI; PASA, 2019) e outros produtos de maior valor agregado (YAN et al., 2022).

O óleo é extraído da matriz utilizando exclusivamente a extração por solvente ou a prensagem mecânica seguida de extração por solvente, sendo o hexano o solvente mais utilizado em nível industrial (LI et al., 2014; PRAMPARO et al., 2002). Recentemente, este éter de petróleo foi classificado à classe II de substâncias carcinogênicas, mutagênicas e reprotóxicas sob a legislação europeia (ABDELLAH et al., 2019; CLAUX et al., 2021). Consequentemente, o uso de hexano pode se restringir a determinadas aplicações no futuro.

A comunidade acadêmica está preocupada com o aumento nas emissões de dióxido de carbono na atmosfera, decorrente da exploração e do uso de substâncias de origem fóssil. O hexano, por sua vez, é uma mistura de isômeros do n-hexano que provém do craqueamento do petróleo, possuindo, então, origem não renovável.

Os solventes verdes são uma alternativa a estas substâncias de origem não renovável aplicáveis à extração de óleo de soja. É possível observar a aplicação de diversos álcoois (COMERLATTO et al., 2021; DAGOSTIN; CARPINÉ; CORAZZA, 2015; DAGOSTIN et al., 2018; PHAN et al., 2009; SAWADA et al., 2014; TODA; SAWADA; RODRIGUES, 2016), éster alquílico (DAGOSTIN; CARPINÉ; CORAZZA, 2015), acetato de etila (DAGOSTIN et al., 2018), α -pineno (BERTOUCHE et al., 2013), 2-metiltetrahidrofurano

(CLAUX et al., 2021), e até água em métodos de extração não convencionais (JUN-QING, 2001) na extração de óleo de soja. O etanol é um solvente renovável muito estudado para esta aplicação (COMERLATTO et al., 2021; DAGOSTIN; CARPINÉ; CORAZZA, 2015; DAGOSTIN et al., 2018; PHAN et al., 2009; POTRICH et al., 2020; SAWADA et al., 2014; TODA; SAWADA; RODRIGUES, 2016), enquanto álcoois de cadeia carbônica maior aparentam ter maior afinidade pelos triacilgliceróis (COMERLATTO et al., 2021; SHARMA; KHARE; GUPTA, 2002; SICAIRE et al., 2015). Apesar do uso de etanol ser atrativo por contribuir no fomento da matriz energética brasileira, este álcool possui miscibilidade parcial com o óleo de soja (FOLLEGATTI-ROMERO, 2010).

Devido à importância de metodologias de seleção de solventes, o presente trabalho busca avaliar os parâmetros de solubilidade de Hansen, o coeficiente de atividade em diluição infinita e os perfis sigma obtidos pela teoria COSMO-SAC para descrever o potencial de cada solvente para cada aplicação. Enquanto os parâmetros de solubilidade de Hansen e o coeficiente de atividade em diluição infinita fornecem uma triagem de solventes, a análise dos perfis sigma e dos próprios parâmetros de solubilidade de Hansen favorecem no entendimento energético das misturas solvente-triglicerídeos.

O tempo, a temperatura e a razão solvente-sólido são variáveis de processo importantes em nível industrial para este tipo de extração sólido-líquido (NAVARRO, 2002). Desta forma, a metodologia de superfície de resposta contribui para otimizar o rendimento das extrações em termos da temperatura e da razão solvente-sólido, assim como, o estudo cinético contribui para determinar em quanto tempo se atinge o equilíbrio. Portanto, modelos empíricos e fenomenológicos são utilizados com o objetivo de compreender a cinética de extração por solventes verdes para posterior análise e interpretação termodinâmica dos resultados.

Índices de qualidade são utilizados para avaliar a qualidade do óleo extraído para aplicações em biocombustíveis e alimentação. Desta forma, é importante analisar a composição dos ácidos graxos do óleo extraído, bem como, a constituição de ácidos graxos livres, mono, di e triacilgliceróis. Ainda, a técnica de espectroscopia por infravermelho com transformada de Fourier fornece uma rápida análise qualitativa de óleos vegetais.

Resumindo, esta dissertação busca ampliar o entendimento sobre a aplicação de solventes verdes na extração de óleo de soja, abordando aspectos relacionados à seleção de solventes pelos parâmetros de solubilidade de Hansen e coeficiente de atividade em diluição infinita obtido pela teoria COSMO-SAC; otimização das variáveis de processo temperatura e razão solvente-sólido no rendimento da extração através da metodologia de superfície de

resposta; modelagem cinética e de transferência de massa utilizando modelos empíricos e fenomenológico; análise termodinâmica das extrações; e a investigação da qualidade do óleo extraído.

1.2 OBJETIVOS

O objetivo geral deste trabalho é avaliar a aplicação de solventes verdes na extração de óleo de soja, através do estudo cinético, termodinâmica e de transferência de massa do processo.

1.2.1 Objetivos específicos

1. Extração de óleo de soja com acetato de etila, 1-butanol e p-cimeno;
2. Estudar a cinética e transferência de massa do processo;
3. Avaliar a termodinâmica das extrações;
4. Investigar a interação entre os solventes e os triglicerídeos através de metodologias de seleção e triagem de solventes;
5. Caracterizar o óleo de soja extraído por meio do espectro do infravermelho, perfil dos ácidos graxos e conteúdo de ácidos graxos livres, mono, di e triacilglicerol.

1.3 ESTRUTURA DA DISSERTAÇÃO

Esta dissertação está dividida em 9 capítulos.

No Capítulo 1 é realizada uma breve introdução à luz da proposta de estudo e as motivações para a elaboração do trabalho.

A revisão bibliográfica sobre o objeto de pesquisa é apresentada no Capítulo 2, no qual é apresentado o estado da arte sobre a aplicação de solventes verdes na extração de óleo de soja, bem como, as abordagens de triagem de solventes e os equacionamentos matemáticos e termodinâmico para descrever este tipo de transporte sólido-líquido.

O Capítulo 3 apresenta a metodologia utilizada neste trabalho para obter os resultados experimentais, a qual foi majoritariamente baseada em planejamento de experimentos.

O Capítulo 4 refere-se ao primeiro artigo desta dissertação, intitulado *Soybean oil extraction using ethyl acetate and 1-butanol: from solvent selection to thermodynamic assessment*, o qual refere-se ao estudo dos solventes acetato de etila e 1-butanol na extração de óleo de soja. Neste trabalho, avaliou-se as metodologias de seleção de solventes através

dos parâmetros de solubilidade de Hansen e do coeficiente de atividade em diluição infinita obtido pela teoria COSMO-SAC. A influência das variáveis temperatura e razão solvente-sólido no rendimento da extração foi avaliada através da metodologia de superfície de resposta utilizando um planejamento composto central. Por fim, a cinética de extração foi modelada e os parâmetros termodinâmicos padrões de entalpia, entropia e energia livre de Gibbs foram calculados. Este artigo foi publicado no periódico *Journal of Industrial and Engineering Chemistry*.

O Capítulo 5 apresenta o segundo artigo que compõe esta dissertação, intitulado *Theoretical and experimental studies on the technical viability of soybean oil extraction with p-cymene*, no qual é realizado um estudo de viabilidade técnica sobre a extração de óleo de soja utilizando p-cimeno. Neste trabalho, a modelagem cinética da extração é associada à reamostragem bootstrap visando reduzir o viés dos estimadores. Este artigo foi submetido para publicação no periódico *Separation and Purification Technology*.

No Capítulo 6 é apresentado o último artigo desta dissertação, intitulado *A novel application of the fractional-order model to green vegetable oil extraction*, no qual é realizada a comparação entre o modelo de potência de primeira ordem usual e de derivada fracionária em diversos casos de extração de óleo de soja presentes na literatura e com as curvas cinéticas obtidas experimentalmente para o 1-butanol, o acetato de etila e o p-cimeno. Este artigo foi submetido para publicação no periódico *Separation and Purification Technology*.

O Capítulo 7 apresenta uma discussão geral dos resultados.

No Capítulo 8 são apresentadas a conclusão e as sugestões de trabalhos futuros.

2 REVISÃO BIBLIOGRÁFICA

2.1 A SOJA E O ÓLEO DE SOJA

A soja é a oleaginosa mais cultivada no mundo, enquanto, segundo o departamento de agricultura dos Estados Unidos (USDA, 2020), o Brasil ocupa o primeiro lugar na sua produção mundial, contribuindo com mais de 30% do montante. Na safra de 2020, a produção de soja brasileira ficou na ordem de 139.500 milhões de toneladas métricas, seguida pelos Estados Unidos com 114.749 (USDA, 2020).

A grande quantidade de óleo e proteínas de alta qualidade, em conjunto com a facilidade de cultivo, destacam a soja na economia mundial (ANWAR et al., 2016; KONG et al., 2019). Apesar do maior retorno financeiro (60-70%) ser resultante da produção do farelo (DIJKSTRA, 2016), a soja convencional contém cerca de 20% de óleo bruto (CLAUX et al., 2021; PERKINS, 1995). O óleo extraído é destinado à alimentação (GERDE et al., 2020), produção de biodiesel (CHEN et al., 2007; LIU et al., 2007) e diesel verde (KIM et al., 2013) e outros (OLIVIERI; DE QUADROS; GIUDICI, 2020; YAN et al., 2022).

O óleo de soja é composto majoritariamente por mono, di e triacilgliceróis, fosfolipídios, material insaponificável, ácidos graxos livres e outros (GERDE et al., 2020). A estrutura básica dos acilgliceróis é composta por uma molécula de glicerol ligada a um, dois ou três ácidos graxos, nos quais, sobretudo, encontram-se: ácidos graxos palmítico (C16:0), esteárico (C18:0), oleico (C18:1), linoleico (C18:2) e linolênico (C18:3) (GERDE et al., 2020). O perfil dos ácidos graxos do óleo de soja é: C16:0 (8-17%), C18:0 (3-30%), C18:1 (25-60%), C18:2 (25-60%) e C18:3 (2-15%) (HAMMOND; GLATZ, 1989). Desta forma, os ácidos graxos classificam-se como saturados, monoinsaturados e poli-insaturados, a depender do número de duplas ligações em sua cadeia carbônica. A Tabela 2.1 apresenta a composição típica do óleo de soja bruto e refinado.

Tabela 2. 1 - Composição típica do óleo de soja bruto e refinado.

Componentes	Unidade	Óleo bruto	Óleo refinado
Triacilgliceróis	(%)	94,4 ^a	> 99 ^b
Fosfolipídios	(%)	3,7 ^a	0,003-0,045 ^b
Material insaponificável	(%)	1,3-1,6 ^a	0,3 ^b
Ácidos graxos livres	(%)	0,3-,7 ^a	< 0,05 ^b
Metais	mg/kg	1-3 ^a	0,12-0,36 ^b

^aGERDE et al., 2020; ^bLIU, 2012.

2.2 MÉTODOS DE EXTRAÇÃO DO ÓLEO BRUTO DE SOJA

O óleo é extraído da matriz utilizando prensagem mecânica ou extração utilizando solventes (MIYASAKA, 1981), a depender do teor de óleo presente. A prensagem mecânica é seguida de extração com solvente a fim de aumentar o rendimento da extração (MIYASAKA, 1981; SHAHIDI, 2005). Ao fazer o uso de solvente, a extração do óleo acontece majoritariamente por dois mecanismos: dissolução e difusão. No primeiro, o óleo livre é simplesmente dissolvido no solvente e, no segundo, o óleo contido nos bolsões e em capilares fibrosos é transferido para a micela por difusão (MIYASAKA, 1981).

Visando aumentar o rendimento da extração e, conseqüentemente, reduzir o teor de óleo residual, busca-se acondicionar a soja por laminação, visando obter flocos com espessura de milésimos de polegada, ou por extrusão, visando obter aglomerados expandidos (MIYASAKA, 1981). Após acondicionamento, o material é submetido a extração por solvente obtendo três produtos principais, o óleo bruto, o farelo e a lecitina (MIYASAKA, 1981).

Sistemas contínuos e descontínuos são utilizados para a extração do óleo. Nos sistemas contínuos, destacam-se os métodos de infusão e de enriquecimento, enquanto nos descontínuos é possível citar os métodos de submersão e de percolação (MIYASAKA, 1981). Quanto aos métodos contínuos, encontram-se os extratores de Hildebrandt, Bollmann, De Smet, Lurgi e Rotocel (ERICKSON, 1980; MIYASAKA, 1981). Principalmente extratores contracorrentes são utilizados e o extrato contém cerca de 25-30% de óleo, o qual é concentrada até 80% ou mais em destilador de simples efeito, seguindo para um segundo estágio de evaporação a fim de concentrar a micela até 95-98% de óleo (SHAHIDI, 2005).

Dentre as variáveis que afetam o processo de extração é possível citar a umidade da matriz, temperatura e pressão do extrator, pureza, vazão e temperatura do solvente, relação solvente-lâminas e tempo de retenção (NAVARRO, 2002). Para o projeto de um extrator, deve-se levar em conta a velocidade para atingir o equilíbrio entre a micela no interior e no exterior da partícula, parâmetro este que depende majoritariamente da viscosidade do solvente e do óleo, tamanho, forma e estrutura interna da matriz (HUI, 1996), além da afinidade entre o óleo e o solvente (BENAZZOUZ et al., 2013).

2.2.1 Uso de solventes verdes

O hexano é o solvente mais utilizado na extração de óleos vegetais (LI et al., 2014; PRAMPARO et al., 2002). Em contrapartida, recentemente este solvente foi classificado à

lista de substâncias carcinogênicas, mutagênicas e reprotóxicas sob a legislação Europeia por apresentar efeitos neuro e reprotóxicos (BENAZZOUZ et al., 2013; CLAUX et al., 2021; LI; SMITH; STEVENS, 2016). Da mesma forma, o uso de solventes e combustíveis provenientes da exploração de combustíveis fósseis contribui com grande parte das emissões de dióxido de carbono na atmosfera. Ao que foi apresentado, o campo científico vem se empenhando a encontrar alternativas renováveis, não tóxicas, não carcinogênicas, não mutagênica, não reprotóxicas e carbono neutro. Por conseguinte, os solventes verdes vêm sendo utilizados na tentativa de substituir o uso destes produtos derivados do petróleo.

Segundo Anastas e Warner (2000), os doze princípios da química verde são:

1. Prevenir o desperdício;
2. Mitigar riscos e efeitos tóxicos com o design de produtos e químicos seguros;
3. Projeto de síntese química menos perigosa ao humano e ao meio ambiente;
4. Utilizar matérias-primas renováveis às oriundas de combustíveis fósseis;
5. Usar catalisadores para reduzir a quantidade estequiométrica de reagentes;
6. Evitar derivações químicas para reduzir a quantidade de reagentes;
7. Reduzir o desperdício e melhorar o rendimento;
8. Utilizar solventes e condições que não contribuam para a formação de *smog* e destruição da camada de ozônio;
9. Aumentar a eficiência energética;
10. Utilizar produtos e reagentes que se degradem após uso;
11. Utilizar o monitoramento em tempo real de processos para evitar a poluição;
12. Minimizar o potencial de explosões, incêndios e emissões ao meio ambiente.

Existem diferentes famílias de solventes verdes, sendo possível citar a utilização de fluido supercrítico, líquidos iônicos e solventes eutéticos profundos, solventes fluorados, líquidos poliméricos, a água, solventes ambientalmente amigáveis (*eco-friendly*) e bio-solventes. Neste sentido, a Tabela 2.2 apresenta a aplicação de diferentes solventes verdes na extração de óleo de soja.

Tabela 2. 2 - Aplicação de diferentes solventes verdes na extração de óleo de soja.

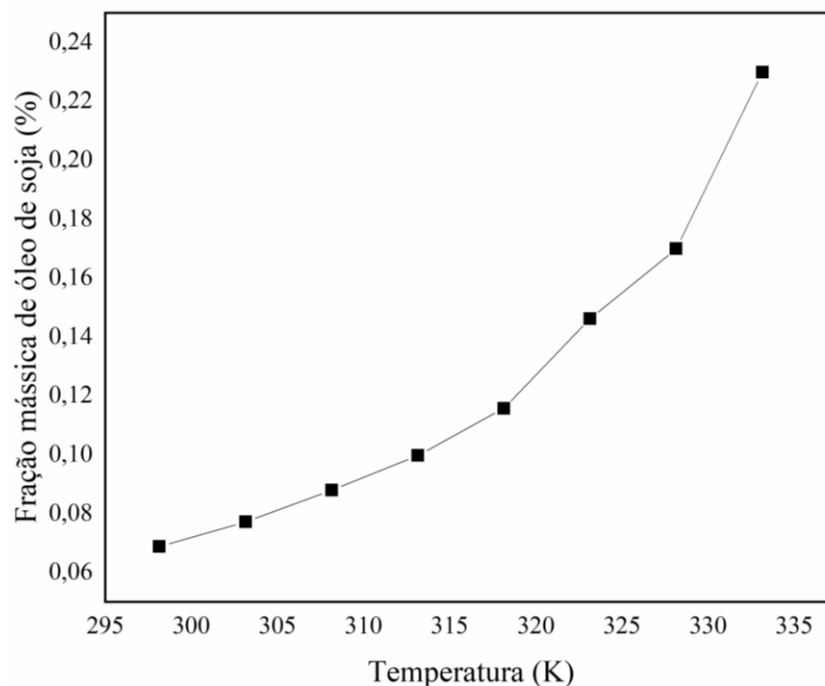
Acondicionamento	Solvente	Técnica	Referência
Moída	CO ₂ supercrítico	Extração supercrítica	JOKIĆ et al., 2010
Aglomerado expandido	Água	Extração subcrítica	NDLELA et al., 2012
Flocos	Isopropanol e etanol, anidro e suas misturas	Extração em leito fixo	COMERLATTO et al., 2021
Flocos	Etanol anidro e hidratado e misturas entre etanol e biodiesel	Batelada	DAGOSTIN; CARPINÉ; CORAZZA, 2015
Aglomerado expandido	Etanol anidro e hidratado	Batelada	TODA; SAWADA; RODRIGUES, 2016
Flocos	Misturas entre etanol e acetato de etila	Batelada	DAGOSTIN et al., 2018
Flocos	2-Metiltetrahidrofurano anidro e hidratado	Batelada sequencial	CLAUX et al., 2021
Moída	α -pineno	Extração Soxhlet	BERTOUCHE et al., 2013
Aglomerado expandido	Etanol anidro e hidratado	Batelada	SAWADA et al., 2014
Moída	Etanol anidro	Extração líquida pressurizada	RODRIGUES; CARDOZO-FILHO; SILVA, 2017
Flocos	Etanol anidro e hidratado	Batelada	RODRIGUES; ARACAVAL; ABREU 2010
Não informado	Etanol, n-propanol e isopropanol em suas misturas, anidros e em azeótropos	Extração Soxhlet	GANDHI et al., 2003
Farinha	t-Butanol, n-propanol, isopropanol e etanol	Particionamento de três fases	SHARMA; KHARE; GUPTA, 2002
Flocos	Etanol	Extrator industrial contínuo	POTRICH et al., 2020
Aglomerado expandido	Etanol	Batelada	FERREIRA et al., 2022

Ao observar os estudos sobre extração de óleo de soja utilizando solventes verdes é evidente a utilização de álcoois, com destaque ao etanol. O uso de etanol vem se apresentando como uma opção viável na substituição do hexano em análises técnicas (COMERLATTO et al., 2021; DAGOSTIN; CARPINÉ; CORAZZA, 2015; FERREIRA et al., 2022; RODRIGUES; ARACAVAL; ABREU, 2010; RODRIGUES; CARDOZO-FILHO; SILVA, 2017; SAWADA et al., 2014; TODA; SAWADA; RODRIGUES, 2016) e técnicas-econômicas (POTRICH et al., 2020), principalmente por reduzir consideravelmente as emissões de dióxido de carbono na atmosfera (POTRICH et al., 2020), bem como, por contribuir na promoção da matriz energética renovável brasileira.

O etanol já foi introduzido industrialmente como solvente na extração de óleo de soja, mas sua aplicação foi interrompida devido ao seu alto custo em relação ao hexano (HRON;

KOLTUN; GRACI, 1982; JOHNSON; LUCAS, 1983). A utilização de etanol hidratado resulta em menores rendimentos de extração de óleo de soja (TODA; SAWADA; RODRIGUES, 2016), enquanto a aplicação de etanol anidro pode ocasionar em acúmulo de água no solvente devido à umidade natural da matéria-prima, atenuando, assim, a relação de equilíbrio de óleo entre a matriz e a micela (ABRAHAM et al., 1993; SILVA et al., 2009). Não obstante, como pode ser observado na Figura 2.1, o etanol e o óleo de soja não apresentam miscibilidade completa.

Figura 2. 1 - Solubilidade do óleo de soja em etanol em função da temperatura.



Fonte: Adaptado de FOLLEGATTI-ROMERO, 2010.

Em comparação ao etanol, o isopropanol possui maior afinidade com óleo de soja (COMERLATTO et al., 2021; SHARMA; KHARE; GUPTA, 2002; SICAIRE et al., 2015). Da mesma forma, a aplicação de isômeros do 1-butanol vem se mostrando promissora (SHARMA; KHARE; GUPTA, 2002).

O estudo de Dagostin et al. (2018) mostra que maiores quantidades de acetato de etila, como cossolvente junto ao etanol, resultam em maiores rendimentos da extração.

Para a extração de óleos vegetais e de microalgas, a aplicação de terpenos, como o d-limoneno, o p-cimeno, e o α e β -pineno, vêm se mostrando oportuna (ABDELLAH et al., 2019; BERTOUICHE et al., 2013; LI et al., 2014; TANZI et al., 2012; TANZI; VIAN;

CHEMAT, 2013), assim como, a aplicação de outros compostos, como o 2-metiltetrahidrofurano (CLAUX et al., 2021; SICAIRES et al., 2021).

Mais informações sobre a aplicação de solventes verdes na extração de óleo de soja podem ser obtidas no artigo de revisão intitulado *Recent advances in green soybean oil extraction: A review* recentemente publicado pelo autor dessa dissertação na revista *Journal of Molecular Liquids* (GASPARETTO; CASTILHOS; SALAU, 2022).

2.3 SELEÇÃO DE SOLVENTES

A solubilidade de qualquer soluto em um solvente é afetada pela energia de rede (do inglês *lattice energy*) e os efeitos de solvatação e de entropia (BLAKE, 2003; EISEN; MARANO; GLAZIER, 2014), uma vez que essas propriedades estão relacionadas à mudança da estrutura do solvente (HAYYAN et al., 2022).

Ferramentas de triagem e seleção de solventes são uma alternativa para buscar substâncias para determinadas aplicações. Os parâmetros de solubilidade de Hansen e o coeficiente de atividade em diluição infinita aparecem como metodologias para tal.

Um bom indicativo de interações entre moléculas é o coeficiente de atividade em diluição infinita (BROUWER; SCHUUR, 2019). Interações eletrostáticas e de van der Waals entre moléculas resultam em desvios positivos ou negativos da lei de Raoult, devido aos efeitos inter e intramoleculares (BROUWER; SCHUUR, 2019). O caso limítrofe descreve quando um soluto está infinitamente diluído em um solvente, sendo que o coeficiente de atividade nesta condição serve como ferramenta de seleção de solventes (BROUWER; SCHUUR, 2019).

A teoria *COnductor-like Screening MOdel – Segment Activity Coefficient* (COSMO-SAC) é uma metodologia *ab initio* que pode ser utilizada para obter o coeficiente de atividade em diluição infinita (LIN; SANDLER, 2002). Os perfis-sigma obtidos pela teoria COSMO-SAC podem ser utilizados como uma maneira de entender o comportamento e a solvatação dos pares soluto-solvente.

Os parâmetros de solubilidade de Hansen (HANSEN, 2007) são utilizados na seleção de solventes (BENZAOUZ et al., 2013; BROUWER; SCHUUR, 2019), bem como, no entendimento energético da mistura (Jimenez et al., 2019). O modelo foi proposto como uma extensão dos parâmetros de solubilidade de Hildebrand por dividir as contribuições de energia em dispersiva, polar e de interação de hidrogênio (BROUWER; SCHUUR, 2019). Neste, energias dispersivas, polares e de interação de hidrogênio descrevem a interação soluto-

solvente na forma de uma diferença relativa de energia (*RED*) (BROUWER; SCHUUR, 2019). Um solvente é considerado para determinada aplicação se este estiver dentro do raio de solubilidade do soluto (R_0). De fato, isto ocorre para razões *RED* menores ou iguais a 1 e quanto menor o *RED* melhor é o potencial de solubilização do solvente.

$$Ra^2 = 4(\delta_{D2} - \delta_{D1})^2 + (\delta_{P2} - \delta_{P1})^2 + (\delta_{H2} - \delta_{H1})^2 \quad (1)$$

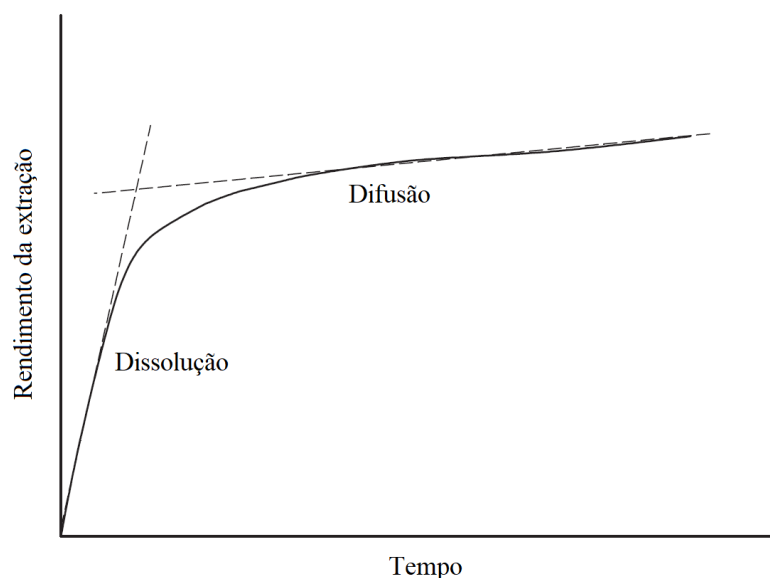
$$RED = \frac{Ra}{R_0} \quad (2)$$

em que Ra representa a distância soluto-solvente, δ são os parâmetros de solubilidade de Hansen para as energias dispersivas (D), polares (P) e de interação de hidrogênio (H) e os subscritos 1 e 2 dizem respeito aos pares soluto e solvente.

2.4 MODELAGEM CINÉTICA E DE TRANSFERÊNCIA DE MASSA NA EXTRAÇÃO DE ÓLEO DE SOJA

A extração de óleo de soja segue uma cinética típica representada pela Figura 2.2, na qual é evidente a ocorrência de dois períodos característicos: dissolução e difusão (CHAN; YUSOFF; NGOH, 2014). No primeiro, o óleo presente na superfície é rapidamente transferido à fase fluida e, no segundo, a difusão do soluto dentro da partícula controla um fluxo de transferência lento.

Figura 2. 2 - Curva típica de extração em batelada utilizando solvente.



Fonte: Adaptado de CHAN; YUSOFF; NGOH, 2014.

Os mecanismos de transferência de massa baseiam-se em fenômenos difusivos e convectivos para descrever o transporte de um componente de uma região de alta concentração para uma de baixa (BERGMAN et al., 2014). Enquanto, a diferença de potencial químico entre essas regiões corresponde à força motriz para a transferência de massa (BERGMAN et al., 2014).

2.4.1 Modelos empíricos

Modelos de ordem de potência são utilizados para descrever a cinética de extração de óleos vegetais (DAGOSTIN; CARPINÉ; CORAZZA, 2015; SANTOS et al., 2015). A Eq. 3 apresenta o modelo geral de ordem de potência e as Eqs. 4 e 5 as soluções analíticas para os casos $m = 1$ (primeira ordem) e $m = 2$ (segunda ordem), respectivamente.

$$\frac{dC}{dt} = k(C_{\infty} - C)^m \quad (3)$$

$$C = C_{\infty} [1 - \exp(-kt)] \quad (4)$$

$$C = \frac{t}{\frac{1}{kC_{\infty}} + \frac{t}{C_{\infty}}} \quad (5)$$

em que C representa a concentração do óleo extraído (g/g DM), C_{∞} a concentração de óleo extraído na condição de equilíbrio (g/g DM), k é a constante de taxa de extração (1/min), t é o tempo de extração (min) e m é a ordem do modelo de potência (-).

Originalmente apresentado por Patricelli et al. (1979) e comumente referido como modelo de So e Macdonald (1986) a Eq. 6 é utilizada para descrever a cinética de processos que ocorrem por mecanismos de lavagem (sobrescrito w) e difusão (sobrescrito d).

$$C = C_{\infty}^w [1 - \exp(-k_w t)] + C_{\infty}^d [1 - \exp(-k_d t)] \quad (6)$$

Em que a concentração de óleo extraída no equilíbrio é determinada pela soma entre C_{∞}^w e C_{∞}^d . Também pode estar presente um segundo termo difusivo o qual representa a difusão muito lenta de compostos menos solúveis, descritos pela presença de substâncias não glicerídicas e frações de óleo ricas em fosfatídeos (KARNOFSKY, 1949). O modelo de So e Macdonald reparameterizado pode ser encontrado em Kostic et al. (2014).

Os modelos de ordem fracionária têm ganhado popularidade devido seu potencial para descrever processos complexos e dinâmicas não lineares. Ao definir uma derivada arbitrária α

para o termo diferencial na Eq. 3 e $m = 1$ é possível obter a solução para o modelo de ordem fracionária usando propriedades genéricas da transformada de Laplace e o derivativo fracionário de Caputo, obtendo

$$C = C_{\infty} \left[1 - \sum_{i=0}^{\infty} \frac{(-kt^{\alpha})^i}{\Gamma(\alpha i + 1)} \right] \quad (7)$$

em que Γ representa a função gama.

2.4.2 Modelo cinético de transferência de massa

Realizando um balanço diferencial de massa para um componente genérico A em uma mistura binária em que o movimento do fluido ocorre devido a um fluxo $\nabla(\rho_A v)$ e por um termo de difusão molecular j_A , obtém-se

$$\frac{\partial \rho_A}{\partial t} + \nabla(\rho_A v) + \nabla j_A = r_A \quad (8)$$

O termo de difusão molecular é definido como

$$j_A = -D_{AB} \nabla \rho_A \quad (9)$$

Dividindo todos os termos da Eq. 8 pela massa molar do componente, chega-se a

$$\frac{\partial C_A}{\partial t} + \nabla(C_A v) = \nabla(D_{AB} \nabla C_A) + R_A \quad (10)$$

$$R_A = \frac{r_A}{M_A} \quad (11)$$

Para temperatura e pressão constante, D_{AB} também será constante

$$\frac{DC_A}{Dt} = D_{AB} (\nabla^2 C_A) + R_A \quad (12)$$

Simplifica-se a Eq. 12 para velocidade do meio nula e fenômeno não reacional

$$\frac{\partial C_A}{\partial t} = D_{AB} (\nabla^2 C_A) \quad (13)$$

Utilizando a abordagem pseudocomponente para o óleo de soja ($C_A = C_p$) e adotando o coeficiente de difusão como o termo de difusão efetiva ($D_{AB} = D_{eff}$) (CRANK, 1979) é possível obter

$$\frac{\partial C_p}{\partial t} = D_{eff} (\nabla^2 C_p) \quad (14)$$

A Eq. 14 pode ser resolvida para coordenadas cartesianas, cilíndricas ou esféricas utilizando o respectivo laplaciano de C_p . São necessárias uma condição inicial (Eq. 15) e duas condições de contorno (Eq. 16 e 17) para resolver a Eq. 14.

$$\frac{\partial C_p}{\partial x} = 0, \text{ para } x = 0 \text{ e } t > 0 \quad (15)$$

$$-D_{eff} \frac{\partial C_p}{\partial x} = k_F (C|_{x=L} - C), \text{ para } x = L \text{ e } t > 0 \quad (16)$$

$$C_p = C_0, \text{ para } 0 \leq x \leq L \text{ e } t = 0 \quad (17)$$

C corresponde a concentração de óleo extraído no solvente e pode ser obtido por (CERUTTI; SOUZA; SOUZA, 2012; COMERLATTO et al., 2021)

$$\frac{\partial C}{\partial t} = a_p k_F (C|_{x=L} - C) \quad (18)$$

$$C = 0, \text{ para } t = 0 \quad (19)$$

Uma alternativa para obter k_F é analisar o caso limite $t \rightarrow 0$, $C \rightarrow 0$, $C_p|_{r=R} \rightarrow C_0$

$$\frac{dC}{dt} = a_p k_F C_0 \quad (20)$$

$$\int_0^C \frac{dC}{C_0} = \int_0^t a_p k_F dt \quad (21)$$

$$\frac{C}{C_0} = a_p k_F t \quad (22)$$

Desta forma, é possível obter k_F por regressão linear utilizando os primeiros 3 pontos experimentais (Souza et al., 2017).

Existe uma relação direta entre os tipos de geometria de placa plana e esférica, conforme apresentado por Comerlatto et al. (2020). Segundo os autores, é possível considerar

as lâminas de soja como esferas de raio $R = 3h/2$, em que h é a espessura da lâmina de soja. Neste sentido, a solução analítica para o caso apresentado pelas Eqs. 14 a 17 e após realizar $\int C_p(t, x) dx$ para geometria esférica será (CHAN; YUSOFF; NGOH, 2014; FRANCO et al., 2007)

$$C = C_\infty \left[1 - 0,8415 \sum_{n=1}^{\infty} B_n \lambda_n \exp\left(-\frac{D_{eff} \lambda_n^2 t}{R^2}\right) \right] \quad (23)$$

$$B_n = \left(\frac{4}{q_n} \right) \frac{\sin(\lambda_n) - \lambda_n \cos(\lambda_n) + \lambda_n}{2\lambda_n - (\sin(\lambda_n))^2} \quad (24)$$

Em que q_n são os autovalores da função

$$\lambda \cdot \cotg(\lambda) + \frac{k_F R}{D_{eff}} = 1 \quad (25)$$

Os primeiros 5 autovalores da Eq. 25 podem ser representados em função de R , k_F e D_{eff} , conforme apresentado por Franco et al. (2007)

$$\lambda_1 = 0,5717 \ln\left(\frac{k_F R}{D_{eff}}\right) + 1,5757 \quad (26)$$

$$\lambda_2 = 0,3776 \ln\left(\frac{k_F R}{D_{eff}}\right) + 4,793 \quad (27)$$

$$\lambda_3 = -0,0045 \ln\left(\frac{k_F R}{D_{eff}}\right)^2 + 0,13 \left(\frac{k_F R}{D_{eff}}\right) + 7,7206 \quad (28)$$

$$\lambda_4 = 0,0743 \ln\left(\frac{k_F R}{D_{eff}}\right) + 10,927 \quad (29)$$

$$\lambda_5 = 0,0618 \ln\left(\frac{k_F R}{D_{eff}}\right) + 14,079 \quad (30)$$

A concentração de óleo na superfície é intrínseca ao fluxo de massa dentro da partícula, que neste caso é difícil de determinar (SANTOS et al., 2015). Desta forma, assume-se a igualdade do fluxo difusivo dentro da partícula à transferência de massa por convecção para a fase fluida (COMERLATTO et al., 2021), sendo comum negligenciar a resistência externa à transferência de massa (CLAUX et al., 2021; DAGOSTIN; CARPINÉ; CORAZZA,

2015; DAGOSTIN et al., 2018) assumindo que o transporte de óleo da superfície para o solvente é instantâneo, desta forma, chega-se à Eq. 31 para geometria plana e à Eq. 32 para geometria esférica.

$$C = C_{\infty} \left[1 - \frac{8}{\pi^2} \sum_{n=1}^{\infty} \frac{1}{(2n+1)^2} \exp\left(-\frac{(2n+1)^2 \pi^2 Dt}{4L^2}\right) \right] \quad (31)$$

$$C = C_{\infty} \left[1 - \frac{6}{\pi^2} \sum_{n=1}^{\infty} \frac{1}{n^2} \exp\left(-\frac{n^2 \pi^2 Dt}{R^2}\right) \right] \quad (32)$$

De maneira geral, para a extração de óleo de soja em batelada, melhores resultados estatísticos são observados para o modelo generalizado de So e Macdonald com um termo difusivo em relação ao modelo cinético de transferência de massa (MTKM) (TODA; SAWADA; RODRIGUES, 2016). A comparação dos modelos de ordem de potência com MTKM foi feita por Dagostin et al. (2015), sendo observado melhores resultados para o modelo de segunda ordem, ainda que a concentração no equilíbrio estimada por MTKM tenha sido utilizada para obter os parâmetros termodinâmico padrões de entalpia, entropia e energia livre de Gibbs. Entretanto, o modelo cinético de transferência de massa vem sendo truncado no primeiro termo da série de Taylor (CLAUX et al., 2021; DAGOSTIN et al., 2018), o que pode não garantir estabilidade e pequena variabilidade para os parâmetros estimados (NICOLIN; ROSSONI; JORGE, 2016). Não menos importante, para extração em leito fixo costuma-se considerar a resistência externa à transferência de massa (COMERLATTO et al., 2021; CERUTTI; SOUZA; SOUZA, 2012) na forma de uma condição de contorno na superfície das partículas de soja para a equação diferencial parcial governante.

2.5 COMENTÁRIOS FINAIS

Neste capítulo abordou-se tópicos referentes a extração de óleo de soja, o qual é um processo de separação de interesse de indústrias de alimentos a biocombustíveis. Observa-se que vários solventes renováveis podem ser utilizados a fim de substituir o uso de hexano, enquanto os parâmetros de solubilidade de Hansen e o coeficiente de atividade em diluição infinita aparecem como metodologias para triagem e seleção de solventes. A modelagem do processo de extração é governada por mecanismos difusivos, sendo comum negligenciar a resistência externa à transferência de massa.

3 METODOLOGIA

3.1 PLANEJAMENTO DE EXPERIMENTOS

Um planejamento composto central 2^2 (níveis ± 1) com 4 pontos axiais ($\alpha = \sqrt{2}$) e triplicata no ponto central foi conduzido para avaliar a influência da temperatura e da razão solvente-sólido no rendimento da extração de óleo de soja. Um modelo estatístico foi ajustado no software R Studio (R CORE TEAM, 2022).

Os parâmetros do modelo estatístico para construir as superfícies de resposta foram avaliados através da análise de variância (ANOVA) simplificada e o modelo final foi submetido aos testes de heterocedasticidade e de Shapiro-Wilk para normalidade. A matriz de planejamento experimental está apresentada na Tabela 3.1.

Tabela 3. 1 - Matriz de planejamento experimental.

Experimento	Temperatura (K)	Razão solvente/sólido (-)
1	298 (-1)	2,5 (-1)
2	328 (1)	2,5 (-1)
3	298 (-1)	7,5 (1)
4	328 (1)	7,5 (1)
5	291,79 ($-\sqrt{2}$)	5 (0)
6	334,21 ($\sqrt{2}$)	5 (0)
7	313 (0)	1,46 ($-\sqrt{2}$)
8	313 (0)	8,54 ($\sqrt{2}$)
9	313 (0)	5 (0)
10	313 (0)	5 (0)
11	313 (0)	5 (0)

3.2 METODOLOGIA EXPERIMENTAL

As lâminas de soja foram gentilmente cedidas pela empresa Granol, unidade de Cachoeira do Sul, localizada no estado do Rio Grande do Sul. Aproximadamente 10 kg de soja foram descarregadas dos cilindros laminadores, embaladas e acondicionadas sob resfriamento até o seu uso.

Hexano (Êxodo científica, 99% de pureza, CAS N° 110-54-3), álcool etílico absoluto (Neon, 99,8% de pureza, CAS N° 64-17-5), 1-butanol (Neon, 99% de pureza, CAS N° 71-36-3), acetato de etila (Sigma Aldrich, 99,8% de pureza, CAS N° 141-78-6) e p-cimeno (Sigma Aldrich, 99,8% de pureza, CAS N° 99-87-6) foram utilizados como solventes puros nas extrações.

A determinação do teor de óleo bruto total nas lâminas de soja foi realizada em extrator Soxhlet no ponto de ebulição dos solventes supracitados seguindo metodologia

adaptada de Comerlatto (2020). Aproximadamente 5 g de lâminas de soja foram extraídas com 150 mL de cada solvente por cerca de 4 horas. Após, o solvente foi removido em rotaevaporador à vácuo e o balão foi submetido à aquecimento em estufa a aproximadamente 24 horas a 80 °C para eliminar quaisquer solventes residuais. O rendimento foi calculado em base seca conforme Eq. 33.

$$\text{Rendimento (g/g DM)} = \frac{\text{massa de óleo (g)}}{\text{massa de lâminas de soja (g)}} \quad (33)$$

A umidade foi determinada por perda por dessecação em estufa a 105 °C por aproximadamente 24 horas (AOCS, 1998).

A espessura média das lâminas foi medida utilizando-se um paquímetro.

A densidade aparente das lâminas de soja foi determinada utilizando um picnômetro de 5 mL seguindo a metodologia disposta em Peçanha (2014).

A distribuição granulométrica das lâminas de soja foi determinada utilizando uma série de peneiras Tyler também seguindo a metodologia presente em Peçanha (2014).

Os experimentos cinéticos foram realizados em banho térmico e o rendimento de cada extração foi determinado gravimetricamente por evaporação do solvente conforme Eq. 54.

A análise qualitativa dos óleos extraídos foi determinada por Espectroscopia por Infravermelho com Transformada de Fourier em um equipamento IR Prestige-21 da Shimadzu®, o qual foi obtido por transmitância direta sobre um cristal de NaCl operando na faixa de 4500 a 400 cm⁻¹.

O perfil dos ácidos graxos do óleo extraído foi determinado por cromatografia gasosa (GC) equipada com detector por ionização de chama (FID) no cromatógrafo a gás GCMS-QP2010 da Shimadzu® utilizando uma coluna capilar Rtx-Wax® (30 m × 0,25 mm × 0,25 μm). Para o preparo dos ésteres metílicos dos ácidos graxos (FAMES, do inglês *fatty acid methyl esters*) utilizou-se a metodologia de Hartman e Lago (HARTMAN; LAGO, 1973) adaptada pela Embrapa (ANTONIASSI et al., 2018), utilizando transesterificação direta com metanol e hidróxido de potássio seguida por esterificação utilizando solução de cloreto de amônio e ácido sulfúrico em metanol. A programação da rampa de aquecimento do equipamento seguiu conforme: partindo de 60 °C aumentou-se a temperatura até 200 °C a uma taxa de 10 °C/min, para então aumentar a 240 °C a uma taxa de 5 °C/min, mantendo isotermicamente por 7 minutos. O injetor e detector foram mantidos a 250 °C, hélio foi utilizado como gás de arraste a 35 cm/s e razão split de 1:60. Os FAMES foram comparados com o tempo de retenção dos padrões internos palmitato de metila (Sigma Aldrich, padrão

analítico, CAS 112-39-0), estearato de metila (Sigma Aldrich, padrão analítico, CAS 112-61-8), oleato de metila (Sigma Aldrich, padrão analítico, CAS 112-62-9), linoleato de metila (Sigma Aldrich, padrão analítico, CAS 112-63-0), e linolenato de metila (Sigma Aldrich, padrão analítico, CAS 301-00-8).

O teor de ácidos graxos livres, monoacilglicerol, diacilglicerol e triacilglicerol também foi determinado por GC-FID no mesmo equipamento de cromatografia a gás utilizado para a determinação do perfil dos ácidos graxos, todavia, utilizando uma coluna capilar ZB-5HT (15 m × 0,32 mm × 0,10 μm). Após ser solubilizado com uma mistura de hexano/heptano (3:1 v/v) o óleo extraído foi injetado diretamente no equipamento. O forno do GC operou sobre as seguintes condições: manutenção isotérmica a 70 °C por 1 minuto, sendo aquecido a uma taxa de 15 °C/min até 190 °C, para então aumentar a temperatura até 260 °C a uma taxa de 15 °C/min, finalmente aumentando até 380 °C a uma taxa de 20 °C/min e mantendo isotermicamente por 5 min. O gás hélio também foi utilizado como gás de arraste a 35 cm/s e razão de split de 1:60. Tricaprina (Sigma Aldrich, padrão analítico, CAS 621-71-6) e heptadecanoato de metila (Sigma Aldrich, padrão analítico, CAS 1731-92-6) foram utilizados como padrões internos para determinar o tempo de retenção dos componentes. Mais detalhes podem ser obtidos em Ribeiro et al. (2018) e um exemplo de cromatograma obtido está apresentado no Apêndice A.

3.3 ESTIMAÇÃO DE PARÂMETROS

O procedimento de estimação de parâmetros visa ajustar um modelo a dados experimentais minimizando uma função objetivo (S). A Eq. 34 representa os mínimos quadrados ponderados, a qual possui significado estatístico de erros randômicos experimentais distribuídos normalmente e assume-se a hipótese de experimento bem-feito e modelo perfeito (SCHWAAB; PINTO, 2007b).

$$S(\theta) = \sum_{i=1}^N \frac{(C_i - \hat{C}_i)^2}{\sigma_i^2} \quad (34)$$

Para variância dos erros de medição constante (σ), a Eq. 34 se transforma na soma dos erros quadráticos (Eq. 35) (SCHWAAB; PINTO, 2007b).

$$S(\theta) = \sum_{i=1}^N (C_i - \hat{C}_i)^2 \quad (35)$$

A otimização da função objetivo pode ser feita utilizando métodos heurísticos, de busca direta ou derivativos. No decorrer deste trabalho, majoritariamente, utilizaram-se procedimentos de otimização híbrida associando um método de otimização global a um método de otimização local, sendo conveniente utilizar uma heurística para obter bons chutes iniciais para os parâmetros e refinar o resultado utilizando algum método derivativo ou de busca direta.

Os métodos de busca direta são simples, robustos e fáceis de aplicar a problemas contendo duas variáveis, enquanto, para um número maior de variáveis, estes acabam não sendo tão eficazes (SILVEIRA, 2015).

Os métodos derivativos fazem uso de derivadas para determinar a direção de busca da otimização, sendo que a avaliação da função objetivo deve ser melhor que a anterior a cada iteração (SILVEIRA, 2015). A direção de busca precisa satisfazer a Eq. 36 para ser considerada ótima

$$\nabla^T f(x)s < 0 \quad (36)$$

Na qual deve ser obedecida a seguinte relação

$$\nabla^T f(x)s^k = |\nabla f(x^k)| |s^k| \cos \theta \quad (37)$$

Para $0 \leq \theta \leq 90^\circ$, a função irá aumentar e não terá nenhuma melhoria, sendo estritamente necessário obedecer a Eq. 38 para garantir a descida do gradiente da função, até que não mude mais no k -ésimo ponto sob determinada tolerância (SILVEIRA, 2015), conforme

$$x^{k+1} = x^k - \lambda^k \nabla f(x^k) \quad (38)$$

Os problemas de otimização podem ser divididos em convexos e não convexos. Fazem parte de problemas de otimização convexos aqueles em que a função objetivo e o conjunto factível de solução são ambos convexos (BERTSEKAS; NEDIC; OZDAGLAR, 2003). Qualquer mínimo local de problemas convexos é um mínimo global. Em contrapartida, a presença de mínimos locais é característica de problemas de otimização não convexos (MISTAKIDIS; STAVROULAKIS, 2013).

Para números elevados de parâmetros a serem estimados, os métodos derivativos e de busca direta podem ser pouco eficazes e robustos na otimização de problemas de mínimos quadrados não lineares, resultando na presença de mínimos locais. Visando solucionar este

problema, os métodos de otimização heurísticos podem ser utilizados para lidar com problemas não convexos de otimização.

O algoritmo de otimização por enxame de partículas (PSO, do inglês *Particle Swarm Optimization*) é uma meta-heurística muito eficaz na busca do mínimo de funções, os métodos de Newton, Levenberg-Marquardt, *Trust – Region – Reflective* e o algoritmo de ponto interior são algoritmos derivativos e o método simplex de Nelder-Mead é um método de busca direta, ambos são capazes de refinar o resultado obtido pelo enxame de partículas a fim de garantir o mínimo global da função objetivo.

O algoritmo de enxame de partículas foi proposto inicialmente com a finalidade de simular o comportamento coletivo de animais (EBERHART E KENNEDY, 1995). O algoritmo inicia com a geração de partículas aleatórias no espaço de busca, no qual cada partícula é caracterizada por um vetor no espaço multidimensional (EBERHART; KENNEDY, 1995; KHANESAR; TESHNEHLAB; SHOOREHDELI, 2007). Ao vetor da partícula está associado um vetor velocidade, que determinará o próximo movimento da partícula no espaço de busca, sendo atualizado conforme os termos de inércia da partícula, a atração da partícula ao melhor ponto associado ao grupo inteiro de partículas e a melhor posição que a partícula já obteve (EBERHART; KENNEDY, 1995; KHANESAR; TESHNEHLAB; SHOOREHDELI, 2007; SCHWAAB et al., 2008).

Um dos algoritmos derivativos mais famosos é o método de Newton, no qual o mínimo da função objetivo em x^k pode ser obtido somando o gradiente da função com a matriz Hessiana multiplicada pela distância de x entre $k-1$ até k , conforme (SILVEIRA, 2015)

$$\nabla f(x^k) + H(x^k)\Delta x^k = 0 \quad (39)$$

Da mesma forma, um dos algoritmos mais eficientes para estimação de parâmetros em problemas de mínimos quadrados não lineares é o algoritmo de Levenberg-Marquardt. Este método de otimização foi publicado primeiramente por Kenneth Levenberg e aperfeiçoado por Donald Marquardt. Dado um chute inicial, o algoritmo visa encontrar, a cada iteração, uma direção $d(\lambda)$ que seja solução do sistema linear

$$\left(J(x^k)^T J(x^k) + \lambda^k I \right) d(\lambda^k) = -J(x^k)^T R(x^k) \quad (40)$$

em que $J(x)$ é a matriz jacobiana de $R(x)$ e λ é uma constante denominada parâmetro de *damping* (SCHWERTNER, 2019).

O algoritmo *Trust – Region – Reflective* é um método iterativo, confiável e robusto capaz de resolver problemas não convexos que aborda as regiões de confiança do modelo, em que os cálculos são feitos sobre um subproblema da região de confiança no qual a função objetivo é minimizada (CONN; GOULD; TOINT, 2000; YUAN, 2000; YUAN, 2015). Neste sentido, um modelo acerca de um chute inicial x_0 é construído em uma sub-região contendo x_0 como uma representação fiel da função objetivo (CONN; GOULD; TOINT, 2000).

O método do ponto interior é capaz de resolver problemas convexos não lineares aplicando o método de Newton a uma sequência de problemas restritos de igualdade ou de versões modificadas da condição de Karush-Kuhn-Tucker (BOYD; VANDENBERGHE, 2003; COLEMAN; LI, 1994; COLEMAN; LI, 1996).

Finalmente, o método simplex de Nelder-Mead é um algoritmo de busca direta para minimização multidimensional irrestrita (LAGARIAS et al., 1998). O método busca minimizar uma função não linear escalar utilizando apenas valores de função, sem qualquer informação implícita ou explícita (LAGARIAS et al., 1998).

A implementação de métodos de otimização pode ser facilitada pelo uso de softwares como o MatLab®, o qual possui rotinas próprias para cada um dos métodos de otimização descritos anteriormente. A Tabela 3.2 apresenta algumas funções e rotinas disponíveis no software MatLab® que foram utilizadas no decorrer desta dissertação. Em resumo, a metodologia híbrida utilizando a função *particleswarm* seguida das rotinas *fmincon* e *fminsearch* foi utilizada na maioria dos problemas de estimação de parâmetros desta dissertação, enquanto a função *lsqnonlin* foi utilizada quando foi necessário obter ganho em performance.

Tabela 3. 2 - Rotinas disponíveis no software MatLab®.

Função	Descrição
<i>lsqnonlin</i>	Resolve problemas de mínimos quadrados não lineares utilizando os algoritmos <i>Trust – Region – Reflective</i> ou de Levenberg-Marquardt
<i>particleswarm</i>	Resolve problemas não lineares através da meta-heurística de enxame de partículas
<i>fmincon</i>	Encontra o mínimo da de problemas não lineares restritos utilizando o algoritmo de ponto interior
<i>fminsearch</i>	Encontra o mínimo de problemas não lineares irrestritos utilizando o método livre de derivadas simplex de Nelder-Mead

A significância dos parâmetros estimados é caracterizada pela matriz de covariâncias definida pela Eq. 41 (BARD, 1974; SCHWAAB; PINTO, 2007b; SCHWAAB; LEMOS; PINTO, 2008).

$$V_{\theta} = s^2 (B_i^T B_i)^{-1} \quad (41)$$

em que B é a matriz de sensibilidade das respostas do modelo, definida pela Eq. 42

$$B_i = \begin{bmatrix} \frac{\partial C_{1,i}}{\partial \theta_1} & \dots & \frac{\partial C_{p,i}}{\partial \theta_1} \\ \vdots & \ddots & \vdots \\ \frac{\partial C_{n,i}}{\partial \theta_1} & \dots & \frac{\partial C_{n,i}}{\partial \theta_p} \end{bmatrix} \quad (42)$$

Na hipótese de modelo perfeito, o resíduo da função objetivo pode ser utilizado para determinar a variância das observações experimentais s^2 (DRAPER; SMITH, 2014; SCHWAAB; PINTO, 2007b; SCHWAAB; LEMOS; PINTO, 2008)

$$s^2 = \frac{S(\hat{\theta})}{n-p} \quad (43)$$

em que n é o número de pontos experimentais e p o número de parâmetros estimados.

A diagonal principal da matriz de covariância contém a variância dos parâmetros estimados e os elementos fora da diagonal caracterizam a correlação entre os parâmetros (SCHWAAB; PINTO, 2007b; SCHWAAB; LEMOS; PINTO, 2008).

$$\rho_{ij} = \frac{v_{ij}}{\sqrt{v_{ii}v_{jj}}} \quad (44)$$

em que v_{ij} é o elemento ij da matriz de covariância dos parâmetros estimados.

Quanto mais próximo os valores absolutos de ρ_{ij} chegam de 1, mais os parâmetros se tornam mais correlacionados, de fato, se a correlação entre os parâmetros atinge valores superiores a 0,9, recomenda-se avaliar a necessidade da inserção do parâmetro (SCHWAAB; PINTO, 2007a).

O intervalo de confiança de máxima verossimilhança de cada parâmetro pode ser obtido por

$$\left[\theta_i - t_{n-p}^{1-\alpha/2} (s^2 v_{ii})^{1/2}, \theta_i + t_{n-p}^{1-\alpha/2} (s^2 v_{ii})^{1/2} \right] \quad (45)$$

em que $t_{n-p}^{1-\alpha/2}$ são os valores de t-Student definido para $n - p$ graus de liberdade a um nível de confiança $(1 - \alpha/2)$.

A tendência ou viés de um determinado parâmetro ocorre se houver diferença entre a média do conjunto de estimativas e o verdadeiro valor do parâmetro estimado. O parâmetro populacional θ é dito não viesado se a esperança (E) do estimador $\hat{\theta}$ for igual a θ (Eq. 46) (MORETTIN; BUSSAB, 2017).

$$E(\hat{\theta}) = \theta \quad (46)$$

Enquanto o viés do parâmetro é a própria diferença $E(\hat{\theta}) - \theta$.

Um algoritmo utilizado para redução do viés dos estimadores é a reamostragem bootstrap, conforme (DAVISON; HINKLEY, 1997; NICOLIN; ROSSONI; JORGE, 2016):

1. Baseado na Eq. 47

$$C(t) = \hat{C}(t) + \varepsilon \quad (47)$$

2. A nova amostra será

$$C(t^*) = \hat{C}(t^*) + \varepsilon^* \quad (48)$$

3. Realizar a estimação de parâmetros de mínimos quadrados não linear
4. Retornar ao passo 1 e repetir pelo menos 100 vezes
5. Fim

Para avaliar o desempenho estatístico dos modelos é usual utilizar o coeficiente de determinação (R^2), a raiz do erro quadrático médio ($RMSE$, do inglês *root mean squared error*) e a distribuição chi-quadrada (χ^2 , do inglês *chi-square distribution*). Para comparar modelos é comum utilizar o coeficiente de determinação ajustado (R_{adj}^2), o critério de informação Akaike (AIC) e o teste exato de Fisher.

4 SOYBEAN OIL EXTRACTION USING ETHYL ACETATE AND 1-BUTANOL: FROM SOLVENT SELECTION TO THERMODYNAMIC ASSESSMENT

Published in: Journal of Industrial and Engineering Chemistry, 113 (2022) 450-460.

DOI: 10.1016/j.jiec.2022.06.020

Henrique Gasparetto, Ana Luiza Barrachini Nunes, Fernanda de Castilhos, Nina Paula
Gonçalves Salau

Chemical Engineering Department, Federal University of Santa Maria, Brazil

ABSTRACT

Soybean oil extraction using two green solvents was investigated from solvent selection to thermodynamics: ethyl acetate and 1-butanol. The screening of the solvents was performed using the Hansen parameters and Infinite Dilution Activity Coefficient (IDAC) obtained through the CONductor-like Screening MOdels - Segment Activity Coefficient (COSMO-SAC) theory. The solvent selection was performed on ethyl acetate and 1-butanol in comparison with ethanol, a well-studied green solvent, and hexane, a non-renewable and industrially used solvent. The effects of temperature and solvent/solid ratio on the yield of soybean oil extraction were investigated through response surface methodology (RSM). The RSM obtained satisfactory statistical results, with R_{adj}^2 of 0.9958 for ethyl acetate and 0.9729 for 1-butanol. The kinetic of the extractions were evaluated using two different models: mass transfer kinetic and So and Macdonald. The last one obtained the best correlation to the data ($R^2 > 0.9964$). The thermodynamic assessment showed endothermic, and spontaneous processes for both solvents. 1-Butanol, ethyl acetate, and hexane have a better performance on the yield of soybean oil extraction than using ethanol; however, ethyl acetate is the best candidate to replace the industrial use of hexane due to its highest rate of soybean oil extraction at the process beginning.

Keywords: Green solvents; Kinetic models; RSM; COSMO-SAC; IDAC.

NOMENCLATURE

AIC - Akaike information criterion

ANOVA - Analysis of variance

COSMO-SAC - CONductor-like Screening MOdels - Segment Activity Coefficient

CRM - Carcinogenic, mutagenic, and reprotoxic

C_0 - Concentration of oil extracted at the equilibrium (g solute/g solid)

C_∞ - Solute concentration at the equilibrium (g solute/g solid)

C_∞^d - Final oil concentration due to diffusion (g solute/g solid)

C_∞^w - Final oil concentration due to the washing stage (g solute/g solid)

DM - Dry mass

FAME - Fatty acid methyl ester

FO - First-order terms

FTIR - Fourier transforms infrared radiation

GC-FID - Gas chromatography with flame ionization detector

IDAC - Infinite Dilution Activity Coefficient

I_{tox} - Acute Toxicity According to the Hodge and Sterner Scale

K - Equilibrium constant (-)

k_d - Kinetic coefficient for the diffusional stage (1/s)

k_w - Kinetic coefficient for the washing stage (1/s)

MTKM - Mass transfer kinetic model

MOPAC - Molecular orbital packages

n - Number of experimental data

p - Number of estimated parameters

PQ - Pure quadratic terms

r - Radius of the solubility sphere for the solute ($\text{MPa}^{1/2}$)

R - Universal gas constant (J/mol.K)

REACH - European Regulation on Registration, Evaluation, Authorization, and Restriction of Chemicals

RED - Relative energy difference (-)

RMSE - Root mean square error

RSM - Response surface methodology

R^2 - Coefficient of determination

R_{adj}^2 - Adjusted coefficient of determination

R_0 - Rate of extraction at the beginning of the process (g/g.s)

SMM - So and Macdonald model

T - Temperature (K)

TWI - Two-way interaction term

y_i - Observed values

\hat{y}_i - Predicted values

\bar{y}_i - Mean of observed values

Greek Symbols

γ_i^∞ - Infinite Dilution Activity Coefficient (-)

δ_d - Hansen parameter of dispersive energy (MPa^{1/2})

δ_h - Hansen parameter of hydrogen-bonding energy (MPa^{1/2})

δ_p - Hansen parameter of polar energy (MPa^{1/2})

ΔG^0 - Standard Gibbs free energy change (J/mol)

ΔH^0 - Standard enthalpy change (J/mol)

ΔS^0 - Standard entropy change (J/mol.K)

Φ - Objective function (-)

χ^2 - Chi-square distribution

4.1 INTRODUCTION

The limited reserve of petroleum oil associated with the deleterious effect of greenhouse gases has directional scientific attention to renewable resources. The academy is engaged all over the world to find potential resources that are renewable, non-toxic, non-carcinogenic, non-mutagenic, non-reprotoxic, and especially carbon dioxide neutral. On this basis, the green solvents are trying to replace the broad industrial use of hexane, which is non-renewable and contributes to huge carbon dioxide emissions. Also, hexane has recently been classified as a carcinogenic, mutagenic, and reprotoxic substance under the REACH regulation and may have restricted applications for industrial use in the future [1].

Soybean (*Glycine max* L.) oil is one of the main sources of lipids for food and biofuels production [2]. The oil extraction can be performed using a mechanical press or solvent extraction. In solvent extraction, the mixture of oil and solvent is evaporated to obtain the crude oil, which can be further refined to remove fatty acids, waxes, phospholipids, and

others, and the oilseed is desolventizing for use in food. The world production of soybean in 2021 was around 381.78 million metric tons, where Brazil occupied the first position in the ranking of the production of soybean in the world [3].

Several studies have been conducted to replace hexane in vegetable oil extraction including the use of ethanol [4,5], isopropanol [6], t-butanol, and butanol [7,8], methyl and ethyl acetate [9,10], 2-methyl tetrahydrofuran [2], α -pinene [11], and even alkyl esters [4]. According to Dagostin et al. [9], the increase in ethyl acetate as a co-solvent in mixtures with ethanol leads to an increase in the yield of soybean oil extraction. The isomers of butanol have been found in the literature as promising solvents for vegetable oil extraction [7,8]. While the study of Sharma et al. [8] concludes that the extraction of soybean oil using t-butanol by the method of three phase partitioning results in a higher yield of extraction than using ethanol, isopropanol, and n-propanol the investigation of Sendzikiene et al. [7] used 1-butanol as higher-order alcohol in a concomitant extraction/transesterification process of rapeseed oil. However, many studies have concluded that ethanol is a promising solvent in soybean oil extraction [4,5,12], the yield of extraction can be lower in comparison with higher-order alcohols, such as the 1-butanol, which may have a better yield of extraction due to its physicochemical properties, especially when evaluating polar, and hydrogen-bonding interactions [7].

The Hansen parameters and the COSMO theory have been used for the screening of solvents in vegetable oil extraction [13]. The Hansen parameters are based on experimental data [14] whereas the COSMO theory is an *ab initio* method to obtain thermodynamic properties [15]. The use of the COSMO theory is suitable to obtain the Infinite Dilution Activity Coefficient (IDAC), which describes the limiting case of a non-ideal behavior where a solute is infinitely dissolved in a solvent [16]. In this context, $\ln(IDAC)$ is often applied as a solvent selection tool [17].

Regarding the mathematical modeling of this process, the first and second-order power-law models in most cases do not represent the best fitting to the kinetic data. Thus, the mass transfer kinetic model (MTKM) and the So and Macdonald model (SMM) have been applied to overcome this issue [2,4,9,18,5]. MTKM is derived from the second law of Fick for diffusion [4] whilst SMM considers that the process occurs by two mechanisms: simple washing and diffusion. However, the mass transfer kinetic model may not be the best model to predict the experimental data because the boundary conditions used to obtain the analytical solution are constant, disregarding the external resistance to mass transfer [19] and this might be inaccurate. The MTKM is usually truncated at the first terms of the Taylor series [2,4,9]

which is insufficient to guarantee a small and stable variability for the effective diffusivity as it is shown by Nicolin et al. [20] for a similar diffusional process.

The thermodynamic analysis of vegetable oil extraction is performed after obtaining the distribution coefficient of oil between phases at each temperature [21]. This distribution coefficient, also referred as equilibrium constant, is finally applied to the van't Hoff equation to obtain the standard enthalpy, entropy, and Gibbs free energy change [4,9]. From the goodness of the thermodynamic fitting as well as through the value of the parameters it is possible to obtain inferences about the quality of the experimental data, besides understanding if the process is endothermic or exothermic, spontaneous, and random and irreversible.

The main subject of this study was to evaluate the extraction of soybean oil using two green solvents: ethyl acetate and 1-butanol. The experimental results were briefly compared with hexane, once this is the solvent industrially used, and ethanol, for being a promising solvent for soybean oil extraction, using the methodologies of solvent selection of Hansen and the prediction of $\ln(IDAC)$ using the COSMO-SAC theory. The best conditions of extraction were obtained using the response surface methodology and the kinetic extraction data of soybean oil was fitted by the models: MTKM and SMM. Finally, a thermodynamics analysis was performed.

4.2 MATERIALS AND METHODS

4.2.1 Material

The soybean flakes used were gently supplied by a Brazilian soybean processing company (Granol, RS, Brazil) and it was stored at - 12 °C until use. The solvents used for the extraction were ethyl acetate (Sigma Aldrich, purity $\geq 99.8\%$, CAS N° 141-78-6), 1-butanol (Neon, purity $\geq 99\%$, CAS N° 71-36-3), ethanol (Neon, purity $\geq 99.8\%$, CAS N° 64-17-5), and hexane (Êxodo científica, purity $\geq 99\%$, CAS N° 110-54-3).

4.2.2 Methods

4.2.2.1 Feedstock Characterization

The soybean flakes were characterized in terms of moisture [22], relative density, thickness, particle size distribution [23], and diameter of Sauter.

4.2.2.2 Screening of Solvent

The Hansen solubility parameters are widely used in industry to select solvents [24]. The solubility is defined in a three-dimensional space, in which the solutes and solvents are located. The solubility is better as closer the solute and solvent parameters are. The relative energy difference (*RED*) indicates the affinity of the solvent with the solute [25]. Eq. 1 describes the solute-solvent distance, where the terms correspond to the main molecular interactions, for dispersive (δ_d), polar (δ_p), and hydrogen-bonding (δ_h) contributions.

$$D = \sqrt{4(\delta_{d, \text{solvent}} - \delta_{d, \text{solute}})^2 + (\delta_{p, \text{solvent}} - \delta_{p, \text{solute}})^2 + (\delta_{h, \text{solvent}} - \delta_{h, \text{solute}})^2} \quad (1)$$

For the *RED* calculation is used Eq. 2.

$$RED = \frac{D}{r} \quad (2)$$

where r is the radius of the solubility sphere.

The CONductor-like Screening MOdel - Real Solvents (COSMO-RS) was the first *ab initio* method developed for the prediction of the Infinite Dilution Activity Coefficient (IDAC) using quantum mechanical calculation [26,15]. Succeeding, based on the COSMO-RS theory, the CONductor-like Screening MOdel - Segment Activity Coefficient (COSMO-SAC) was proposed by Lin and Sandler [27] as a model that uses quantum chemistry and considers the molecules as a collection of surface segments. Besides, the infinite dilution activity coefficient, also referred to γ_i^∞ , is a convenient manner to predict the behavior of liquid-liquid equilibrium as a solvent selection tool [17]. Based on this, this study has used the COSMO-SAC theory coupled with σ -profiles from molecular orbital packages (MOPAC) to obtain the $\ln(\gamma_i^\infty)$ using the open-source software JCOSMO developed by the research group: [28,29,30].

4.2.2.3 Experimental Procedure

4.2.2.3.1 Extraction of Soybean Oil

For the response surface methodology (RSM) study the extractions were performed in different soybean flakes: solvent mass ratios and temperatures until the equilibrium condition (reached around 120 minutes). The equilibrium condition was based on what was found in the

literature [4,9,31], the temperature range used was defined to cover the industrial condition [13] as well the solvent-to-solid ratios [12,32] used in the RSM study.

For the kinetic study with ethyl acetate and 1-butanol, the extractions were performed individually in tubes of 50 mL in a constant ratio of 1:7, for the temperatures of 298.15, 313.15, and 328.15 K for each solvent, in the following extraction times: 1, 2, 4, 8, 10, 15, 30, 60, 90 and 120 minutes. For comparison purposes, the same kinetic study was performed with hexane and ethanol for the temperature of 328.15 K. The experimental apparatus used in the RSM, and kinetic studies are presented in the supplementary material (Fig. S.1).

To obtain the maximum yield of soybean oil extraction for ethyl acetate, 1-butanol, and hexane, the Soxhlet extractions were performed, whereas around 5 grams of soya flakes were extracted with 150 mL of each solvent for 4 hours in a Soxhlet apparatus (MA491/6, Marconi, Brazil).

At the end of each extraction, the raffinate and the extract were separated, and the mass of soybean oil extracted was determined gravimetrically after complete evaporation of the solvent. The extractions were made at least in triplicate for the kinetic study and to obtain the maximum yield of soybean oil extraction through Soxhlet. The yield of each extraction was determined through Eq. 3 in respect to the dry mass (DM) of soybean flakes.

$$\text{Yield (g/g DM)} = \frac{\text{Mass of crude oil (g)}}{\text{Mass of dry soybean flakes (g)}} \quad (3)$$

The crude oils produced after 120 minutes of extraction at 328 K were used for determining the fatty acid profile and to obtain the FTIR spectra for each solvent because this is the temperature industrially used [13].

4.2.2.3.2 Determination of Fatty Acid Composition

The fatty acid profile of the soybean oil extracted for each solvent was determined by gas chromatography with flame ionization detector (GC-FID) after transmethylation of fatty acids using the methodology of Hartman and Lago (1973) [33] and a solution of ammonium chloride and sulfuric acid in methanol as the esterifying agent. The analyses were performed using an Rtx®-Wax capillary column (30 m × 0.25 mm × 0.25 μm) and helium as carrier gas at the velocity of 35 cm/s. The oven temperature program was operated as follows: the initial temperature at 333 K for 2 minutes, increasing at a rate of 10 K/min to 473 K and a rate of 5 K/min from 473 to 513 K, held isothermally as 513 K for 7 minutes. The injector and the

detector were operating at 523 K. FAMES were identified in comparison with the internal standards: methyl palmitate (Sigma Aldrich, analytical standard, CAS 112-39-0), methyl stearate (Sigma Aldrich, analytical standard, CAS 112-61-8), methyl oleate (Sigma Aldrich, analytical standard, CAS 112-62-9), methyl linoleate (Sigma Aldrich, analytical standard, CAS 112-63-0) and methyl linolenate (Sigma Aldrich, analytical standard, CAS 301-00-8). All the data were obtained at least in triplicate.

4.2.2.3.3 Component Analysis

The technique of Fourier transforms infrared radiation (FTIR) is one of the trending analytical tools in the analysis of edible oils [34]. This technique is useful because the intensities of the bands are proportional to the concentration of the compounds [35]. The equipment used for the analysis was an IRPrestige-21 from Shimadzu Ltda., equipped with a liquid detection accessory used for direct transmittance on a NaCl crystal from 500 to 4000 $1/\text{cm}$.

4.2.2.4 Modeling and Simulation

4.2.2.4.1 Response Surface Methodology

The response surface methodology was used to investigate the effect of temperature (x_1) and solvent/solid ratio (x_2) on the yield of oil extraction from the soybean flakes. For ethyl acetate and 1-butanol, the experimental design was created and evaluated in the software R Studio using the *rsm* library. The effects were evaluated through a central composite design ($\alpha = \sqrt{2}$) with triplicates at the central point. The statistical significance of the model was determined by the analysis of variance (ANOVA), Fischer and Student's tests, as well as the coefficient of determination (R^2) and the adjusted coefficient of determination (R_{adj}^2). Besides, the Shapiro-Wilk normality test was performed to verify the normality of the residues and the Breusch-Pagan test for heteroscedasticity.

4.2.2.4.2 Kinetic and Thermodynamic Modeling

The kinetics and thermodynamics parameters were fitted by nonlinear regression using the MatLab® built-in function *particleswarm* for Particle Swarming Optimization (PSO). This function was hybridized either with the built-in function *fmincon* for constrained

minimization or with the built-in function *fminsearch* for unconstrained minimization. The objective function used is given by Eq. 4.

$$\Phi = \sum_{i=1}^n (y_i - \hat{y}_i)^2 \quad (4)$$

where Φ is the sum of squares errors, y_i is the observed values, \hat{y}_i is the predicted values, and n is the number of experimental data.

To describe the experimental data two mathematical models were used: the mass transfer kinetic model (MTKM) and the model proposed by So and Macdonald [36], which is going to be referred to as SMM. The first (Eq. 5) is an approximation based on the first law of Fick for diffusion and it was used by Dagostin et al. [4], Dagostin et al. [9], and Claux et al. [2] to describe the oil extraction from soybean flakes.

$$C = C_{\infty} \left[1 - \frac{8}{\pi^2} \sum_{n=0}^{\infty} \frac{1}{(2n+1)^2} \exp\left(-\frac{(2n+1)^2 \pi^2 D t}{4L^2}\right) \right] \quad (5)$$

where C_{∞} is the concentration of the oil removed at the equilibrium (g/g DM), t is the extraction time (s), D is the diffusivity of the oil inside the particle (m²/s) and L is the half of the thickness of the slab (m).

The So and Macdonald model (represented by Eqs. 6 and 7) was also used by several authors [37,38,5] for modeling vegetable oil extractions.

$$C = C_{\infty}^w [1 - \exp(-k_w t)] + C_{\infty}^d [1 - \exp(-k_d t)] \quad (6)$$

$$C_{\infty} = C_{\infty}^w + C_{\infty}^d \quad (7)$$

where C_{∞}^w and C_{∞}^d are the concentrations of the oil removed at the equilibrium for the washing (g/g DM) and the diffusional (g/g DM) stages, respectively, k_w is the kinetic constant for the washing step (1/s) and k_d is the kinetic constant for the diffusion step (1/s).

As the knowledge of the rate of extraction at the industrial level is very important it was evaluated through Eq. 8, which describes the rate of the extraction at the beginning of the process [37].

$$R_0 = \left(\frac{dC}{dt} \right)_{t=0} \quad (8)$$

For the thermodynamics analysis, the distribution coefficient (K) for the solid-liquid extraction was calculated by Eq. 9.

$$K = \frac{C_{\infty}}{C_0 - C_{\infty}} \quad (9)$$

where C_0 is the initial concentration of oil in the soybean (g/g DM) and C_{∞} is the concentration of soybean oil removed in the equilibrium (g/g DM). The relation between K and the thermodynamics parameters of standard enthalpy change (ΔH^0) and standard entropy change (ΔS^0) is given by Eq. 10 and for the standard Gibbs free energy change (ΔG^0) by Eq. 11.

$$K = \exp\left(-\frac{\Delta H^0}{RT} + \frac{\Delta S^0}{R}\right) \quad (10)$$

$$\Delta G^0 = \Delta H^0 - T\Delta S^0 \quad (11)$$

4.2.2.5 Model Evaluation

The coefficient of determination (R^2), chi-square distribution (χ^2), and the root mean square error ($RMSE$) were used to assess the goodness of the fittings of the experimental data with the models.

$$R^2 = 1 - \frac{\sum_{i=1}^n (y_i - \hat{y}_i)^2}{\sum_{i=1}^n (y_i - \bar{y})^2} \quad (12)$$

$$\chi^2 = \sum_{i=1}^n \frac{(y_i - \hat{y}_i)^2}{y_i} \quad (13)$$

$$RMSE = \sqrt{\frac{1}{n} \sum_{i=1}^n (y_i - \hat{y}_i)^2} \quad (14)$$

To compare the models were used the Akaike information criterion (AIC) and the adjusted coefficient of determination (R_{adj}^2).

$$AIC = 2p + n \times \ln\left(\frac{\sum_{i=1}^n (y_i - \hat{y}_i)^2}{n}\right) \quad (15)$$

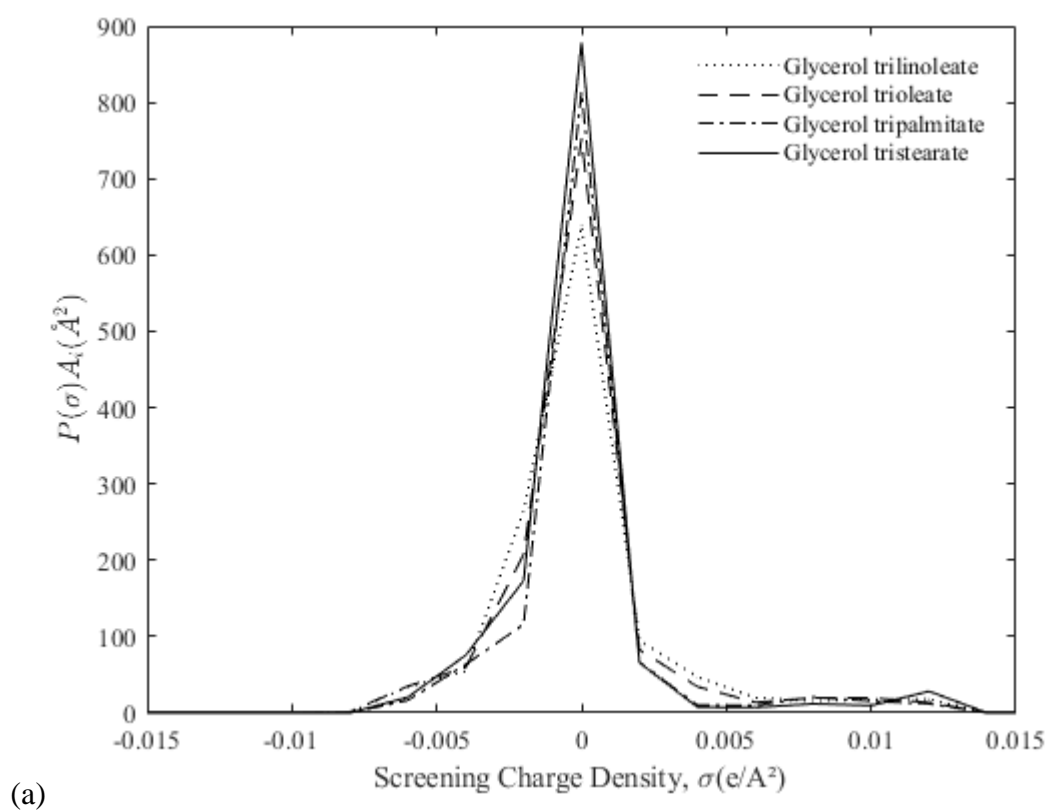
$$R_{adj}^2 = 1 - \frac{(n-1)(1-R^2)}{(n-p-1)} \quad (16)$$

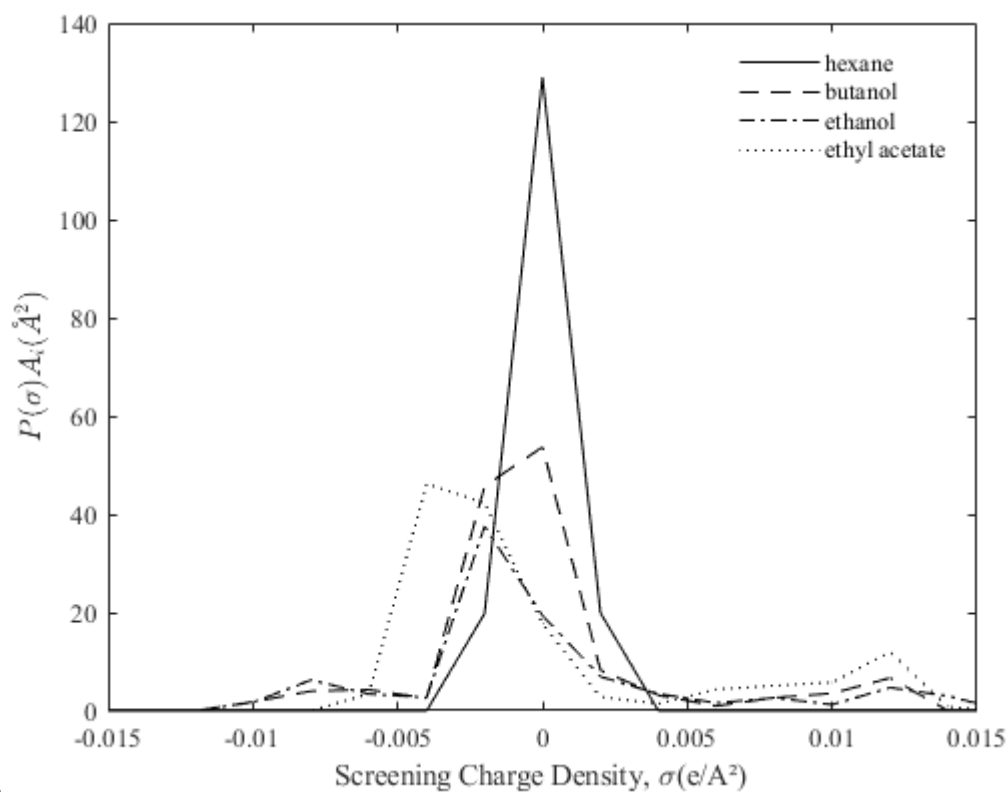
where \bar{y} is the mean of observed values, and p is the number of estimated parameters.

4.3 RESULTS AND DISCUSSION

4.3.1 Screening of Solvents

The sigma profiles of four triacylglycerols and each solvent obtained from JCOSMO are shown in Fig. 4.1.





(b) Figure 4. 1 - Sigma profiles obtained from JCOSMO using COSMO-SAC (MOPAC) theory for (a) the triacylglycerols and (b) the solvents.

It can be seen from Fig. 4.1 that there are no significant differences between the sigma profiles of the triacylglycerols as well among the solvents. Considering the similarity of the sigma profiles between hexane, ethyl acetate, 1-butanol, and ethanol it can be affirmed that all of them have similar attractive and repulsive forces over the triacylglycerols. However, the difference in their solubility might be due to the number of neutral segments and their molecular configuration [39]. By the sigma-profile analysis, the more stable system is created with hexane due to its total neutral segments followed by 1-butanol once it has the biggest molecular structure with well-established regions of hydrogen-bond donation and acceptance.

The analysis of the solubility in terms of the sigma-profile plays the role in that “like dissolves like”. It shall be expected that solvents with higher charge density in the neutral region would be more prone to have a higher affinity with the triacylglycerols; besides solvents that present small positive induced charge peaks due to the occurrence of double bonds in the oxygens of the respective fatty acids [40]. In fact, the most important evidence obtained from the sigma-profile is the similarity between the screening charge density of the pair solute-solvent. As it was previously mentioned, in this case the similarity is mostly evidenced for the triacylglycerol-hexane mixture, which is corroborated by the calculation of

the infinite dilution activity coefficient by this method.

The *RED* calculations for hexane, ethyl acetate, 1-butanol, and ethanol and $\ln(IDAC)$ obtained using the JCOSMO are shown in Table 4.1, where, for the soybean oil, the radius of the solubility sphere used was $9.57 \text{ MPa}^{1/2}$, and $\delta_d = 15.33$, $\delta_p = 3.77$ and $\delta_h = 6.87$ [14]. The other parameters for the solvents were obtained from Benazzouz et al. [41]. Table 4.1 also presents some interesting properties of these solvents. Analyzing the *RED* from Table 4.1 it can be seen a lower unbalance of energy for the mixture of ethyl acetate/soybean oil than using hexane, 1-butanol, and ethanol, respectively. However, the $\ln(\gamma_i^\infty)$ have shown that the affinity of hexane with different triacylglycerols is higher than using 1-butanol, ethyl acetate, and ethanol, respectively. 1-Butanol has a higher boiling point as well as a higher viscosity, whereas its higher viscosity can lower the rate of extraction. The green solvents have I_{tox} between 5-4 and the hexane has the best index of acute toxicity, however, it is the only one included in the list of carcinogenic, mutagenic, and reprotoxic substances for having neurotoxic and reprotoxic effects. Not less important, the affinity with the organic phase is higher ($\log(P_{o/w}) > 0$) for hexane, 1-butanol, and ethyl acetate in comparison to what is found for ethanol ($\log(P_{o/w}) < 0$), which is corroborated by its partial miscibility with vegetable oil [42].

Table 4. 1 - *RED* and $\ln(IDAC)$ calculations for hexane, ethyl acetate, and 1-butanol.

Property	Hexane	Ethyl acetate	1-butanol	Ethanol
<i>RED</i> ^a	0.82	0.19	0.96	1.41
$\ln(\gamma_i^\infty)$ COSMO-SAC ^b	0.53	4.54	0.84	5.90
Boiling point (K)	341.15 [41]	350.15 [41]	391.15 [41]	352.15 [41]
$\log(P_{o/w})$ ^c	3.90	0.73	0.88	-0.31
Viscosity (mPa.s)				
298.15 K	0.30 [43]	0.43 [43]	2.60 [45]	1.23 [47]
313.15 K	0.27 [43]	0.37 [43]	1.80 [45]	0.91 [47]
328.15 K	0.24 [46]	0.30 [44]	1.43 [45]	0.65 [47]
I_{tox}	6 [41]	5 [41]	4 [41]	5 [41]
CRM effects	neurotoxic and reprotoxic	no CRM effect	no CRM effect	no CRM effect

^afor soybean oil, independent of temperature; ^baverage calculation, at 328.15 K, for the following triacylglycerols: glycerol tristearate, glycerol trioleate, glycerol tripalmitate, and glycerol trilinoleate; ^cobtained from PubChem platform

4.3.2 Soybean and Soybean Oil Characterization

The soybean slabs had a moisture content of 10.70 ± 0.2 wt%, an average thickness of 0.37 ± 0.09 mm, and an average diameter of Sauter of 0.1033 mm. Its relative density was about 1.1508 ± 0.0372 and the samples used had the following diameter distribution: ∞ mesh

(0.56 wt%), 16 mesh (2.68 wt%), 14 mesh (6.42 wt%), 10 mesh (5.51 wt%), 9 mesh (5.01 wt%), 8 mesh (45.12 wt%) and 4 mesh (34.70 wt%).

The yields of the Soxhlet extractions are within 24.28 and 27.86 g/g DM, which is following the average content of lipids in the soybean seeds of 20% [2,48,5]. The high yield of the Soxhlet extraction using 1-butanol is justified due to its high boiling point once the Soxhlet extraction shall operate at the boiling point of the solvent and the temperature is responsible for increasing the efficiency of the extraction [49].

As can be seen in Table 4.2, the three crude oils have similar fatty acid profiles ($p > 0.05$) with mainly palmitic acid (C16:0), stearic acid (C18:0), oleic acid (C18:1), linoleic acid (C18:2), and linolenic acid (C18:3), which agrees with the literature [50,5].

Table 4. 2 - Extraction yields and fatty acids profile of the soybean oil extracted with hexane, ethyl acetate, and 1-butanol.

Items	Hexane	Ethyl acetate	1-Butanol
Extraction yield (g/g DM)	24.28 ± 1.58	25.33 ± 0.44	27.86 ± 1.14
Fatty acid (relative %)			
C16:0, palmitic acid	10.84 ± 0.12	10.86 ± 0.14	11.08 ± 0.08
C18:0, stearic acid	3.81 ± 0.09	3.88 ± 0.01	3.78 ± 0.05
C18:1, oleic acid	23.18 ± 0.89	22.14 ± 0.26	21.73 ± 0.35
C18:2, linoleic acid	55.07 ± 0.84	55.66 ± 0.20	56.43 ± 0.48
C18:3, linolenic acid	5.27 ± 0.09	5.79 ± 0.05	5.53 ± 0.21
Others	1.83 ± 0.26	1.67 ± 0.04	1.45 ± 0.45

The FTIR results of the oils extracted with hexane, ethyl acetate, and 1-butanol are shown in Fig. 4.2.

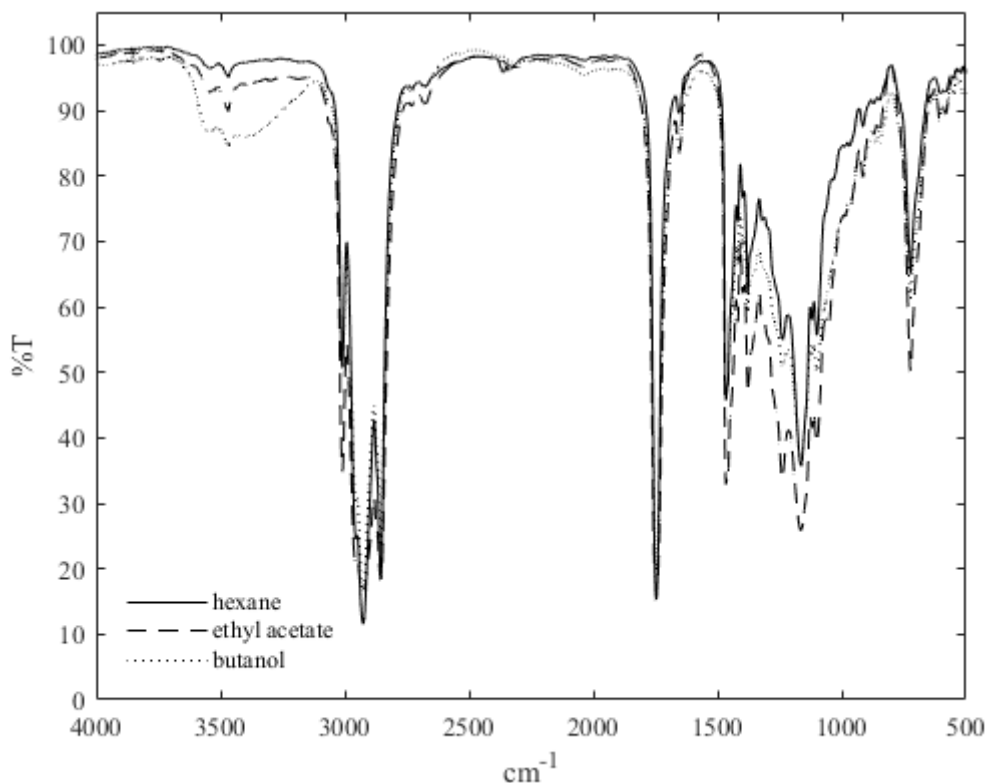


Figure 4. 2 - FTIR spectra of soybean oil extracted with hexane, ethyl acetate, and 1-butanol in the region of 4500 to 500 1/cm.

The spectra are dominated by some peaks at 3467, 3009, 2926, 2855, 1746, 1655, 1466, 1377, 1164 and 723 1/cm. The absorbance results for the region of 3467 1/cm are designated to the O-H stretching vibration of hydroperoxide. The band around 3009 1/cm is due to the C-H stretching vibration of the cis-double bond. Oils with a high proportion of linolenic and linoleic acyl groups show higher frequency data at this point than those with a high proportion of oleic [35]. The bands at 2926 and 2855 1/cm are due to aliphatic CH_2 stretching vibrations, asymmetric and symmetric, respectively. According to that, it can be assumed that the oils are rich in polyunsaturated acyl groups due to the high value of the frequency of those bands. The value of 1655 1/cm is assigned to the C=C stretching vibration of cis olefins. The peak at 1746 1/cm is from C=O stretching vibrations of aldehydes and ketones. Also, the peaks at 1466 and 1377 1/cm arise from CH_2 and CH_3 scissoring vibration of ethers. The peak at 1164 1/cm is associated with C-O stretching vibration, while the last peak (723 1/cm) arose from CH_2 rocking mode. In general, the typical transmittance bands of triacylglycerols in the infrared are assigned to C=O stretching vibrations (1746 1/cm) and C-O stretching vibrations (1164 1/cm). The aliphatic CH_2 stretching vibrations asymmetric and

symmetric (2926 and 2855 1/cm) correspond to the fatty acids from the triacylglycerols. Those spectra observations are supported by the results of other studies [51,35].

4.3.3 RSM Results

In Table 4.3, the planning matrix is presented along with the experimental data for both of the solvents. Analyzing the Shapiro-Wilk normality test for ethyl acetate there was no indication of non-normality for the residues once the p-value was equal to 0.5652 and it shall be greater than the alpha level (0.05 for 95% of significance) for the non-rejection of the null hypothesis (that the population is normally distributed). At the same time, it was possible to verify simultaneous and individual homoscedasticity for the variables, in other words, the variance of the errors is constant. It may be highlighted that the central points for each solvent were very similar, indicating the reliability of the results.

Table 4. 3 - Summary of the experiment design at equilibrium condition (120 minutes).

Run	Factors				Ethyl acetate	1-Butanol
	Temperature (K)	Solvent/solid mass ratio	x_1	x_2	Yield (g/g DM)	Yield (g/g DM)
1	298	2.5	-1	-1	0.1079	0.1360
2	328	2.5	1	-1	0.1189	0.1541
3	298	7.5	-1	1	0.1646	0.1798
4	328	7.5	1	1	0.2094	0.2069
5	291.79	5	$-\sqrt{2}$	0	0.1502	0.1647
6	334.21	5	$\sqrt{2}$	0	0.1883	0.2058
7	313	1.46	0	$-\sqrt{2}$	0.0708	0.1311
8	313	8.54	0	$\sqrt{2}$	0.1818	0.1991
9 ^a	313	5	0	0	0.1786	0.1594
10 ^a	313	5	0	0	0.1759	0.1610
11 ^a	313	5	0	0	0.1809	0.1647

^aCentral point

Table 4. 4 - ANOVA for the yield of extraction using ethyl acetate.

	DF	Sum of squares	Mean of squares	F-value	p-value	
FO (x_1, x_2)	2	0.0131	0.0065	902.04	4.02×10^{-7}	significant
PQ (x_1^2, x_2^2)	2	0.0037	0.0018	258.51	8.98×10^{-6}	significant
TWI ($x_1: x_2$)	1	0.0003	0.0003	39.31	0.0015	significant
Residuals	5	3.62×10^{-5}	7.2×10^{-6}			
Lack of fit	3	2.40×10^{-5}	8×10^{-6}	1.32	0.4594	not significant
Pure error	2	1.22×10^{-5}	0.61×10^{-5}			

where DF denotes degree of freedom; $R^2 = 0.9979$; $R_{adj}^2 = 0.9958$

The model adjusted for ethyl acetate is presented in Eq. 17, where x_1 and x_2 are the coded variables. The simplified analysis of variance (ANOVA) is presented in Table 4.4

considering FO as the first-order terms, PQ as the pure quadratic terms, and TWI as the two-way interaction term.

$$\text{Yield (g / g DM)} = 0.1785 + 0.0137x_1 + 0.038x_2 - 0.004x_1^2 - 0.0255x_2^2 + 0.0084x_1x_2 \quad (17)$$

For ethyl acetate, the adjusted model has a high value of R^2 and R_{adj}^2 . The p-values for the FO, PQ, and TWI show that these terms are significant. Comparing the F calculated with those tabulated ($F = 6.6079$ and $F = 5.7861$) it can be affirmed that all the terms have predictive importance. In the same way, the lack of fit is not significant because the p-value is higher than the significance and the F calculated is less than the tabulated ($F = 19.1643$), so the hypothesis of lack of fit is rejected.

Table 4. 5 - Analysis of variance for the yield of extraction using 1-butanol.

	DF	Sum of squares	Mean of squares	F-value	p-value	
FO (x_1, x_2)	2	0.0059	0.0029	163.60	1.33×10^{-6}	significant
PQ (x_1)	1	0.0006	0.0006	35.24	5.78×10^{-4}	significant
Residuals	7	0.0001	1.82×10^{-5}			
Lack of fit	5	0.0001	2.26×10^{-5}	2.96	0.2713	not significant
Pure error	2	1.52×10^{-5}	7.6×10^{-6}			

where DF denotes degree of freedom; $R^2 = 0.9811$; $R_{adj}^2 = 0.9729$

The awesomeness of using the response surface methodology for modeling the extraction of soybean oil using ethyl acetate was also verified for the soybean oil extractions with 1-butanol. The significance of the model was verified for the first-order parameters and temperature as the pure quadratic term. Disregarding the second-order term for solvent/solid ratio and the two-way interaction parameters that it was possible to verify the normality of the residues (p-value = 0.8355) and simultaneous and individual homoscedasticity for the variables. Thus, the model is presented in Eq. 18, where x_1 and x_2 are the coded variables, and the simplified ANOVA is in Table 4.5.

$$\text{Yield (g / g DM)} = 0.1619 + 0.0129x_1 + 0.0241x_2 + 0.0102x_1^2 \quad (18)$$

As can be seen in Table 4.5 the FO and the PQ parameters were significant and the F calculated was higher than the tabulated, $F = 4.737$ and $F = 5.591$. The lack of fit was not significant, and the F calculated was less than the tabulated, $F = 19.296$, indicating the rejection of the lack of fit hypothesis. Still, the adjusted R^2 was 0.9729, indicating that only

2.71% of the variation in the yield of extraction cannot be explained by this model. The correlation between the experimental and predicted values of oil yields for both of the solvents is shown in Fig. 4.3, whereas it can be seen lower deviations from the experimental points to the straight line for both solvents, corroborating its statistical results previously presented.

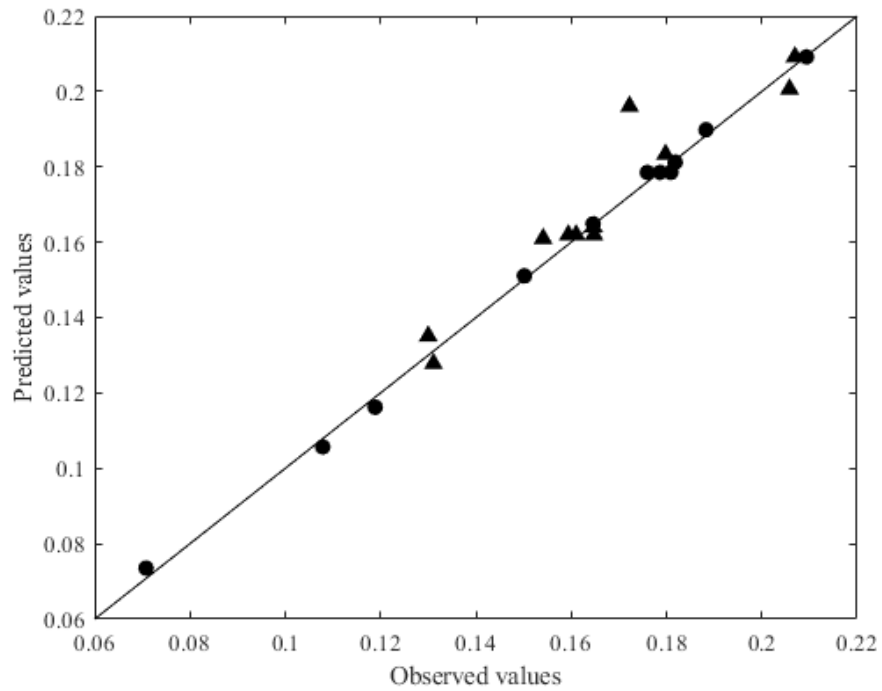
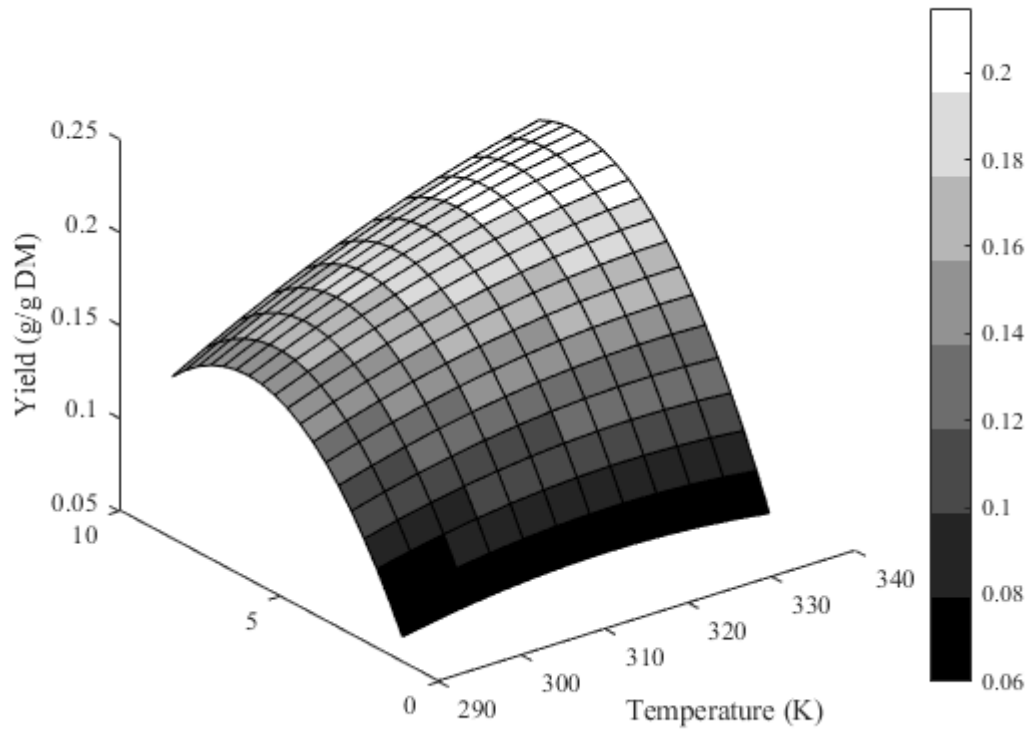
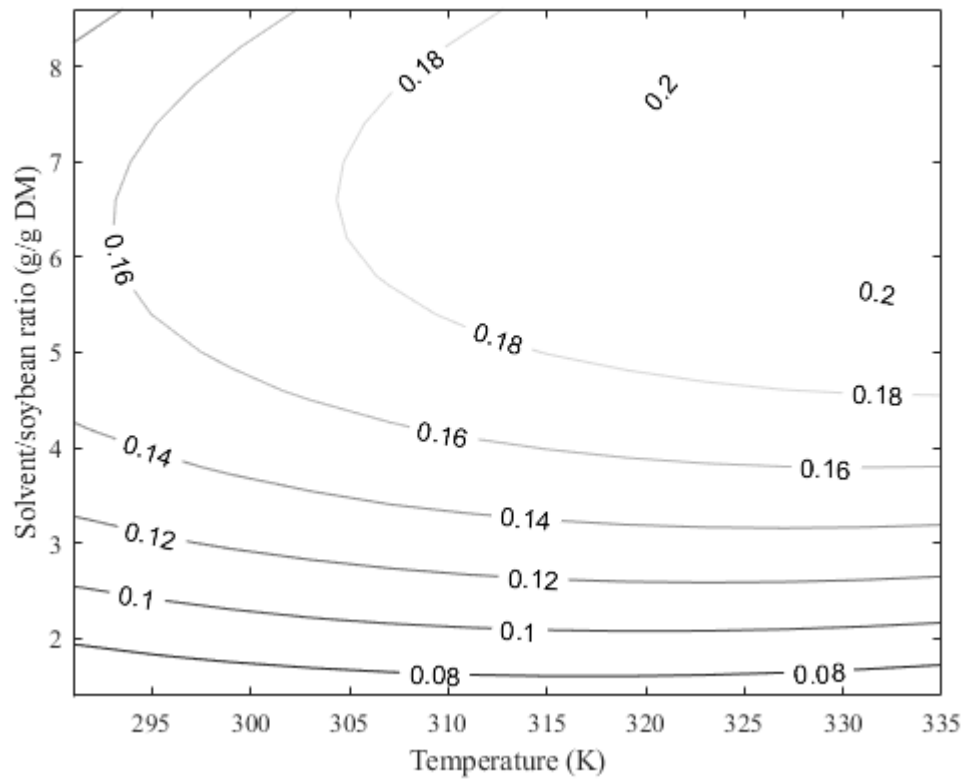


Figure 4. 3 - Observed vs. Predicted values for the extraction of soybean oil using ethyl acetate (●) and 1-butanol (▲).

The contour and perspective plot for each model are shown in Figs. 4.4 and 4.5, for each solvent. It can be seen that the use of both solvents has similar perspective plots once the yield of extraction tends to increase with both increases in temperature and solvent/solid ratio. For the kinetic study, it was chosen to use a solvent/solid ratio of 7 for both solvents based on the RSM results.

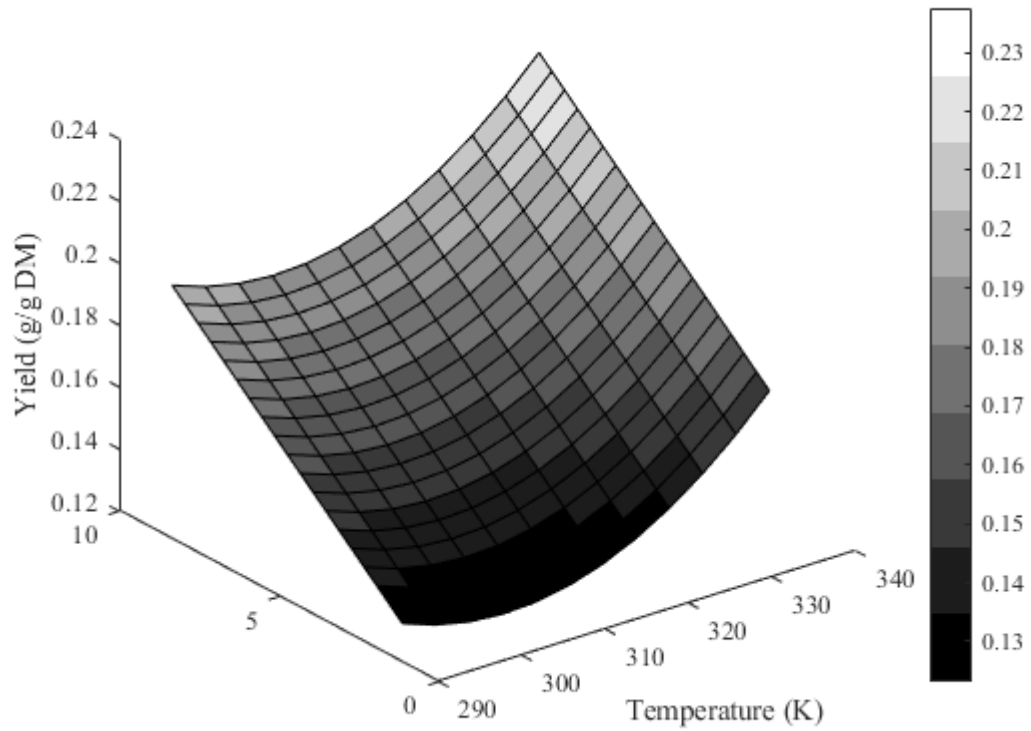


(a) Solvent/soybean ratio (g/g)

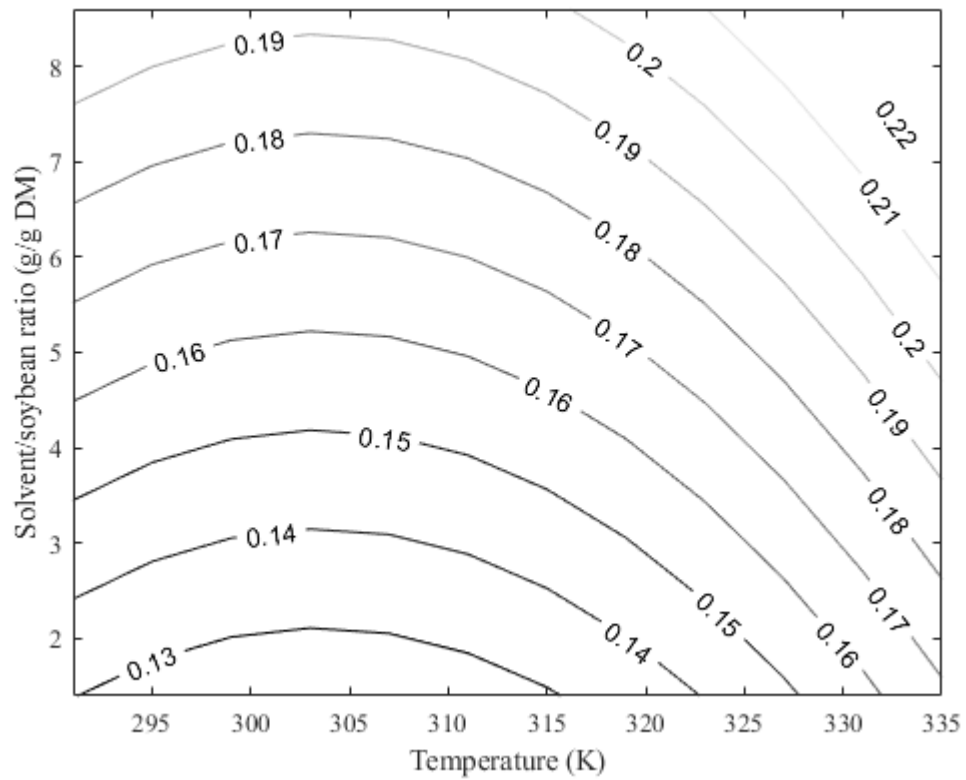


(b)

Figure 4. 4 - (a) Perspective and (b) contour plot for the yield of extraction using ethyl acetate.



(a) Solvent/soybean ratio (g/g)



(b)

Figure 4. 5 - (a) Perspective and (b) contour plot for the yield of extraction using 1-butanol.

4.3.4 Kinetic Modeling and Mass Transfer Analysis

The kinetic parameters are presented in Table 4.6 for the mass transfer kinetic model and in Table 4.7 for the So and Macdonald model. Firstly, the stability of the parameters regarding the number of terms in the Taylor series was analyzed for both of the solvents. The results are detailed in the supplementary material (Figs. S.2 and S.3) and are according to what was stated by Nicolin et al. [20]. The estimated parameters are not independent of the number of terms, however, general stability at the 100th term is observed, and this truncation was used to perform the non-linear regression. For the MTKM parameters, it is possible to see that the equilibrium coefficients are very similar for both solvents. However, the highest difference is in the D/L^2 , where the extractions using ethyl acetate have the highest values for this parameter.

Table 4. 6 - Estimated parameters for the mass transfer kinetic model.

Solvent	T (K)	Parameters	R^2	χ^2	$RMSE$
Ethyl acetate	298.15	$C_\infty = 0.1805$ $D/L^2 = 5.12 \times 10^{-4}$ 1/s	0.9780	0.0043	0.0012
	313.15	$C_\infty = 0.1913$ $D/L^2 = 8.98 \times 10^{-4}$ 1/s	0.9676	0.0064	0.0029
	328.15	$C_\infty = 0.1981$ $D/L^2 = 1.19 \times 10^{-3}$ 1/s	0.9730	0.0056	0.0038
1-butanol	298.15	$C_\infty = 0.1740$ $D/L^2 = 1.82 \times 10^{-4}$ 1/s	0.9927	0.0014	1.20×10^{-3}
	313.15	$C_\infty = 0.1907$ $D/L^2 = 2.15 \times 10^{-4}$ 1/s	0.9848	0.0031	0.0021
	328.15	$C_\infty = 0.2177$ $D/L^2 = 2.65 \times 10^{-4}$ 1/s	0.9972	7.27×10^{-4}	0.0011

The same happens when using the So and Macdonald model. The equilibrium constants are very similar even when compared with the MTKM model. However, the SMM considers one extra step beyond diffusion, the washing. It can be noticed that the highest gain in the extraction is due to diffusion once the equilibrium constant for the diffusional stage is usually higher than for washing. This indicates that the process occurs mainly through diffusion, although the washing is also important due to the gain of performance when evaluating the statistical parameters.

Table 4. 7 - Estimated parameters for the So and Macdonald model.

Solvent	T (K)	Parameters	R^2	χ^2	RMSE
Ethyl acetate	298.15	$C_{\infty}^w = 0.0587$	0.9989	1.50×10^{-4}	1.19×10^{-4}
		$k_w = 0.0230$ 1/s			
		$C_{\infty}^d = 0.1261$			
	313.15	$k_d = 8.26 \times 10^{-4}$ 1/s	0.9964	7.21×10^{-4}	9.53×10^{-4}
		$C_{\infty} = 0.1848$			
		$C_{\infty}^w = 0.0846$			
	328.15	$k_w = 0.0198$ 1/s	0.9972	5.85×10^{-4}	7.71×10^{-4}
		$C_{\infty}^d = 0.1131$			
		$k_d = 1.09 \times 10^{-3}$ 1/s			
1-butanol	298.15	$C_{\infty} = 0.1977$	0.9980	3.77×10^{-4}	1.56×10^{-4}
		$C_{\infty}^w = 0.1246$			
		$k_w = 0.0112$ 1/s			
	313.15	$C_{\infty}^d = 0.0833$	0.9985	3.12×10^{-4}	6.06×10^{-5}
		$k_d = 8.43 \times 10^{-4}$ 1/s			
		$C_{\infty} = 0.2079$			
	328.15	$C_{\infty}^w = 0.0429$	0.9974	6.88×10^{-4}	1.30×10^{-3}
		$k_w = 0.0097$ 1/s			
		$C_{\infty}^d = 0.1433$			
313.15	$k_d = 3.18 \times 10^{-4}$ 1/s	0.9985	3.12×10^{-4}	6.06×10^{-5}	
	$C_{\infty} = 0.1862$				
	$C_{\infty}^w = 0.0527$				
328.15	$k_w = 0.0119$ 1/s	0.9974	6.88×10^{-4}	1.30×10^{-3}	
	$C_{\infty}^d = 0.1544$				
	$k_d = 3.31 \times 10^{-4}$ 1/s				
328.15	$C_{\infty} = 0.2071$	0.9974	6.88×10^{-4}	1.30×10^{-3}	
	$C_{\infty}^w = 0.0355$				
	$k_w = 0.0226$ 1/s				
328.15	$C_{\infty}^d = 0.1815$	0.9974	6.88×10^{-4}	1.30×10^{-3}	
	$k_d = 6.85 \times 10^{-4}$ 1/s				
	$C_{\infty} = 0.2170$				

In general, both of the models presented high values for the coefficient of determination, although the best was the So and Macdonald model because it has the bests R^2 and the lowest χ^2 and $RMSE$. For the MTKM the values of R_{adj}^2 were between 0.9676 and 0.9972 and the AIC were between -94.80 to -117.75. While for SMM the values of R_{adj}^2 were between 0.9963 and 0.9989 and the AIC were between -113.54 and -132.25, confirming the best correlation to the data. The kinetic curves with the experimental data and the simulation of the models can be seen in Fig. 4.6.

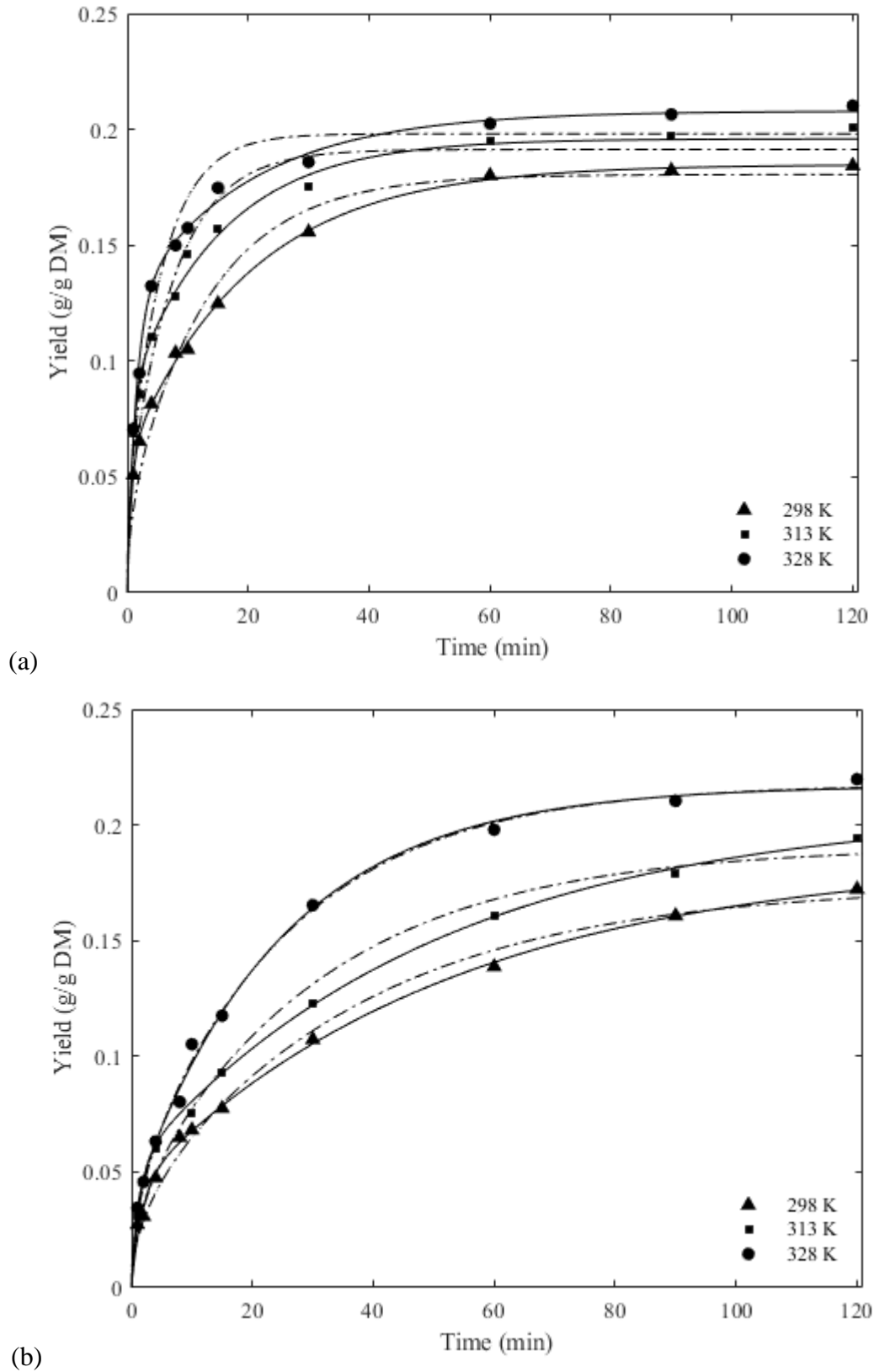


Figure 4. 6 - Experimental and predicted yields of extraction for the mass transfer kinetic model (dash-dotted line) and the So and Macdonald model (continuous line) for (a) ethyl acetate and (b) 1-butanol at a solvent-to-soybean ratio of 7 and different temperatures.

The R_0 was obtained for the kinetic curves at 328.15 K for ethyl acetate, 1-butanol, hexane, and ethanol, after its parameter estimation using the So and Macdonald model. The kinetic curves and the rates of extraction are presented in Figs. 4.7 and 4.8.

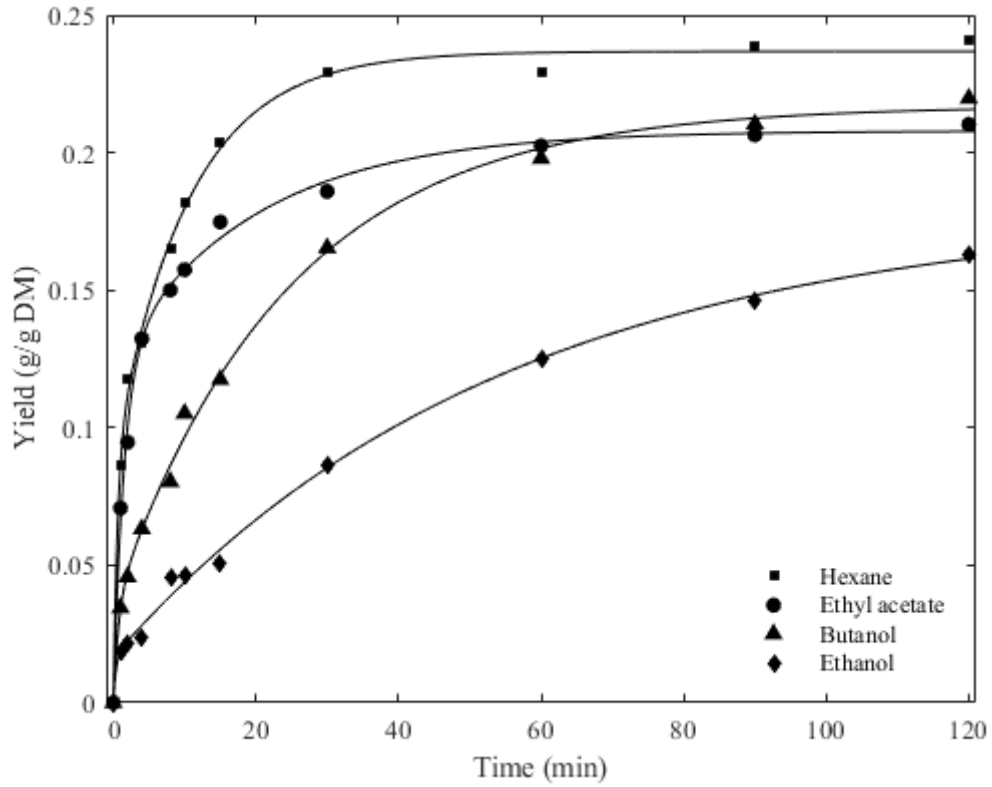


Figure 4. 7 - Experimental and predicted yields of extraction for ethyl acetate, 1-butanol, ethanol, and hexane at 328.15 K using the solvent-to-solid ratio of 7.

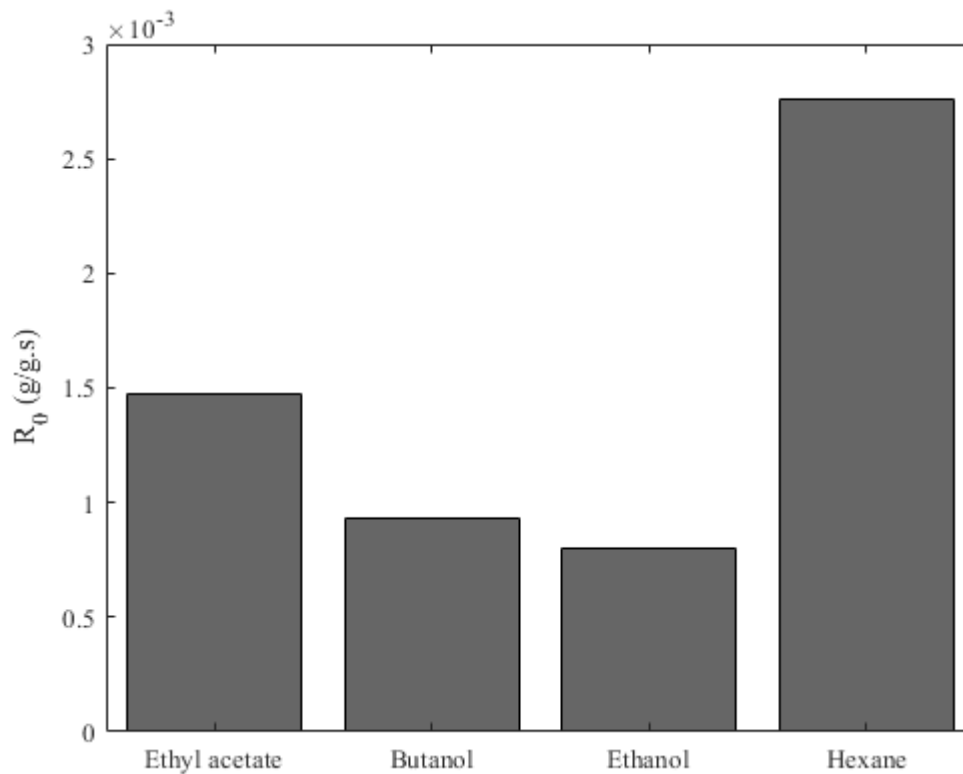


Figure 4. 8 - Rate of extraction at the beginning of the process at 328.15 K for each solvent using the solvent-to-solid ratio of 7.

Evaluating Figs. 4.7 and 4.8 it can be seen that hexane and ethyl acetate have similar kinetic curves; however, hexane achieves a higher yield of soybean oil extraction, and the rate at the beginning of the process has a big difference. This difference may be justified due to its viscosity, once hexane has the lowest viscosity of the solvents used in this study. It shall be highlighted that the solubility of a solute in a solvent is not affected by the viscosity of the solvent. Notwithstanding, the viscosity of the solvent directly affects the extraction rate once the migration of the solute in the medium depends on the diffusion coefficient, which is highly dependent on viscosity [52,53]. Besides, the extraction rate also is dependent on the highest possible solute concentration in the solvent at determined conditions of temperature and pressure. These two considerations can be found in more detail in Seager et al. (2018) [54]. As a general conclusion, the highest initial extraction rate for hexane is corroborated by its lower viscosity and best solubility parameters (see Table 4.1). Although, the higher theoretical solubility parameter for 1-butanol is counterbalanced through its viscosity, which is the highest. Ethanol has the worst solubilization capacity and high viscosity, and ethyl acetate has the closest viscosity to hexane, however, its solubilization of soybean oil might not be considered similar to hexane.

It is interesting to see that 1-butanol has a better solubility effect than using ethanol, which was in accordance with its Hansen parameters and $\ln(IDAC)$ values. However, 1-butanol has a smaller rate of extraction than hexane and ethyl acetate. Again, this can be justified due to its higher viscosity, which is higher even when compared to ethanol. At the end of the extraction (120 minutes), it can be seen that hexane has the highest yield of extraction, followed by 1-butanol, ethyl acetate, and ethanol. From the techniques of solvent selection used, the infinite dilution activity coefficient obtained using the COSMO-SAC (MOPAC) theory correctly described the behavior of using all the solvents once $\gamma_{Hexane}^{\infty} < \gamma_{1-Butanol}^{\infty} < \gamma_{Ethyl\ acetate}^{\infty} < \gamma_{Ethanol}^{\infty}$. However, the Hansen parameters could not describe this behavior accurately.

In general, 1-butanol has a better yield of extraction than using ethanol, although its high viscosity might be related to a decrease in the rate of extraction. Also, the high boiling point of 1-butanol can hinder the direct substitution of hexane. Ethyl acetate has a higher R_0 and a lower boiling point than 1-butanol, being a good candidate for the replacement of the industrial use of hexane in soybean oil extractions.

The estimated parameters for the MTKM and the SMM are according to what was found in the literature. Table 4.8 presents a data compilation of parameters available in the literature for extractions with different solvents and temperatures.

Table 4. 8 - Diffusivity coefficients and mass transfer parameters for So and Macdonald model for soybean extraction reported by several authors.

Soybean	D (m ² /s)	k_w (1/s)	k_d (1/s)	Solvent	T (K)	Reference
Pellets	1.84×10 ⁻⁸ to 2.65×10 ⁻⁸	-	-	Trichloroethylene	328	[55]
Collets	4.42×10 ⁻¹¹ to 5.36×10 ⁻¹¹	4.83×10 ⁻³ to 5.83×10 ⁻³	3.33×10 ⁻⁴ to 5×10 ⁻⁴	Ethanol 99%	313, 323, 333	[5]
Collets	3.61×10 ⁻¹¹ to 4.27×10 ⁻¹¹	4.67×10 ⁻³ to 0.01	3.33×10 ⁻⁴ to 6.67×10 ⁻⁴	Ethanol 94%	313, 323, 333	[5]
Flakes	8.95×10 ⁻¹⁰ to 1.15×10 ⁻⁸	-	-	Hexane	298, 328	[2]
Flakes	1.88×10 ⁻⁹ to 1.35×10 ⁻⁸	-	-	2-MeTHF ^a	298, 328, 338	[2]
Flakes	1.17×10 ⁻⁹ to 1.09×10 ⁻⁸	-	-	2-MeTHF ^a 95.5%	298, 328, 338	[2]
Flakes	5.98×10 ⁻¹⁰ to 9.04×10 ⁻¹⁰	-	-	Ethanol	298, 313, 328	[4]
Flakes	5.44×10 ⁻¹⁰ to 7.69×10 ⁻¹⁰	-	-	Ethanol with biodiesel (5%)	298, 313, 328	[4]
Flakes	3.87×10 ⁻¹⁰ to 1.06×10 ⁻⁹	-	-	Ethanol with biodiesel (10%)	298, 313, 328	[4]
Flakes	4.87×10 ⁻¹⁰ to 1.21×10 ⁻⁹	-	-	Ethanol with ethyl acetate (5%)	298, 313, 328	[9]
Flakes	4.17×10 ⁻¹⁰ to 1.45×10 ⁻⁹	-	-	Ethanol with ethyl acetate (10%)	298, 313, 328	[9]
Flakes	1.14×10 ⁻¹¹ to 2.36×10 ⁻¹¹	-	-	Mixtures of ethanol and isopropyl alcohol	303, 313, 323	[6]
Flakes	1.75×10 ⁻¹¹ to 4.07×10 ⁻¹⁰	0.0112 to 0.0230	8.27×10 ⁻⁴ to 1.09×10 ⁻³	Ethyl acetate	298.15, 313.15, 328.15	This work
Flakes	6.22×10 ⁻¹² to 9.07×10 ⁻¹²	0.0097 to 0.0226	3.18×10 ⁻⁴ to 6.85×10 ⁻⁴	1-Butanol	298.15, 313.15, 328.15	This work

^a2-MeTHF: 2-Methyltetrahydrofuran

4.3.5 Thermodynamic Analysis

The thermodynamic analysis was performed using the concentration of soybean oil removed in the equilibrium estimated from the SMM to calculate the equilibrium constant, once it had the best correlation with the experimental data. The thermodynamic parameters estimated (ΔH^0 and ΔS^0) and calculated (ΔG^0) are shown in Table 4.9 for both solvents.

Table 4. 9 - Thermodynamic assessment for the soybean oil extraction using ethyl acetate and 1-butanol.

Solvent	T (K)	K	ΔH^0 (kJ/mol)	ΔS^0 (J/mol.K)	ΔG^0 (kJ/mol)	R^2
Ethyl acetate	298.15	2.6965	14.3500	56.3730	-2.4576	0.9999
	313.15	3.5537			-3.3032	
	328.15	4.5760			-4.1487	
1-butanol	298.15	2.0141	14.4849	54.7242	-1.8311	0.9785
	313.15	2.8946			-2.6519	
	328.15	3.5201			-3.4785	

It can be seen from Table 4.9 that the thermodynamic assessment was better for ethyl acetate than 1-butanol once its R^2 was higher. However, the correlation for both of the solvents was satisfactory. The estimated standard enthalpy change was positive, indicating endotherm processes, and it was higher when using 1-butanol than using ethyl acetate. The positive values of the standard entropy change indicate that the processes are irreversible and random. The negative values of the standard Gibbs free energy change indicate that the extractions were spontaneous, being more favorable when using ethyl acetate than 1-butanol. Not less important, the value of ΔH^0 for 1-butanol is higher once the extraction rate is highly dependent on the increase in temperature. These results are similar to what was found in other studies [56,57].

4.4 CONCLUSIONS

The extraction of soybean oil using ethyl acetate and 1-butanol was investigated. It can be concluded that the response surface methodology could correctly describe the effect of the temperature and solvent/solid ratio on the yield of the extractions. The vegetable oils obtained using the green solvents tested have a similar fatty acid profile and FTIR spectra to the oil obtained when using hexane. As the kinetic of the oil extraction was well described by the So and Macdonald model, it can be concluded that the mass transfer due to washing is important to describe this solid-liquid extraction, however, the highest gain in the yield of soybean oil extraction is related to diffusion. The thermodynamic analysis showed irreversible, endotherms, and spontaneous processes. Finally, 1-butanol has a better solubility capacity than ethanol for soybean oil, although ethyl acetate is the best candidate for the replacement of the industrial use of hexane due to its highest rate of soybean oil extraction at the beginning of the process and its lower boiling point.

CONFLICT OF INTERESTS

The authors report no declaration of interest.

ACKNOWLEDGMENT

The authors are grateful for the financial support and scholarships of the Human Resources Program of the National Agency for Petroleum, Natural Gas and Biofuels – PRH-ANP through the Human Resources Training Program for Petroleum and Biofuels Processing (PRH 52.1).

REFERENCES

- [1] M.H. Abdellah, L. Liu, C.A. Scholes, B.D. Freeman, S.E. Kentish. Organic Solvent Nanofiltration of Binary Vegetable Oil/Terpene Mixtures: Experiments and Modelling. *Journal of Membrane Science*, 573 (2019) 694–703. <https://doi.org/10.1016/j.memsci.2018.12.026>
- [2] O. Claux, V. Rapinel, P. Goupy, N. Patouillard, M.A. Vian, L. Jacques, F. Chemat. Dry and Aqueous 2-Methyloxolane as Green Solvents for Simultaneous Production of Soybean Oil and Defatted Meal. *ACS Sustainable Chemistry & Engineering*, 9 (2021) 7211–7223. <https://doi.org/10.1021/acssuschemeng.0c09252>
- [3] United States Department of Agriculture. Soybean 2021 World Production. https://ipad.fas.usda.gov/cropexplorer/cropview/commodityView.aspx?cropid=2222000&sel_year=2021&rankby=Production, 2021 (accessed 14 December 2021)
- [4] J.L.A. Dagostin, D. Carpiné, M.L. Corazza. Extraction of Soybean Oil Using Ethanol and Mixtures with Alkyl Esters (Biodiesel) as Co-Solvent: Kinetics and Thermodynamics. *Industrial Crops and Products*, 74 (2015) 69–75. <https://doi.org/10.1016/j.indcrop.2015.04.054>
- [5] T.A. Toda, M.M. Sawada, C.E.C. Rodrigues. Kinetics of Soybean Oil Extraction Using Ethanol as Solvent: Experimental Data and Modeling. *Food and Bioproducts Processing*, 98 (2016) 1–10. <https://doi.org/10.1016/j.fbp.2015.12.003>
- [6] A. Comerlatto, F.A. Voll, A.L. Daga, É. Fontana. Mass Transfer in Soybean Oil Extraction Using Ethanol/Isopropyl Alcohol Mixtures. *International Journal of Heat and Mass Transfer*, 165 (2021) 120630. <https://doi.org/10.1016/j.ijheatmasstransfer.2020.120630>
- [7] E. Sendzikiene, V. Makareviciene, M. Gumbyte. Reactive Extraction and Fermental Transesterification of Rapeseed Oil with 1-butanol in Diesel Fuel Media. *Fuel Processing Technology*, 138 (2015) 758–764. <https://doi.org/10.1016/j.fuproc.2015.07.020>
- [8] A. Sharma, S.K. Khare, M.N. Gupta. Three Phase Partitioning for Extraction of Oil from Soybean. *Bioresource Technology*, 85 (2002) 327–329. [https://doi.org/10.1016/s0960-8524\(02\)00138-4](https://doi.org/10.1016/s0960-8524(02)00138-4)
- [9] J.L.A. Dagostin, D. Carpiné, P.R.S. dos Santos, M.L. Corazza. Liquid-Liquid Equilibrium and Kinetics of Ethanolic Extraction of Soybean Oil Using Ethyl Acetate as Co-Solvent. *Brazilian Journal of Chemical Engineering*, 35 (2018) 415–428. <https://doi.org/10.1590/0104-6632.20180352s20160175>
- [10] B.T.F. de Mello, I.J. Iwassa, R.P. Cuco, V.A.S. Garcia, C. da Silva. Methyl Acetate as Solvent in Pressurized Liquid Extraction of Crambe Seed Oil. *The Journal of Supercritical Fluids*, 145 (2019) 66–73. <https://doi.org/10.1016/j.supflu.2018.11.024>
- [11] S. Bertouche, V. Tomao, A. Hellal, C. Boutekedjiret, F. Chemat. First Approach on Edible Oil Determination in Oilseeds Products Using Alpha-Pinene. *Journal of Essential Oil Research*, 25 (2013) 439–443. <https://doi.org/10.1080/10412905.2013.782473>

- [12] E. Potrich, S.C. Miyoshi, P.F.S. Machado, F.F. Furlan, M.P.A. Ribeiro, P.W. Tardioli, R.L.C. Giordano, A.J.G. Cruz, R.C. Giordano. Replacing Hexane by Ethanol for Soybean Oil Extraction: Modeling, Simulation, and Techno-Economic-Environmental Analysis. *Journal of Cleaner Production*, 244 (2020) 118660. <https://doi.org/10.1016/j.jclepro.2019.118660>
- [13] A. Sicaire, M. Vian, F. Fine, F. Joffre, P. Carré, S. Tostainm F. Chemat. Alternative Bio-Based Solvents for Extraction of Fat and Oils: Solubility Prediction, Global Yield, Extraction Kinetics, Chemical Composition and Cost of Manufacturing. *International Journal of Molecular Sciences*, 16 (2015) 8430–8453. <https://doi.org/10.3390/ijms16048430>
- [14] M.M. Batista, R. Guirardello, M.A. Krähenbühl. Determination of the Hansen Solubility Parameters of Vegetable Oils, Biodiesel, Diesel, and Biodiesel–Diesel Blends. *Journal of the American Oil Chemists' Society*, 92 (2014) 95–109. <https://doi.org/10.1007/s11746-014-2575-2>
- [15] A. Klamt, F. Eckert, W. Arlt. COSMO-RS: An Alternative to Simulation for Calculating Thermodynamic Properties of Liquid Mixtures. *Annual Review of Chemical and Biomolecular Engineering*, 1 (2010) 101-122. <https://doi.org/10.1146/annurev-chembioeng-073009-100903>
- [16] P. Alessi, M. Fermeglia, I. Kikic. Significance of Dilute Regions. *Fluid Phase Equilibria*, 70 (1991) 239–250. [https://doi.org/10.1016/0378-3812\(91\)85037-u](https://doi.org/10.1016/0378-3812(91)85037-u)
- [17] T. Brouwer, B. Schuur. Model Performances Evaluated for Infinite Dilution Activity Coefficients Prediction at 298.15 K. *Industrial & Engineering Chemistry Research*, 58 (2019) 8903–8914. <https://doi.org/10.1021/acs.iecr.9b00727>
- [18] C.E.C. Rodrigues, N.M. Longo, C.C. Silva, K.K. Aracava, B.R. Garavazo. Ethanolic extraction of soybean oil: oil solubility equilibria and kinetic studies. *Chemical Engineering Transactions*, 24 (2011). <https://doi.org/10.3303/CET1124136>
- [19] J. Crank. *The Mathematics of Diffusion*. Clarendon Press, 1975.
- [20] D.J. Nicolin, D.F. Rossoni, L.M.M. Jorge. Study of Uncertainty in the Fitting of Diffusivity of Fick's Second Law of Diffusion with the Use of Bootstrap Method. *Journal of Food Engineering*, 184 (2016) 63–68. <https://doi.org/10.1016/j.jfoodeng.2016.03.024>
- [21] C.E.C. Rodrigues, K.K. Aracava, F.N. Abreu. Thermodynamic and statistical analysis of soybean oil extraction process using renewable solvent. *International Journal of Food Science and Technology*, 45 (2010) 2407-2414. <https://doi.org/10.1111/j.1365-2621.2010.02417.x>
- [22] AOCS, 1998. *Official Methods and Recommended Practices of the American Oil Chemists' Society*, AOCS Press, Champaign, USA.
- [23] R.P. Peçanha. *Sistemas particulados #: Operações unitárias envolvendo partículas e fluidos*. Elsevier, 2014.
- [24] C.M. Hansen. *Hansen Solubility Parameters a User's Handbook*. CRC Press, Taylor & Francis Group, 2018.

- [25] S. Chemat. *Edible Oils Extraction, Processing, and Applications*. CRC Press, 2017.
- [26] F. Eckert, A. Klamt. Fast Solvent Screening via Quantum Chemistry: COSMO-RS Approach. *AIChE Journal*, 48 (2002) 369–385. <https://doi.org/10.1002/aic.690480220>
- [27] S. Lin, S.I. Sandler. A Priori Phase Equilibrium Prediction from a Segment Contribution Solvation Model. *Industrial & Engineering Chemistry Research*, 41 (2001) 899-913. <https://doi.org/10.1021/ie001047w>
- [28] R.P. Gerber, R. P. Soares. Assessing the Reliability of Predictive Activity Coefficient Models for Molecules Consisting of Several Functional Groups. *Brazilian Journal of Chemical Engineering*, 30 (2013) 1–11. <https://doi.org/10.1590/s0104-66322013000100002>
- [29] R.P. Gerber, R.P. Soares. Prediction of Infinite-Dilution Activity Coefficients Using UNIFAC and COSMO-SAC Variants. *Industrial & Engineering Chemistry Research*, 49 (2010) 7488–7496. <https://doi.org/10.1021/ie901947m>
- [30] R.P. Soares. The Combinatorial Term for COSMO-Based Activity Coefficient Models. *Industrial & Engineering Chemistry Research*, 50 (2011) 3060–3063. <https://doi.org/10.1021/ie102087p>
- [31] É.R. Oliveira, G.R. Carvalho, M.Â. Cirillo, F. Queiroz. Effect Of Ecofriendly Bio-Based Solvents on Oil Extraction from Green Coffee Bean and Its Industrial Press Cake. *Brazilian Journal of Chemical Engineering*, 36 (2019) 1739–1753. <https://doi.org/10.1590/0104-6632.20190364s20190102>
- [32] C.E.C. Rodrigues, R. Oliveira. Response Surface Methodology Applied to the Analysis of Rice Bran Oil Extraction Process with Ethanol. *International Journal of Food Science & Technology*, 45 (2010) 813–820. <https://doi.org/10.1111/j.1365-2621.2010.02202.x>
- [33] L. Hartman, R.C. Lago. Rapid preparation of fatty acid methyl esters from lipids. *Laboratory Practice*, 22 (1973) 475-494.
- [34] M.D. Guillén, N. Cabo. Some of the Most Significant Changes in the Fourier Transform Infrared Spectra of Edible Oils under Oxidative Conditions. *Journal of the Science of Food and Agriculture*, 80 (2000) 2028–2036. [https://doi.org/10.1002/1097-0010\(200011\)80:14<2028::aid-jsfa713>3.0.co;2-4](https://doi.org/10.1002/1097-0010(200011)80:14<2028::aid-jsfa713>3.0.co;2-4)
- [35] E. Zahir, R. Saeed, M.A. Hameed, A. Yousuf. Study of Physicochemical Properties of Edible Oil and Evaluation of Frying Oil Quality by Fourier Transform-Infrared (FT-IR) Spectroscopy. *Arabian Journal of Chemistry*, 10 (2017) S3870-S3876. <https://doi.org/10.1016/j.arabjc.2014.05.025>
- [36] G. C. So, D.G. Macdonald. Kinetics of Oil Extraction from Canola (Rapeseed). *The Canadian Journal of Chemical Engineering*, 64 (1986) 80–86. <https://doi.org/10.1002/cjce.5450640112>
- [37] F. Amarni, H. Kadi. Kinetics Study of Microwave-Assisted Solvent Extraction of Oil from Olive Cake Using Hexane. *Innovative Food Science & Emerging Technologies*, 11 (2010) 322–327. <https://doi.org/10.1016/j.ifset.2010.01.002>

- [38] S. Meziane, M. Kadi, O. Lamrous. Kinetic Study of Oil Extraction from Olive Foot Cake. *Grasas y Aceites*, 57 (2006) 175-179. <https://doi.org/10.3989/gya.2006.v57.i2.34>
- [39] C.L. Silveira, A.C. Galvão, W.S. Robazza, J.V.T. Feyh. Modeling and Parameters Estimation for the Solubility Calculations of Nicotinamide Using UNIFAC and COSMO-Based Models. *Fluid Phase Equilibria*, 535 (2021) 112970. <https://doi.org/10.1016/j.fluid.2021.112970>
- [40] M.M. Cascant, C. Breil, S. Garrigues, M. de la Guardia, A.S. Fabiano-Tixier, F. Chemat. A green analytical chemistry approach for lipid extraction: computation methods in the selection of green solvents as alternative solvents. *Analytical and Bioanalytical Chemistry*, 409 (2017) 3527-3539. <https://doi.org/10.1007/s00216-017-0323-9>
- [41] A. Benazzouz, L. Moity, C. Pierlot, M. Sergent, V. Molinier, J. Aubry. Selection of a Greener Set of Solvents Evenly Spread in the Hansen Space by Space-Filling Design. *Industrial & Engineering Chemistry Research*, 52 (2013) 16585–16597. <https://doi.org/10.1021/ie402410w>
- [42] L.A. Follegatti-Romero, M. Lanza, C.A.S da Silva, E.A.C. Batista, A. Meirelles. Mutual Solubility of Pseudobinary Systems Containing Vegetable Oils and Anhydrous Ethanol from (298.15 to 333.15) K. *Journal of Chemical & Engineering Data*, 55 (2010) 2750–2756. <https://doi.org/10.1021/je900983x>
- [43] H. Modarress, M.Mohsen-Nia. Experimental and theoretical studies of viscosities of ternary mixture [2-propanol+ethyl acetate+hexane] and its binary constituents at 298.15, 308.15 and 313.15 K. *Physics and Chemistry of Liquids: An International Journal*. 44 (2006) 67-76. <https://dx.doi.org/10.1080/00319100500337203>
- [44] T. Zhu, H. Gong, M. Dong. Density and viscosity of CO₂ + ethyl acetate binary systems from 308.15 to 338.15 K and 15 to 45 MPa. *Fluid Phase Equilibria*. 537 (2021) 112988. <https://doi.org/10.1016/j.fluid.2021.112988>
- [45] J. Zambrano, M.C. Martín, Á. Martín, J.J. Segovia. Viscosities of binary mixtures containing 1-butanol + 2,2,4-trimethylpentane or + 1,2,4-trimethylbenzene at high pressures for the thermophysical characterization of biofuels. *The Journal of Chemical Thermodynamics*. 102 (2016) 140-146. <https://dx.doi.org/10.1016/j.jct.2016.07.008>
- [46] M.F. Bolotnikov, Y.A. Neruchev. Viscosities and Densities of Binary Mixtures of Hexane with 1-Chlorohexane between 293.15 and 333.15 K. *J. Journal of Chemical Engineering Data*. 48 (2003) 739-741. <https://doi.org/10.1021/je034002l>
- [47] A. Todorut, A. Molea, I. Barabás. Predicting the Temperature and Composition – Dependent Density and Viscosity of Diesel Fuel – Ethanol Blends. *Periodica Polytechnica Chemical Engineering*, 64 (2020) 213-220. <https://doi.org/10.3311/PPch.14757>
- [48] M.M. Sawada, L.L. Venâncio, T.A. Toda, C.E.C. Rodrigues. Effects of Different Alcoholic Extraction Conditions on Soybean Oil Yield, Fatty Acid Composition and Protein Solubility of Defatted Meal. *Food Research International*, 62 (2014) 662–670. <https://doi.org/10.1016/j.foodres.2014.04.039>

- [49] K.A. Santos, C.M. de Aguiar, E.A. da Silva. Evaluation of Favela Seed Oil Extraction with Alternative Solvents and Pressurized-Liquid Ethanol. *The Journal of Supercritical Fluids*, 169 (2021) 105125. <https://doi.org/10.1016/j.supflu.2020.105125>
- [50] G.M. Rodrigues, L. Cardozo-Filho, C. da Silva. Pressurized Liquid Extraction of Oil from Soybean Seeds. *The Canadian Journal of Chemical Engineering*, 95 (2017) 2383–2389. <https://doi.org/10.1002/cjce.22922>
- [51] T. Aktar, E. Adal. Determining the Arrhenius Kinetics of Avocado Oil: Oxidative Stability under Rancimat Test Conditions. *Foods*, 8 (2019) 236. <https://doi.org/10.3390/foods8070236>
- [52] I. Avramov. Relationship between diffusion, self-diffusion and viscosity. *Journal of Non-Crystalline Solids*, 355 (2009) 745-747. <https://doi.org/10.1016/j.jnoncrysol.2009.02.009>
- [53] D.F. Boucher, J.C. Brier, J.O. Osburn. Extraction of Oil from Porous Solid. *Transactions of the American Institute of Chemical Engineers*, 38 (1942) 967-993.
- [54] R.J. Seager, A.J. Acevedo, F. Spill, M.H. Zaman. Solid dissolution in a fluid solvent is characterized by the interplay of surface area-dependent diffusion and physical fragmentation. *Scientific reports*, 8 (2018) 7711. <https://doi.org/10.1038/s41598-018-25821-x>
- [55] R.C. Chorny, J.H. Krasuk. Extraction for Different Geometries. Constant Diffusivity. *Industrial & Engineering Chemistry Process Design and Development*, 5 (1966) 206–208. <https://doi.org/10.1021/i260018a019>
- [56] S. Meziane, H. Kadi. Kinetics and Thermodynamics of Oil Extraction from Olive Cake. *Journal of the American Oil Chemists' Society*, 85 (2008) 391–396. <https://doi.org/10.1007/s11746-008-1205-2>
- [57] S.B. dos Santos, M.A. Martins, A.L. Caneschi, P.R.M. Aguiar, J.S.R. Coimbra. Kinetics and Thermodynamics of Oil Extraction from *Jatropha curcas* L. Using Ethanol as a Solvent. *International Journal of Chemical Engineering*, 2015 (2015) 1–9. <https://doi.org/10.1155/2015/871236>

SUPPLEMENTARY MATERIAL

Soybean oil extraction using ethyl acetate and 1-butanol: from solvent selection to thermodynamic assessment

Henrique Gasparetto, Ana Luiza Barrachini Nunes, Fernanda de Castilhos, Nina Paula Gonçalves Salau*

Chemical Engineering Department, Universidade Federal de Santa Maria, Brazil

*To whom all correspondence should be addressed. E-mail: ninasalau@ufsm.br

Address: Chemical Engineering Department, UFSM – Av. Roraima, 1000, Cidade Universitária - Bairro Camobi. 97105-900 Santa Maria, RS – Brazil.

Phone: +55-55-3220-8448

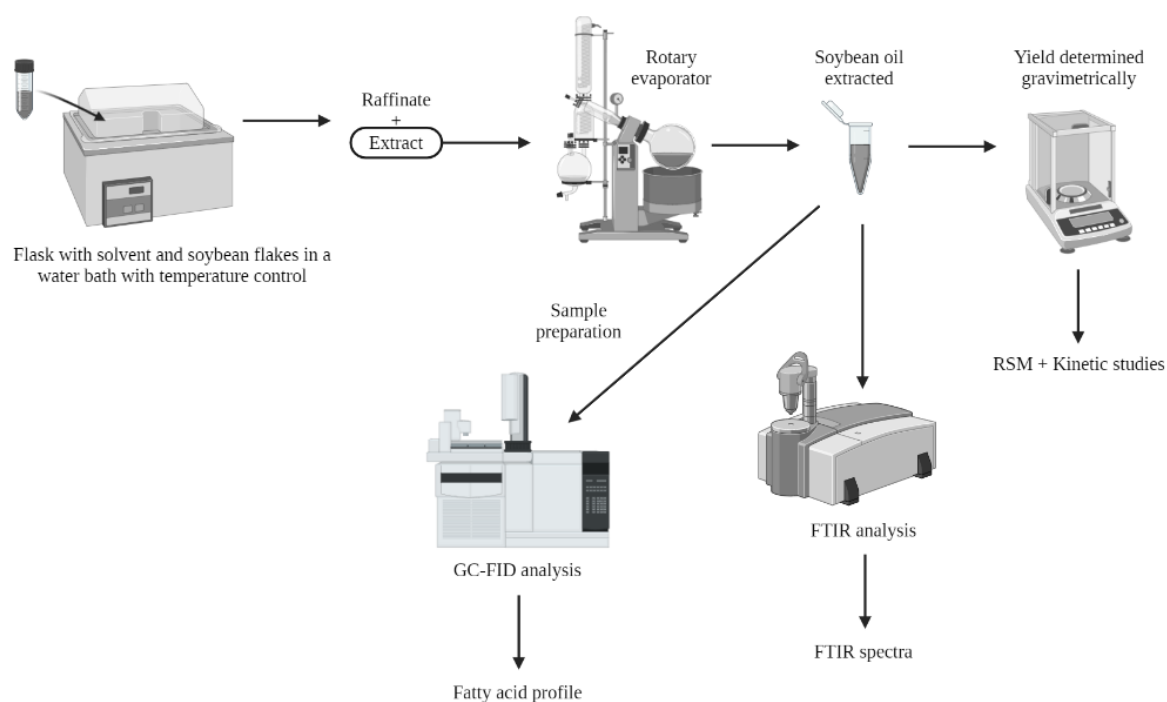
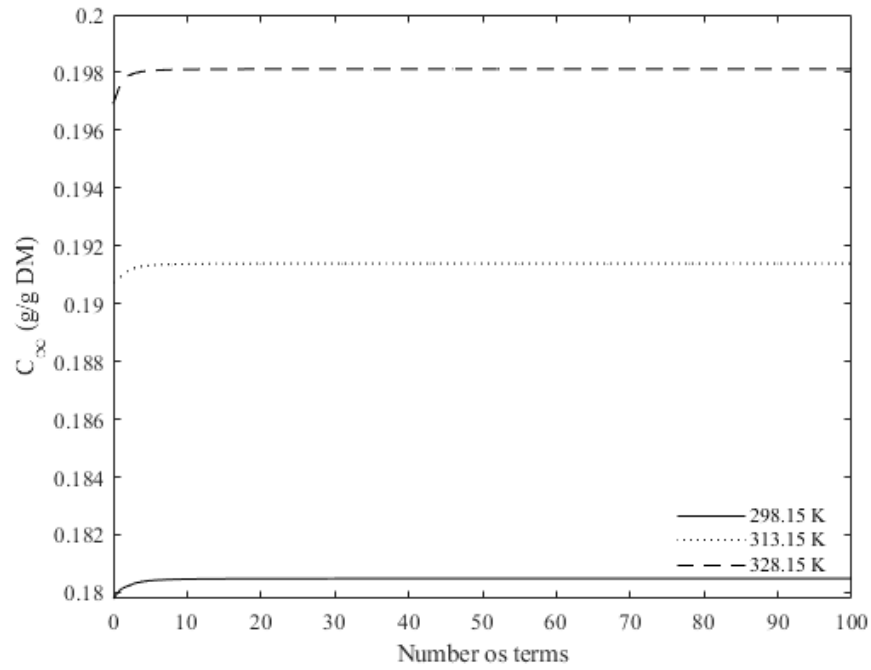
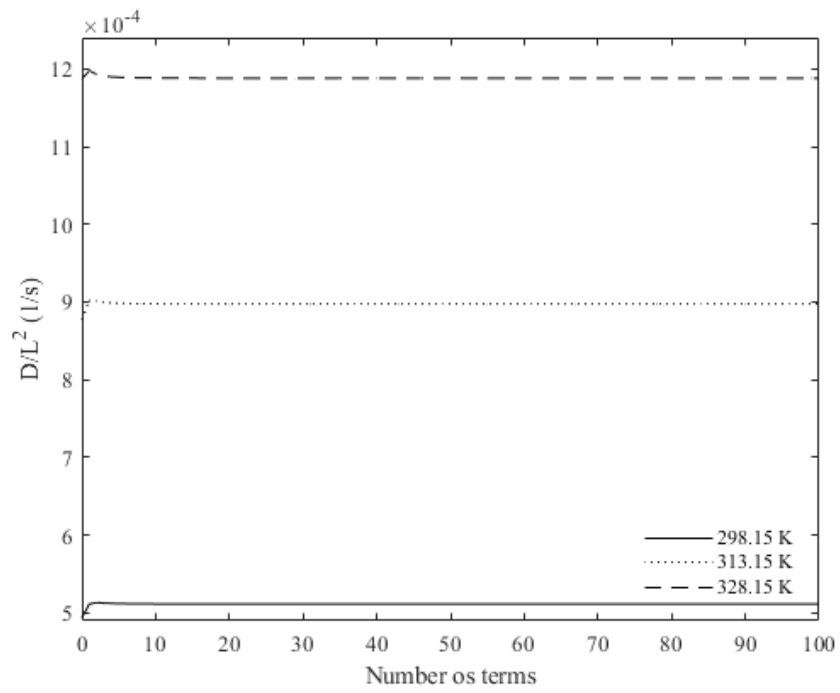


Figure S. 1 - Experimental apparatus.

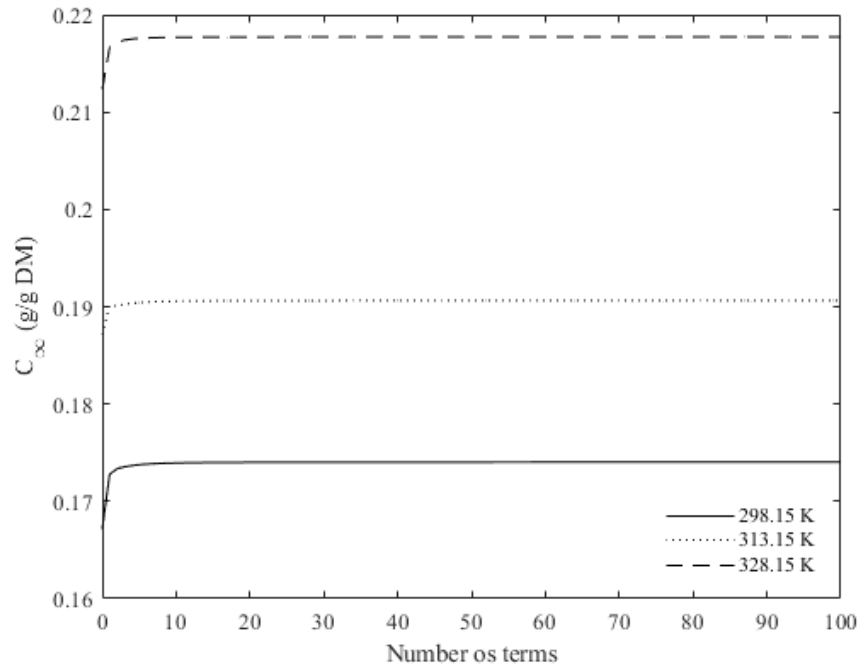


(a)

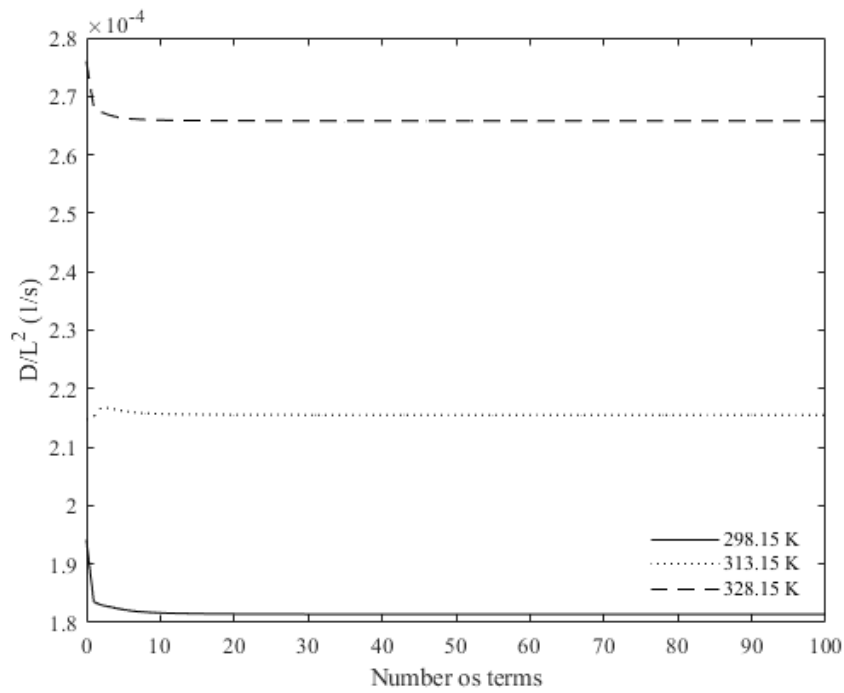


(b)

Figure S. 2 - Parameters stability for ethyl acetate as function of the number of terms of the mass transfer kinetic model for (a) C_∞ , and (b) D/L^2 .



(a)



(b)

Figure S. 3 - Parameters stability for 1-butanol as function of the number of terms of the mass transfer kinetic model for (a) C_{∞} , and (b) D/L^2 .

5 THEORETICAL AND EXPERIMENTAL STUDIES ON TECHNICAL VIABILITY OF SOYBEAN OIL EXTRACTION WITH P-CYMENE

Henrique Gasparetto, Fernanda de Castilhos, Nina Paula Gonçalves Salau

Chemical Engineering Department, Federal University of Santa Maria, Brazil

ABSTRACT

Oil was extracted from soybean using terpene as a green solvent. Against this background, the technical viability of replacing hexane with p-cymene was evaluated. First, insights into solvent selection and infinite dilution activity coefficient were obtained by, respectively, Hansen solubility parameters and COSMO-SAC theory. Equilibrium extraction yields were assessed using response surface methodology and each model was considered statistically significant. The kinetics and thermodynamics of the oil extraction were obtained and evaluated by the bootstrap method, taking into account bias reduction. This first reported use of p-cymene in soybean oil extraction has shown that it is associated with better yields than using hexane at 328.15 K. P-cymene has not affected the typical oil quality. The bootstrap method was able to reduce the bias of the estimators, correct the probability confidence interval for the So and Macdonald models, and increase the correlation coefficient for the thermodynamic assessment from 0.9387 to 0.9533.

Keywords: Solid-liquid extraction; green solvent; kinetic; thermodynamic; fatty acid profile; FTIR; solvent selection.

NOMENCLATURE

Abbreviations

ANOVA – Analysis of variance

BS – Bootstrap Resampling

COSMO – CONductor-like Screening MOdels

DAG – Diacylglycerol

DM – Dry mass

FFA – Free fatty acids

FID – Flame ionization detector

FOM – First-order model

FTIR – Fourier-transform infrared spectroscopy

GAMESS – General Atomic and Molecular Electronic Structure System

GC – Gas chromatography

MAG – Monoacylglycerol

MOPAC – Molecular Orbital Packages

MUFAs – Monounsaturated fatty acids

MTKM – Mass transfer kinetic model

PSO – Particle Swarm Optimization

PUFAs – Polyunsaturated fatty acids

RSM – Response surface methodology

SAC – Segment Activity Coefficient

SFAs – Saturated fatty acids

SMM – So and Macdonald Model

SOM – Second-order model

TAG – Triacylglycerol

Variables

AIC – Akaike information criterion [-]

C_i – Observed values [g/g DM]

\hat{C}_i – Predicted values [g/g DM]

\bar{C}_i – Mean of observed values [g/g DM]

C_0 – Initial oil concentration in the solid matrix [g/g DM]

- C_{∞} – Solute concentration at the equilibrium [g/g DM]
 D_{eff} – Diffusivity of the solute inside the particle [$m^2 \cdot min^{-1}$]
 F – Fisher's calculated value [-]
 $IDAC$ - Infinite Dilution Activity Coefficient [-]
 K – Equilibrium constant [-]
 k – Extraction rate constant [min^{-1}]
 m – Temperature extraction coefficient [-]
 n – Number of observations [-]
 p – Number of parameters of the model [-]
 R – Universal gas constant [$8.3144 J \cdot mol^{-1} \cdot K^{-1}$]
 R^2 – Coefficient of determination [-]
 R_{adj}^2 – Adjusted coefficient of determination [-]
 R_0 – Radius of the solubility sphere for the solute [$MPa^{1/2}$]
 R_a – Distance between the solute and the solvent on the Hansen solubility space [$MPa^{1/2}$]
 RED – Relative energy difference [-]
 $RMSE$ – Root-mean-square error [-]
 S – Objective function [-]
 T – Temperature [K]
 v_{ii} – i-th diagonal element of the covariance matrix of the model parameters [-]
 Y_0 – Extraction yield at 273.15 K [g/g DM]

Greek Symbols

- δ – Hansen parameter [$MPa^{1/2}$]
 ΔG^0 – Standard Gibbs free energy change [$kJ \cdot mol^{-1}$]
 ΔH^0 – Standard enthalpy change [$kJ \cdot mol^{-1}$]
 ΔS^0 – Standard entropy change [$kJ \cdot mol^{-1} \cdot K^{-1}$]
 χ^2 – Chi-square distribution [-]
 ε – Error [g/g DM]
 α – Significance level [-]

Subscripts and superscripts

- l – Model with a lower number of parameters

2 – Model with a higher number of parameters

D – Dispersive forces

P – Polar forces

H – Hydrogen-bond interactions forces

d – Diffusional stage

w – Washing stage

5.1 INTRODUCTION

Soybean (*Glycine max*) is one of the most cultivated grains in the world. In particular, its oil portion is specially intended for food (Gerde et al., 2020; Tomita et al., 2014), for the production of biofuels (Kim et al., 2013), and for producing plasticizers (Olivieri et al., 2020). The oil is commonly extracted from the matrix using a mechanical press (Cheng and Rosentrater, 2019) and solvent extraction (Cheng et al., 2018). The solvent extraction using hexane is the most used process due to its high yield of soybean oil production (Cheng and Rosentrater, 2017), although hexane has been recently included in the list of carcinogenic, mutagenic, and reprotoxic substances under European regulation (Benazzouz et al., 2013; Claux et al., 2021; Li et al., 2016). In this context, hexane may be banned from this type of industrial application in the future (Abdellah et al., 2019).

The limited reserve of natural resources has directed scientific attention to renewable processes and materials. Petroleum-derived products are widely known to contribute to massive carbon dioxide emissions (Potrich et al., 2020), which are not reabsorbed by nature in their life cycle (Vineyard and Ingwersen, 2016). Green solvents are being extensively studied to replace hexane use and be considered renewable resources (Rodrigues et al., 2014) in respect of their neutrality on carbon dioxide emissions (Capello et al., 2007). Besides the previously mentioned advantages of using green solvents in vegetable oil extraction, the extraction yield can be improved due to the better solubilization of the triacylglycerols (Caschant et al., 2017; Gasparetto et al., 2022a; Sicaire et al., 2015).

Many types of green solvents have been studied for soybean oil extraction: ethanol (Comerlatto et al., 2021; Dagostin et al., 2015; Dagostin et al., 2018; Phan et al., 2009; Toda et al., 2016), isopropanol (Comerlatto et al., 2021), 1-butanol (Gasparetto et al., 2022b), 2-methyl tetrahydrofuran (Claux et al., 2021), ethyl acetate (Dagostin et al., 2018; Gasparetto et al., 2022b), alkyl esters (Dagostin et al., 2015), alpha-pinene (Bertouche et al., 2013), and others (Abdellah et al., 2019; Abdellah et al., 2020; Sharma et al., 2012). The hydrated form

of the solvent (Claux et al., 2021; Dagostin et al., 2015; Toda et al., 2016) and co-solvents (Dagostin et al., 2015; Dagostin et al., 2018) were also investigated. Terpenes have been appearing as suitable substitutes for oil extraction of oilseeds (Li et al., 2014) and microalgae (Tanzi et al., 2012; Tanzi et al., 2013), being noticed an effort to use D-limonene (Tanzi et al., 2012; Tanzi et al., 2013), alpha-pinene (Bertouche et al., 2013; Tanzi et al., 2012; Tanzi et al., 2013), and p-cymene (Abdellah et al., 2019; Abdellah et al., 2020; Li et al., 2014; Naik et al., 2021; Tanzi et al., 2012; Tanzi et al., 2013).

P-cymene was applied in many applications; it can be mentioned for its use in bitter gourd (Naik et al., 2021) and rapeseed (Li et al., 2014) oil extraction. For rapeseed, p-cymene achieved the highest yield of oil extraction in comparison with n-hexane, ethanol, isopropanol, butanol, alpha-pinene, and D-limonene. However, from the terpenes, only alpha-pinene was used for soybean oil extraction, where better extraction yields were achieved than using n-hexane (Bertouche et al., 2013).

Obtaining the oil's fatty acid profile is suitable to describe the main constituents of triglycerides because they are responsible for the cetane number of its respective biofuels (Pinzi et al., 2013), and some are related to dietary benefits (Srivastava and Semwal, 2013). It is interesting to obtain the composition of the oil regarding free fatty acids (FFA), monoacylglycerols, and diacylglycerols for evaluating if hydrolysis has occurred to any extent (Pacheco et al., 2014). FFA impact negatively the quality of an extracted oil (Toda et al., 2016) and the transesterification reaction if the oil is destined to produce biodiesel (Pasiadis et al., 2009). Fourier-transform infrared spectroscopy (FTIR) has been applied to analyze vegetable oils (Rohman et al., 2020; Valand et al., 2020) because it is an essential technique for the analysis of organic compounds (Rai et al., 2015). FTIR technique is suitable for obtaining a fast, easy, and brief screening of the oil composition while verifying if the oil is clean and free from solvent.

Regarding to extraction modeling, diffusive models based on the second law of Fick are being used to describe the kinetics of the solid-liquid extractions and further evaluate their thermodynamics (Dagostin et al., 2015; Dagostin et al., 2018; Toda et al., 2016). The mass flow is intrinsically related to the concentration gradient inside the particle, which is difficult to determine (Santos et al., 2015). The power-law models have also been used (Dagostin et al., 2015). Furthermore, the So and Macdonald Model (SMM) has been one of the best models to predict vegetable oil extraction using many solvents (Meziane and Kadi, 2008; Toda et al., 2016).

For parameter estimation, combining the use of a deterministic method after obtaining an initial guess with a heuristic approach can be an option to find the global minimum of optimization problems. Different techniques, such as the bootstrap method, can evaluate uncertainties related to the problems. Bootstrap is an approach for obtaining new samples through statistics. This technique is used to consider the uncertainty of the fitting and reduce the bias of the estimators (Efron and Tibshirani, 1994).

For the extraction of vegetable oils, the thermodynamic analysis is carried out after obtaining the partition coefficient between the phases, as reported in the works of Rodrigues et al., 2010 and Dagostin et al. (2015). The equilibrium relationship of oil extracted at each temperature is related to the standards enthalpy, entropy, and Gibbs free energy changes. Some additional thermodynamic parameters related to the molecular configuration of the compounds turn possible to evaluate candidates for solvent extraction. On this basis arise the analysis of dispersive, polar, and hydrogen-bonding interaction using Hansen solubility parameters (Hansen, 2018) and the infinite dilution activity coefficient (Brouwer and Schuur, 2019) obtained through the CONductor-like Screening Model – Segment Activity Coefficient (COSMO-SAC) theory (Lin and Sandler, 2001).

This study aims at evaluating the technical feasibility of the first reported application of p-cymene in soybean oil extraction. To obtain a brief screening and describe the many interactions between the triacylglycerols with p-cymene and hexane, the Hansen solubility parameters and the infinite dilution activity coefficient obtained through the COSMO-SAC theory were used. The influence of the temperature and the solvent-to-solid mass ratio on the yield of soybean oil extraction at equilibrium were evaluated using the response surface methodology (RSM). The oil extracted at different temperatures was evaluated by its fatty acid profile, FFA, MAG, DAG, and TAG composition, and FTIR spectra. The extraction kinetics was modeled using the first and second-order models, mass transfer kinetic model, and So and Macdonald model. The best model was determined statistically and assessed to the bootstrap method to reduce the bias of the estimators. Finally, the thermodynamics assessment of the extraction was determined and evaluated to describe the physicochemical properties of the process and the reliability of the experimental results.

5.2 MATERIALS AND METHODS

5.2.1 Material

The soy-crushing company Granol (Cachoeira do Sul, Brazil) gently provided the soybean flakes, which were kept at $-12\text{ }^{\circ}\text{C}$ until use. The solvents used for the extractions were p-cymene (Sigma Aldrich, purity 99.8%, CAS N° 141-78-6), and hexane (Êxodo científica, purity $\geq 99\%$, CAS N° 110-54-3).

5.2.2 Methods

5.2.2.1 Experimental procedures

According to Gasparetto et al. (2022b), the soybean flakes were characterized in terms of moisture, relative density, and thickness.

The extractions were individually performed in 50 mL polypropylene flasks inside a bath with temperature control for the RSM and the kinetic studies. The yield of each soybean oil extraction was obtained gravimetrically by Eq. 1.

$$\text{Yield (g/g DM)} = \frac{\text{Mass of soybean oil extracted (g)}}{\text{Mass of dry soybean flakes (g)}} \quad (1)$$

The best solvent-to-solid mass ratio was achieved after applying the response surface methodology. Then the kinetic curves were obtained for the time interval from 0 to 120 minutes (1, 2, 4, 8, 10, 15, 30, 60, 90, and 120 minutes) for the temperatures of 298.15 K, 313.15 K, 328.15 K, and 343.15 K. Each kinetic extraction experiment was performed in triplicate.

Soxhlet extractions were performed to obtain the initial oil concentration in the soybean flakes with 150 mL of each solvent at its boiling point. Around 5 grams of soybean flakes were extracted in 3 hours for p-cymene and 4 hours for hexane. The lower extraction time for p-cymene was chosen due to its higher boiling point. Soxhlet extractions were performed in triplicate.

The fatty acid profile of the soybean oil extracted was obtained after transmethylation of the respective fatty acids using gas chromatography (GC) with a flame ionization detector (FID) in a GCMS-QP2010 gas chromatographic system (Shimadzu) using an Rtx®-Wax capillary column measuring 30 m in length, 0.25 mm as internal diameter, and 0.25 μm in film thickness, operating with helium as carrier gas. The preparation of fatty acids methyl esters was based on Hartman and Lago (1973), using a solution of ammonium chloride and

sulfuric acid in methanol as esterifying agents (Nunes and Castilhos, 2020). The fatty acid profile was determined in triplicate.

The free fatty acid, monoacylglycerols, diacylglycerol, and triacylglycerol contents were determined by GC-FID using a ZB-5HT capillary column measuring 15 m in length, 0.32 mm as internal diameter, and 0.10 μm in film thickness, in the same gas chromatography system previously mentioned. Two drops of the oil extracted were diluted with a hexane/heptane (3:1 v/v) mixture and directly injected into the GC system without further sample preparation. More details can be obtained in Ribeiro et al. (2018). The FFA, MAG, DAG, and TAG contents were determined in triplicate.

The FTIR spectra were acquired by direct transmittance using a liquid film over a crystal of NaCl in an IR Prestige 21 equipment (Shimadzu). The spectra were analyzed in the range of 500 to 4500 cm^{-1} with 45 scans and a resolution of 2.0 cm^{-1} .

5.2.2.2 Modeling and simulation

5.2.2.2.1 Solvent selection

To obtain insight into solvent selection, the JCOSMO software, developed by the Virtual Laboratory for Property Prediction research group (Soares, 2011; Gerber and Soares, 2010; Gerber and Soares, 2013), was used to obtain the sigma profiles for the main triacylglycerols present in soybean oil, and for the solvents p-cymene and hexane. The sigma profiles generated by the Molecular Orbital Packages (MOPAC2009, 2008) were used to obtain the infinite dilution activity coefficient (IDAC) for each pair solute-solvent using the COnductor-like Screening MOdel – Segment Activity Coefficient (COSMO-SAC). The COSMO-based models calculate properties from the interaction between molecules based on their electronic densities (Coto et al., 2021), where the IDAC is a robust tool applied to solvent selection (Brouwer and Schuur, 2019). The JCOSMO sigma profiles were accomplished using the General Atomic and Molecular Electronic Structure System (GAMESS) by the procedure described in Ferrarini et al. (2018).

The relative energy distance (*RED*) between the solvents and soybean oil, obtained using the Hansen parameters, was also evaluated for p-cymene and hexane. The RED was calculated using the parameters obtained from Benazzouz et al. (2013) and Batista et al. (2014), and Eqs. 2 and 3.

$$Ra^2 = 4(\delta_{D1} - \delta_{D2})^2 + (\delta_{P1} - \delta_{P2})^2 + (\delta_{H1} - \delta_{H2})^2 \quad (2)$$

$$RED = \frac{Ra}{R_0} \quad (3)$$

where δ is the Hansen parameter for dispersive (subscript D), polar (subscript P), and hydrogen-bond interactions forces (subscript H), for the solvent (1) and the solute (2), Ra is the distance between the solute and the solvent on the Hansen solubility space ($\text{MPa}^{1/2}$) and R_0 is the radius of the solubility sphere ($\text{MPa}^{1/2}$).

5.2.2.2.2 Response surface methodology

Second-order polynomial models have been successfully applied to predict vegetable oil extraction (Rai et al., 2015). The influence of temperature and solvent-to-solid mass ratio (independent variables) on the yield of soybean oil extraction (dependent variable) using p-cymene was evaluated by the response surface methodology (RSM), while statistical metrics and tests evaluated the model performance.

5.2.2.2.3 Kinetic and thermodynamic

Power-law models have been extensively applied for modeling solid-liquid extraction (Dagostin et al., 2015; Mgoma et al., 2021; Santos et al., 2015; Sarip et al., 2016; Tomito et al., 2014). The first (Eq. 4) and second-order (Eq. 5) power-law models were applied to soybean oil extraction by Dagostin et al. (2015).

$$C = C_{\infty} (1 - e^{-kt}) \quad (4)$$

$$C = \frac{t}{\frac{t}{C_{\infty}} + \frac{1}{kC_{\infty}}} \quad (5)$$

where C_{∞} is the yield of soybean oil extraction at the equilibrium condition (g/g DM), t is the extraction time (min), and k is the extraction rate constant (min^{-1}).

Dagostin et al. (2015) have introduced a mass transfer kinetic model (MTKM) (Eq. 6) to describe soybean oil extraction using anhydrous ethanol and ethanol with co-solvents. This model was further applied by Claux et al. (2021) to describe the kinetics of soybean oil extraction using anhydrous and hydrated 2-MeTHF, and by Gasparetto et al. (2022b) to describe soybean oil extraction using absolute ethyl acetate and absolute 1-butanol. The

following assumptions were made to solve Fick's second law (Chan et al., 2013; Claux et al., 2021; Dagostin et al., 2015; Gasparetto et al., 2022a):

- a) Soybean flakes are symmetrical and porous particles measuring $2L$.
- b) The initial concentration of soybean oil is constant in the solid particle.
- c) The concentration of soybean oil in the flakes depends on time and thickness.
- d) The extraction process is a diffusive phenomenon where the effective diffusivity is time-independent.
- e) External mass transfer resistance is negligible.
- f) The concentration of soybean oil at the interface is kept constant and equal to zero.

$$C = C_{\infty} \left[1 - \frac{8}{\pi^2} \sum_{n=0}^{\infty} \frac{1}{(2n+1)^2} \exp\left(-\frac{(2n+1)^2 \pi^2 D_{eff} t}{4L^2}\right) \right] \quad (6)$$

where L is the half of the thickness of the slab (m), and D_{eff} is the effective diffusivity of the solute inside the particle ($\text{m}^2 \cdot \text{min}^{-1}$).

From Nicolin et al. (2016) and Gasparetto et al. (2022b), it can be concluded that mass transfer based models should not be truncated in the first term to ensure general stability and a smaller confidence interval for the parameters. Therefore, in this work, the MTKM equation was truncated at the 100th term to perform the nonlinear regression.

So and Macdonald Model (SMM) with four parameters (Eqs. 7 and 8) has been used to describe many types of vegetable oil extraction that occur through washing and diffusion (Gasparetto et al., 2022a; Gasparetto et al., 2022b; Kostić et al., 2014; Toda et al., 2016).

$$C = C_{\infty}^w [1 - \exp(-k_w t)] + C_{\infty}^d [1 - \exp(-k_d t)] \quad (7)$$

$$C_{\infty} = C_{\infty}^w + C_{\infty}^d \quad (8)$$

where C_{∞}^w is the yield of soybean oil extraction at the equilibrium condition for the washing stage (g/g DM), C_{∞}^d is the yield of soybean oil extraction at the equilibrium condition for the diffusional stage (g/g DM), k_w is the extraction rate constant for the washing stage (min^{-1}), and k_d is the extraction rate constant for the diffusional stage (min^{-1}).

Finally, Eqs. 9 to 11 are used for the thermodynamic analysis. The distribution coefficient (K) was calculated using the C_{∞} obtained after model fitting.

$$K = \frac{C_{\infty}}{C_0 - C_{\infty}} \quad (9)$$

$$K = \exp\left(-\frac{\Delta H^0}{RT} + \frac{\Delta S^0}{R}\right) \quad (10)$$

$$\Delta G^0 = \Delta H^0 - T\Delta S^0 \quad (11)$$

where C_0 is the initial oil concentration in the soybean flakes (g/g DM), T is the temperature of extraction (K), R is the universal gas constant (8.3144 J.mol⁻¹K⁻¹), ΔH^0 is the standard enthalpy change (J.mol⁻¹), ΔS^0 is the standard entropy change (J.mol⁻¹K⁻¹), and ΔG^0 is the standard Gibbs free energy change (J.mol⁻¹).

5.2.2.2.4 Uncertainties evaluation and parameters estimation

Parameter estimation for the best model was assigned to the bootstrap resampling method to consider the uncertainty of the fitting, using the following algorithm (Davison and Hinkley, 1997; Nicolin et al., 2016).

1. Based on Eq. 12

$$C(t) = \hat{C}(t) + \varepsilon \quad (12)$$

where \hat{C}_i is the estimated value, and with the error ε following an independent and identically Gaussian distribution with mean zero and variance σ^2 ;

2. Replace t for t^* and ε for $\varepsilon - \bar{\varepsilon}$, where the superscript “*” denotes the new sample

$$C(t^*) = \hat{C}(t^*) + \varepsilon^* \quad (13)$$

3. Do the nonlinear parameter estimation.
4. Return to step 1 and repeat the process at least 100 times.
5. Stop.

The algorithm development and application were made using the software Matlab®. In the nonlinear parameter estimation of kinetic models was used the built-in function *particleswarm* for Particle Swarming Optimization (PSO) (Kennedy and Eberhart, 1995; Mezura-Montes and Coello, 2011; Pedersen, 2010) hybridized with the built-in function *fmincon* for constrained optimization using the interior-point algorithm (Byrd et al., 2000; Byrd and Mary, 1999; Coleman and Li, 1994; Coleman and Li, 1996; Gill et al., 1981; Han,

1977; Powell, 1978a; Powell, 1978b; Waltz et al., 2006). A constrained optimization solver was required because all the kinetic parameters are higher than zero (lower bound), the equilibrium concentrations shall respect the maximum value of 1 (100%), and the parameters related to the mass transfer are usually lower than 10 (upper bound).

To obtain the bootstrap samples was chosen the built-in function *lsqnonlin* using the Levenberg-Marquardt algorithm (Coleman and Li, 1994; Coleman and Li, 1996; Levenberg, 1944; Marquardt, 1963; Moré, 1977; Moré et al., 1980; Powell, 1970) for considerable gain in performance. Finally, the built-in function *particleswarm* hybridized with the built-in function *fminsearch* (Lagarias et al., 1998) was selected to perform the thermodynamic analysis because the thermodynamic parameters are not necessarily strictly inside a bound.

All the methods were assessed to the sum of the square errors as the objective function (Eq. 14).

$$S(\theta) = \sum_{i=1}^n (C_i - \hat{C}_i)^2 \quad (14)$$

where θ are the model parameters, C_i is the observed value, and n is the number of observations.

The likelihood confidence interval of the parameters for 95% of confidence was obtained using the methodology fully described in Schwaab et al. (2008). Shortly, the likelihood interval of a parameter i is obtained through the t-Student variable defined for $n - p$ degrees of freedom for the confidence of $(1 - \alpha/2)$ (Eq. 15).

$$\theta_i \pm t_{n-p}^{1-\alpha/2} \left(\frac{S(\hat{\theta})}{(n-p) v_{ii}} \right)^{1/2} \quad (15)$$

where v_{ii} is the i-th diagonal element of the covariance matrix of the model parameters, and the superscript “ \wedge ” denotes the estimate of the minimum point.

5.2.2.3 Statistical evaluation

To assess the goodness of the fittings was used the coefficient of determination (R^2), the chi-square distribution (χ^2), and the root-mean-square error (*RMSE*). The models were compared through the Akaike information criterion (*AIC*), the adjusted coefficient of determination (R_{adj}^2), and Fischer’s exact test.

$$R^2 = 1 - \frac{\sum_{i=1}^n (C_i - \hat{C}_i)^2}{\sum_{i=1}^n (C_i - \bar{C}_i)^2} \quad (16)$$

$$\chi^2 = \sum_{i=1}^n \frac{(C_i - \hat{C}_i)^2}{C_i} \quad (17)$$

$$RMSE = \sqrt{\frac{1}{n} \sum_{i=1}^n (C_i - \hat{C}_i)^2} \quad (18)$$

$$AIC = 2p + n \times \ln \left(\frac{\sum_{i=1}^n (C_i - \hat{C}_i)}{n} \right) \quad (19)$$

$$R_{adj}^2 = 1 - \frac{(n-1)(1-R^2)}{(n-p-1)} \quad (20)$$

$$F = \frac{\left(\frac{S_1 - S_2}{P_2 - P_1} \right)}{\left(\frac{S_2}{n - p_2} \right)} \quad (21)$$

where \bar{C}_i is the mean of the observations, and subscripts 1 and 2 refer to the model with a lower number of parameters and a higher number of parameters, respectively.

5.3 RESULTS AND DISCUSSION

5.3.1 Insights on solvent selection

It can be seen from Fig. 5.1 that there are no significant differences between the sigma profiles for the triacylglycerols constituted by different fatty acids. The sigma profile of p-cymene and hexane suggests similar attractive and repulsive forces over the triacylglycerol. The difference in the extraction yield might be related to a small contribution of hydrogen-bond donors and acceptance by p-cymene, which is not observed for hexane. As a result, the triacylglycerol/p-cymene mixture might be energetically more favorable due to the formation of homologous pairs.

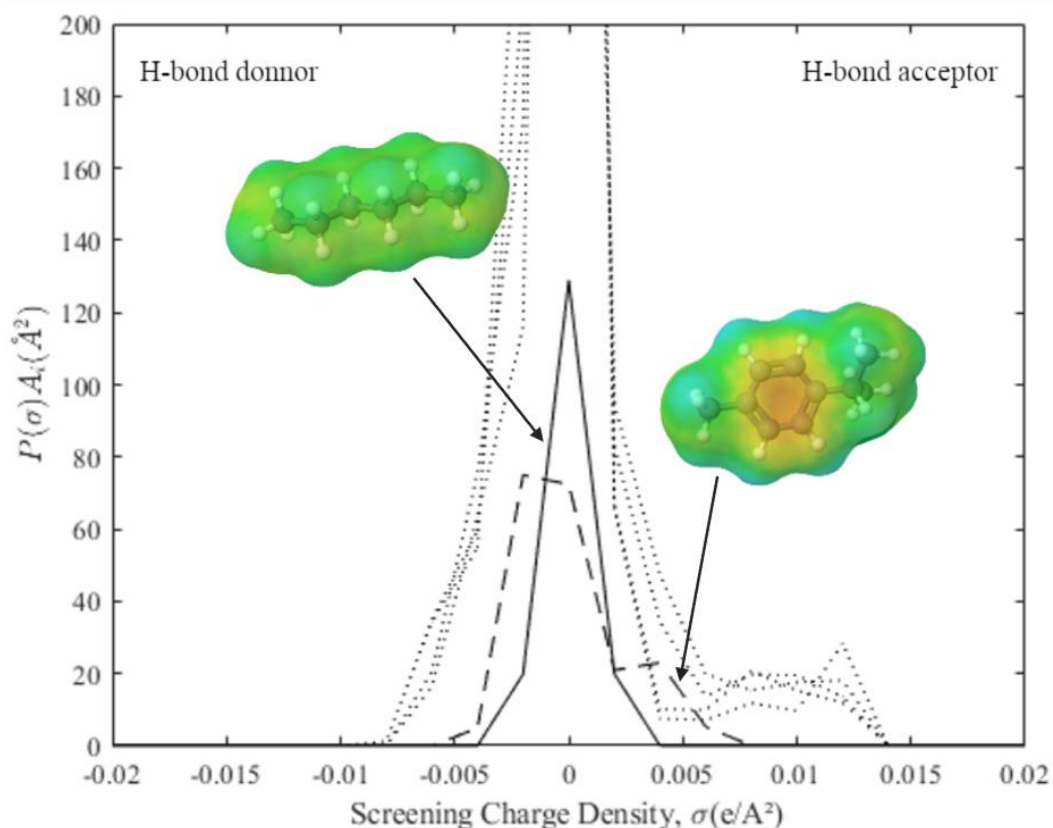


Figure 5. 1 - Sigma-profile of different triacylglycerols (dotted lines) in comparison with p-cymene (dashed line) and hexane (continuous line).

The smaller the relative energy distance (*RED*) and the $\ln(IDAC)$, the better the solubilization of a solute in a solvent. From the software JCOSMO, the $\ln(IDAC)$ was obtained at 328.15 K because this is the temperature industrially used (Sicaire et al., 2015); the average value for the mixtures between p-cymene and glyceryl trilinoleate, glyceryl trioleate, glyceryl tripalmitate, and glyceryl tristearate was -0.64, while for hexane the value was 0.54. For p-cymene, the *RED* calculated is 0.85 and 0.82 for hexane. The $\ln(IDAC)$ suggests that p-cymene has a better performance on solubilizing triacylglycerols, while from the *RED* analysis it might be stated that they have similar potentials.

5.3.2 Soybean and soybean oil characterization

The soybean flakes used were retained in the sieves of 10 mesh. It had moisture of 10.70 ± 0.2 wt%, a thickness of 0.37 ± 0.09 mm, and an apparent relative density equal to 1.1508 ± 0.0372 .

The soybean oil extraction at the boiling point of p-cymene obtained a yield of 31.63 ± 1.50 g/g DM compared to 24.28 ± 1.11 g/g DM for hexane. The extraction yield for hexane is according to what was found in the literature (Claux et al., 2021; Dagostin et al., 2015; Toda et al., 2016). The higher yield for p-cymene is justified because the Soxhlet extraction operates at the boiling point of the solvent, which is 450.15 K for p-cymene compared to 342.15 K for hexane. For example, the increase in temperature is used in pressurized liquid extractions due to the oil recovery improvement when working with higher temperatures (Mello et al., 2019; Rodrigues et al., 2017; Santos et al., 2021). Besides, for p-cymene, there is the opportunity of working in higher temperatures without using high pressures to keep the solvent in the liquid phase. Similarly, p-cymene might be able to remove other solutes than lipids and nonpolar components.

The fatty acid profile of the oil obtained for the different extraction temperatures is presented in Table 5.1. There are no significant differences by Tukey test ($p < 0.05$) between the fatty acid profile for the different extraction temperatures. The fatty acid profile agrees with those found in other studies (Chen et al., 2014; Rodrigues et al., 2010; Rodrigues et al., 2014; Sawada et al., 2014). This fatty acid constitution is similar to the typical composition of rice bran oil (Oliveira et al., 2012; Sawada et al., 2014), which is favorable for the production of biofuels due to the higher cetane number of the respective ester (Pinzi et al., 2013). The composition of saturated fatty acids (SFAs), monounsaturated fatty acids (MUFAs), and polyunsaturated fatty acids (PUFAs) was calculated based on the fatty acid composition.

It can be seen that the soybean oil extracted is mainly composed of linolenic, oleic, and palmitic acid. The oxidative stability of the oil is improved when it has a high content of saturated ethyl esters containing up to 16 carbons and monounsaturated esters (Jimenez et al., 2019). As the relative fatty acid composition of the oil is mainly up to 16 carbons with a high portion of monounsaturated esters, it can be affirmed that the oil has high oxidative stability.

Table 5. 1 - Fatty acid profile of the soybean oil extracted with p-cymene.

Fatty acid (%m/m)	Temperature			
	298.15	313.15	328.15	343.15
C16:0, palmitic acid	12.36 ^a ± 0.04	11.71 ^a ± 0.03	12.94 ^a ± 0.01	14.27 ^a ± 2.01
C18:0, stearic acid	4.66 ^b ± 0.00	4.36 ^b ± 0.01	4.77 ^b ± 0.03	5.38 ^b ± 0.78
C18:1, oleic acid	24.93 ^c ± 0.07	23.63 ^c ± 0.06	25.35 ^c ± 0.12	26.94 ^c ± 2.69
C18:2, linoleic acid	50.22 ^d ± 0.28	52.68 ^d ± 0.12	49.28 ^d ± 0.12	45.25 ^d ± 5.64
C18:3, linolenic acid	4.55 ^e ± 0.02	5.27 ^e ± 0.03	4.29 ^e ± 0.02	3.70 ^e ± 1.37
Others	3.28 ^f ± 0.41	2.35 ^f ± 0.07	3.36 ^f ± 0.04	4.45 ^f ± 1.54
ΣSFAs	17.59 ^g ± 0.03	16.46 ^g ± 0.04	18.33 ^g ± 0.02	20.60 ^g ± 3.22
ΣMUFAs	25.78 ^h ± 0.03	24.20 ^h ± 0.08	26.24 ^h ± 0.12	28.23 ^h ± 3.24
ΣPUFAs	56.63 ⁱ ± 0.06	59.34 ⁱ ± 0.10	55.43 ⁱ ± 0.14	51.16 ⁱ ± 6.45

^{a-i}Within a row, means without a common superscript differ ($p < 0.05$).

Table 5.2 summarizes the main components of the soybean oil extracted at each temperature regarding the free fatty acids (FFA), monoacylglycerols (MAG), diacylglycerols (DAG), and triacylglycerols (TAG) contents. The overall results from Table 5.2 are according to what has been found in the work of Pacheco et al. (2014). Tukey test with a 95% level indicated no significant differences between FFA, MAG, DAG, and TAG content extracted at different temperatures. However, the relative composition of free fatty acids in the final product tends to be lower with the increase in temperature. This might result from the fact that free fatty acids can be extracted more efficiently than MAG, DAG, and TAG at lower temperatures due to steric hindrance.

Table 5. 2 - Mean composition of the soybean oil extracted with p-cymene at each temperature.

Compound (%)	298.15 K	313.15 K	328.15 K	343.15 K
FFA	2.54 ^a ± 0.24	1.71 ^a ± 0.05	0.76 ^a ± 0.11	0.95 ^a ± 0.01
MAG	0.40 ^b ± 0.01	0.46 ^b ± 0.17	0.27 ^b ± 0.14	0.40 ^b ± 0.01
DAG	7.28 ^c ± 0.42	4.64 ^c ± 0.02	3.16 ^c ± 0.26	3.79 ^c ± 0.01
TAG	89.79 ^d ± 0.19	93.19 ^d ± 0.14	95.81 ^d ± 0.29	94.86 ^d ± 0.00

^{abcd}Within a row, means without a common superscript differ ($p < 0.05$).

The FTIR spectra of the extracted oil are presented in Fig. 5.2. The prominent identified peaks and their respective functional group assignments are shown in Table 5.3.

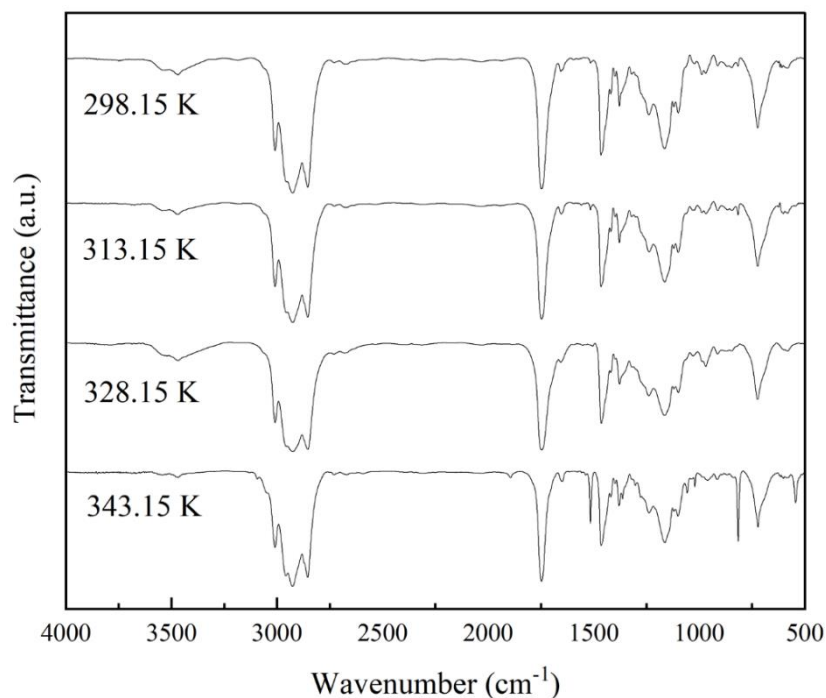


Figure 5. 2 - Fourier-transform infrared spectra of the soybean oil extracted with p-cymene in different temperatures.

Table 5. 3 - The extracted oil's prominent FTIR spectra peaks and their assignments.

Wavenumber (cm ⁻¹)	Functional group assignment
3,468	-OH stretching of hydroperoxide and FFAs of ≡C-H (Saeed and Naz, 2019)
3,009	-C-H stretching of the cis-double bound in unsaturated fatty acids (Saeed and Naz, 2019)
2,925	Asymmetric -C-H(-CH ₂) stretching (Srivastava and Semwal, 2013)
2,855	Symmetric -C-H(-CH ₂) stretching (Srivastava and Semwal, 2013; Aktar and Adal, 2019)
1,746	Aliphatic ester -C=O stretching (Saeed and Naz, 2019; Zahir et al., 2017); C=O stretching vibrations of aldehydes and ketones (Quiñones-Islas et al., 2013)
1,655	C=C stretching vibration of cis olefins (Quiñones-Islas et al., 2013; Zahir et al., 2017)
1,466	-C-H(-CH ₂) asymmetrical bending (Mitrea et al., 2022); CH ₂ scissoring vibrations of ethers (Aktar and Adal, 2019; Quiñones-Islas et al., 2013)
1,378	-C-H(-CH ₃) symmetrical bending (Mitrea et al., 2022); CH ₃ scissoring vibrations of ethers (Aktar and Adal, 2019; Quiñones-Islas et al., 2013).
1,164	-C-O stretching vibration (Mitrea et al., 2022; Aktar and Adal, 2019)
723	CH ₂ rocking mode (Aktar and Adal, 2019; Quiñones-Islas et al., 2013); bending -(CH ₂) _n - (Srivastava and Semwal, 2013)

The FTIR spectra is supported by what was found in other studies (Aktar and Adal, 2019; Naik et al., 2021; Quiñones-Islas et al., 2013; Saeed and Naz, 2019; Srivastava and Semwal, 2015; Zahir et al., 2017). The peak at 3009 cm⁻¹ is related to the linolenic and linoleic acyl groups (Zahir et al., 2017). The peaks at 2925 and 2855 cm⁻¹ confirm the presence of aldehydes (Saeed and Naz, 2019) and their richness in the polyunsaturated acyl

group (Aktar and Adal, 2019). The strong peak in 1746 cm^{-1} confirms that the oil has a high nutritional value (Srivastava and Semwal, 2013) related to the ester linkage attaching fatty acid to the glycerol of triglycerides (Naik et al., 2021). The peaks between 1500 and 900 cm^{-1} are assigned as the fingerprint region of lipids (Voort et al., 2008).

5.3.3 Response surface methodology results

The factors (temperature and solvent-to-solid mass ratio) and response (extraction yield at the equilibrium) for soybean oil extraction using p-cymene are presented in Table 5.4. The slight variation in the extraction yield between the central point indicates the reliability of the experimental results.

Table 5. 4 - Factors and responses for soybean oil extraction using p-cymene.

Run	Factors				Yield (g/g DM)
	Temperature (K)	Solvent-to-solid ratio (-)	x_1	x_2	
1	298.15	2.5	-1	-1	0.2296
2	328.15	2.5	1	-1	0.2481
3	298.15	7.5	-1	1	0.2344
4	328.15	7.5	1	1	0.2520
5	291.94	5	$-\sqrt{2}$	0	0.2227
6	334.36	5	$\sqrt{2}$	0	0.2526
7	313.15	1.46	0	$-\sqrt{2}$	0.2333
8	313.15	8.54	0	$\sqrt{2}$	0.2391
9 ^a	313.15	5	0	0	0.2507
10 ^a	313.15	5	0	0	0.2461
11 ^a	313.15	5	0	0	0.2487

^aCentral point

The parameter estimation was performed using the function *lm* from the *rsm* library in the open-source software R Studio (R Core Team, 2021). The simplified analysis of variance (ANOVA) is presented in Table 5.5, along with the standard error, t-value, and p-value for each parameter. The interaction term and the pure quadratic term for temperature were statistically considered insignificant since the p-values calculated were higher than the confidence level ($p < 0.05$).

Table 5. 5 - ANOVA for the yield of soybean oil extraction using p-cymene.

Coefficients	Estimate	Standard error	t-value	p-value	
Intercept	0.2485	0.0018	137.4342	3.87×10^{-10}	significant
x_1	0.0098	0.0011	8.8488	3.06×10^{-10}	significant
x_2	0.0021	0.0011	1.9089	0.1145	not significant
$x_1:x_2$	-0.0002	0.0016	-0.1386	0.8952	not significant
x_1^2	-0.0044	0.0013	-3.3400	0.0206	significant
x_2^2	-0.0051	0.0013	-3.8953	0.0115	significant

The model which describes the soybean oil extraction at the equilibrium as a function of temperature and the solvent-to-solid mass ratio is presented in Eq. 22. The R^2 is 0.9193, the R^2_{adj} is 0.8848, the F-statistic calculated for the model with 95% confidence is 26.6, and the p-value is 3.359×10^{-4} . The model is considered statistically significant because the p-value is lower than 0.05, and the F calculated is higher than the F tabulated ($F(3,7)_{0.05} = 4.3468$).

$$\text{Yield (g/g DM)} = 0.2485 + 0.0098x_1 - 0.0044x_1^2 - 0.0051x_2^2 \quad (22)$$

The Shapiro-Wilk normality test was performed to verify the hypothesis of the non-normality of the residues. As the p-value obtained ($p = 0.3836$) for the test was higher than the level of confidence of 95% ($p > 0.05$), the hypothesis of non-normality of the residues was rejected. The Breusch-Pagan test for heteroskedasticity was performed using the *olsrr* library; consequently, the error variance was verified to be constant. The perspective plot is presented in Fig. 5.3. Based on the RSM results, the solvent-to-solid mass ratio of 4 was used in the kinetic study due to lower solvent availability. However, the stationary points are around 330 K for the temperature and 5 for the solvent-to-solid mass ratio.

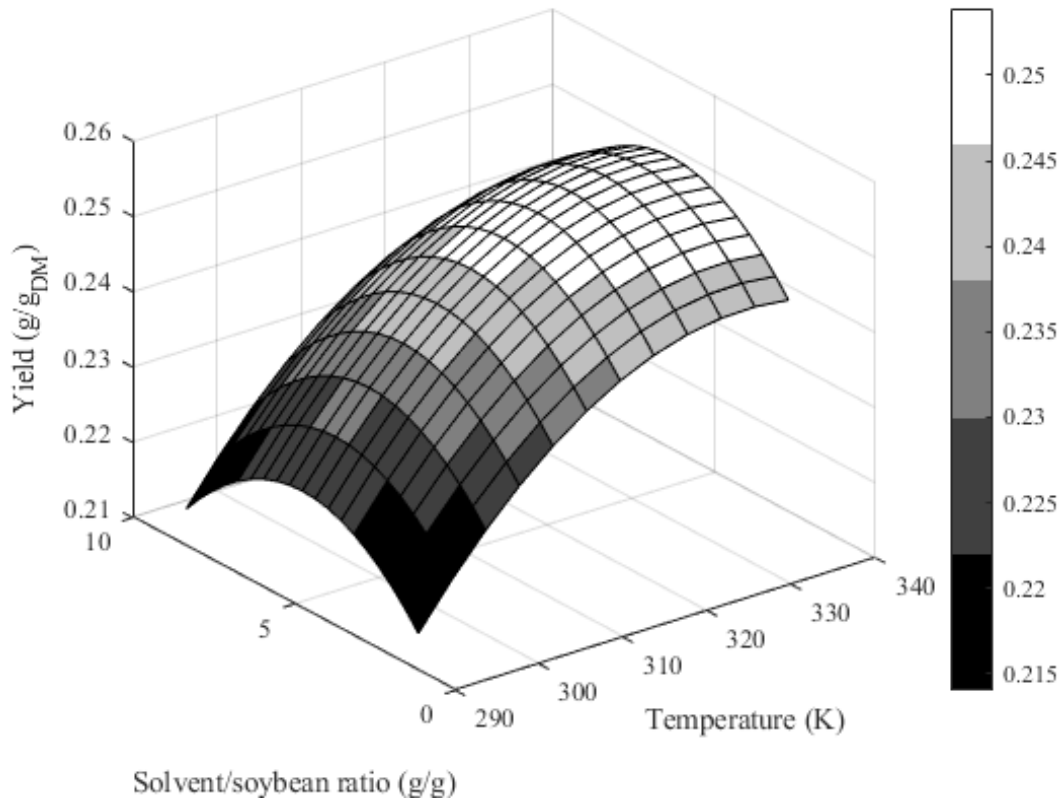


Figure 5. 3 - The perspective plot of soybean oil extraction using p-cymene.

The decrease in the yield of soybean oil extraction for high solvent-to-solid mass ratios might be related to the ability of the soybean oil, immediately extracted, to work as a co-solvent during the extraction in case of weak dilute solution. The unbalance of energy is reduced by increasing the volumetric fraction of vegetable oil in the solvent with a linear dependence. Theoretically, the best solvent would be the vegetable oil itself; however, there would not have driving forces to cause the mass transference from the solid to the bulk phase. The temperature has a positive effect on the extraction yield. As the temperature increases, the cohesive energy density of the molecule decreases.

5.3.4 Kinetic and thermodynamic analysis

The estimated mass transfer coefficients and concentration at equilibrium for the models within its statistical metrics are presented in Tables 5.6 to 5.9, along with its likelihood confidence intervals.

Table 5. 6 - Mass transfer coefficients and concentrations at equilibrium with the likelihood confidence interval and its statistical metrics for the first-order model (FOM).

T (K)	k (min^{-1})	C_{∞} (g/g DM)	R^2	χ^2	RMSE
298.15	0.1938 0.1218-0.3432	0.2072 0.1840-0.2314	0.9539	0.0108	0.0031
313.15	0.2511 0.1543-0.4496	0.2155 0.1930-0.2399	0.9528	0.0113	0.0045
328.15	0.2628 0.1521-0.5005	0.2266 0.2013-0.2543	0.9459	0.0131	0.0072
343.15	0.3738 0.1990-0.7474	0.2435 0.2166-0.2727	0.9350	0.0159	0.0093

Table 5. 7 - Mass transfer coefficients and concentrations at equilibrium with the likelihood confidence interval and statistical metrics for the second-order model (SOM).

T (K)	k (min^{-1})	C_{∞} (g/g DM)	R^2	χ^2	RMSE
298.15	1.3025 0.9718-1.7668	0.2237 0.2120-0.2359	0.9918	0.0019	8.7154×10^{-4}
313.15	1.6288 1.2451-2.1657	0.2323 0.2215-0.2433	0.9925	0.0018	8.8128×10^{-4}
328.15	1.5957 1.1941-2.1595	0.2447 0.2328-0.2571	0.9917	0.0020	0.0032
343.15	2.0670 1.4603-3.0062	0.2624 0.2482-0.2771	0.9877	0.0030	0.0048

Table 5. 8 - Mass transfer coefficients and concentrations at equilibrium with the likelihood confidence interval and its statistical metrics for MTKM.

T (K)	D/L^2 (min^{-1})	C_{∞} (g/g DM)	R^2	χ^2	RMSE
298.15	0.0522 0.0403-0.0687	0.2135 0.2013-0.2261	0.9887	0.0026	0.0012
313.15	0.0668 0.0503-0.0911	0.2221 0.2089-0.2357	0.9864	0.0032	0.0025
328.15	0.0676 0.0480-0.0990	0.2345 0.2180-0.2516	0.9811	0.0046	0.0048
343.15	0.0923 0.0574-0.1625	0.2519 0.2302-0.2749	0.9672	0.0080	0.0068

Table 5. 9 - Mass transfer coefficients and concentrations at equilibrium with the likelihood confidence interval and its statistical metrics for SMM.

<i>T</i> (K)	<i>k_d</i> (min ⁻¹)	<i>k_w</i> (min ⁻¹)	<i>C_∞^d</i> (g/g DM)	<i>C_∞^w</i> (g/g DM)	<i>C_∞</i> (g/g DM)	<i>R</i> ²	χ^2	<i>RMSE</i>
298.15	0.0826 0.0556-0.1379	0.9254 0.5263-10.0000	0.1343 0.1045-0.1784	0.0830 0.0387-0.1082	0.2173	0.9965	8.1051×10 ⁻⁴	6.9661×10 ⁻⁴
313.15	0.1142 0.0491-0.9391	1.6155 0.0904-10.0000	0.1483 0.0947-0.1818	0.0773 0.0399-0.1412	0.2256	0.9961	9.3764×10 ⁻⁴	0.0013
328.15	0.0851 0.0414-0.6347	0.9375 0.0656-10.0000	0.1286 0.0812-0.1831	0.1120 0.0542-0.1638	0.2406	0.9961	9.5833×10 ⁻⁴	0.0029
343.15	0.0952 0.0590-0.1827	1.2436 0.7417-10.0000	0.1292 0.0851-0.1800	0.1320 0.0757-0.1658	0.2612	0.9952	0.0012	0.0040

From Table 5.9, it can be seen that the likelihood confidence interval for k_w reaches the upper bound for the searching space used in the algorithm of particle swarm optimization, which was 10. It indicates that the contour of the SMM might be disjoint and unbounded (Schwaab et al., 2008) for being a complex nonlinear function with four parameters. Besides, the estimation of likelihood confidence intervals for bounded parameters needs a correction (Wu and Neale, 2012) that sometimes can be difficult to implement (Pritikin et al., 2017).

The statistical comparison of the models is presented in Tables 5.10 and 5.11. In Table 5.10, the Akaike information criterion and the adjusted coefficient of determination are presented. The best statistical metrics are associated with the SMM, followed by the SOM.

Table 5. 10 - Comparison of the models.

	<i>S</i>	<i>AIC</i>	R_{adj}^2	<i>S</i>	<i>AIC</i>	R_{adj}^2
<i>T (K)</i>		<i>FOM</i>			<i>SOM</i>	
298.15	0.0024	-88.6873	0.9488	4.3017×10^{-4}	-107.6416	0.9909
313.15	0.0026	-87.8979	0.9476	4.0948×10^{-4}	-108.1837	0.9917
328.15	0.0033	-85.2786	0.9399	5.0433×10^{-4}	-105.8918	0.9908
343.15	0.0044	-82.1451	0.9278	8.2784×10^{-4}	-100.4404	0.9863
<i>T (K)</i>		<i>MTKM</i>			<i>SMM</i>	
298.15	5.9123×10^{-4}	-104.1433	0.9874	1.8100×10^{-4}	-113.1642	0.9951
313.15	7.4519×10^{-4}	-101.5975	0.9849	2.1561×10^{-4}	-111.2393	0.9944
328.15	0.0011	-96.8331	0.9790	2.3983×10^{-4}	-110.0683	0.9944
343.15	0.0022	-89.6679	0.9636	3.2497×10^{-4}	-106.7263	0.9931

Notwithstanding, Fisher's test presented in Table 5.11 was performed to guarantee that the SMM has a better statistical result than the ones given by the models with fewer parameters. None of the models with two parameters can be considered statistically similar to the SMM for all the temperatures. From that, it can be stated that the kinetics of extraction of soybean oil using p-cymene occurs in two steps, washing and diffusion (So and Macdonald, 1986), which follows what has been found in the studies of Claux et al. (2021) and Kostić et al. (2014).

Table 5. 11 - F calculated for the models with two parameters compared to the So and Macdonald model in which $F_{crit}(2,7)_{0.05} = 4.734$.

<i>T (K)</i>	<i>FOM</i>	<i>SOM</i>	<i>MTKM</i>
298.15	98.0773	11.0130	18.1317
313.15	88.4705	7.1934	19.6495
328.15	102.0789	8.8229	28.6926
343.15	100.3177	12.3795	46.1588

This paper mainly used bootstrap resampling to assess the uncertainty of the fitting for the best model. Thus, to guarantee the reduction of the bias of the parameters, the nonlinear parameter estimation was performed on the original data with the bootstrap samples.

For the SMM case using bootstrap samples (see Table 5.12), the likelihood confidence intervals for k_w are not equal to the upper bound of the search space and have less variability than those in Table 5.9. Besides, the bootstrap technique has corrected the likelihood confidence interval. However, as it occurs in the work of Toda et al. (2016), there is still no temperature dependence for the mass transfer parameters k_d and k_w . The statistical parameters were not calculated because those metrics have no improvement. The results were compared through the coefficient of determination for the temperature dependence of C_∞ , and the thermodynamic assessment, with and without bias-reduction. The estimated parameters and their likelihood confidence intervals are presented in Table 5.12 for p-cymene in different temperatures and hexane at 328.15 K for comparison purposes.

Table 5. 12 - Mass transfer coefficients and concentrations at equilibrium condition with bootstrap resampling and the likelihood confidence interval for p-cymene and hexane.

T (K)	k_d (min⁻¹)	k_w (min⁻¹)	C_∞^d (g/g DM)	C_∞^w (g/g DM)	C_∞ (g/g DM)
p-cymene 298.15	0.0764 0.0761-0.0767	1.0555 1.0486-1.0616	0.1323 0.1320-0.1325	0.0864 0.0862-0.0867	0.2187
p-cymene 313.15	0.1017 0.1013-0.1020	1.5137 1.5005-1.5270	0.1411 0.1408-0.1413	0.0868 0.0865-0.0870	0.2279
p-cymene 328.15	0.0721 0.07919-0.0723	0.7827 0.7799-0.7852	0.1188 0.1185-0.1190	0.1278 0.1276-0.1280	0.2466
p-cymene 343.15	0.0863 0.0862-0.0867	1.0139 1.0129-1.0184	0.1226 0.1225-0.1229	0.1447 0.1444-0.1448	0.2673
hexane 328.15	0.0990 0.0987-0.0992	1.8908 1.8712-1.9048	0.1542 0.1540-0.1544	0.0814 0.0812-0.0816	0.2356

The average experimental data with the bootstrap samples and the simulations are presented in Fig. 5.4. It can be seen from the simulations at 328.15 K that p-cymene has presented a higher yield of soybean oil extraction than what is observed for hexane. Although its kinetic curves are very similar, the estimated yield of soybean oil extraction in the equilibrium at 328.15 K using p-cymene was higher. This is an interesting finding, and it could be hypothesized that p-cymene might be a candidate to replace the industrial use of hexane from a technical standpoint. Therefore, it can be stated that the $\ln(IDAC)$ obtained using the COSMO-SAC theory was capable of describing the better yield of soybean oil extraction for p-cymene than for hexane.

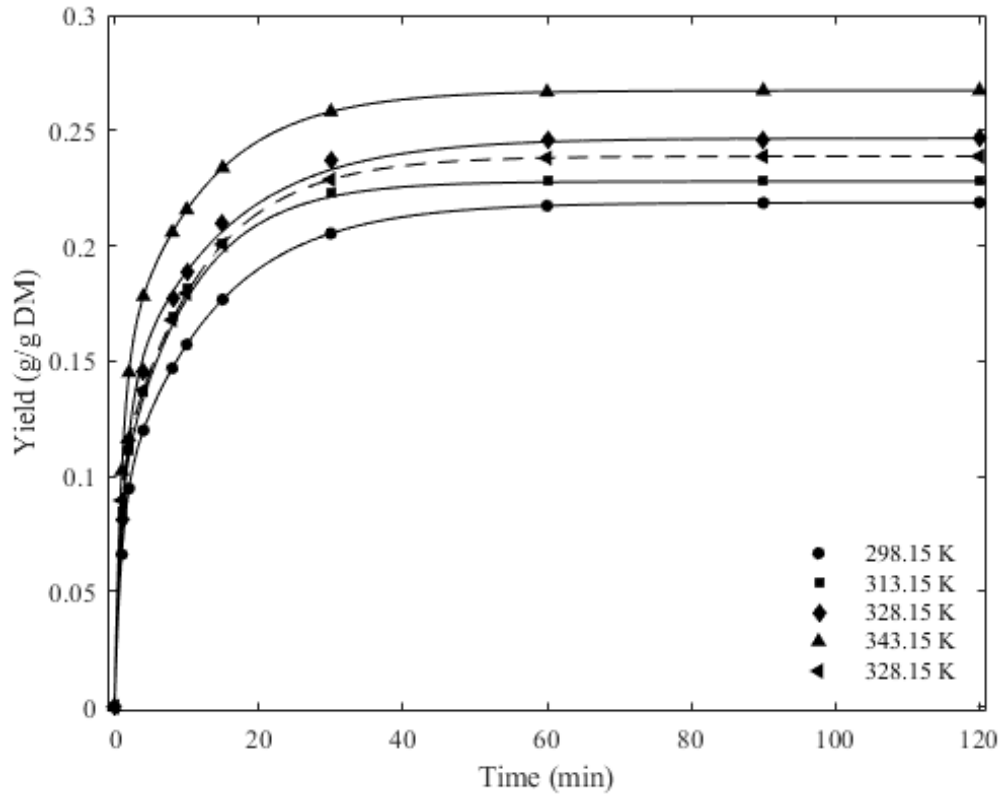


Figure 5. 4 - Average between the experimental data and the bootstrap samples and simulation of soybean oil extraction using p-cymene (continuous line) and hexane (dashed line).

Ibemesi and Attah (1990) used Eq. 23 to describe the effect of temperature on oil extraction yield at the equilibrium (C_{∞}).

$$C_{\infty} = Y_0 m^{\frac{T-273.15}{10}} \quad (23)$$

where Y_0 is the extraction yield at 273.15 K (g/g DM), and m is the temperature extraction coefficient (-).

This analysis was performed for the SMM with and without bootstrap samples. In the first case, a higher R^2 resulted from the efforts to minimize the bias for C_{∞} . The parameters m and Y_0 , when using bootstrap samples, were 1.0472 and 0.1923 g/g DM, respectively, with R^2 equal to 0.9826. In the case without bootstrap samples, i.e., when not using uncertainty calculation, the parameters m and Y_0 were 1.0427 and 0.1931 g/g DM, respectively, with R^2 equal to 0.9753. Despite the concentration of soybean oil extracted at the equilibrium is intrinsically related to the temperature, the mass transfer parameters for the SMM do not have temperature dependence. From what has previously been mentioned, the higher R^2 obtained

when using the bootstrap resampling shows that the method can reduce the bias of the estimators.

Not less important, the same analysis was performed to obtain the standard enthalpy, standard entropy, and standard Gibbs free energy changes, and the same result was observed. It can be seen in Table 5.13 that the coefficient of correlation has a slight advantage when using the bootstrap method.

Table 5. 13 - Thermodynamic assessment with and without bootstrap resampling (BS).

Case	T (K)	K	ΔH^0 (kJ.mol ⁻¹)	ΔS^0 (kJ.mol ⁻¹ .K ⁻¹)	ΔG^0 (kJ.mol ⁻¹)	R ²
with BS	298.15	2.2389	19.3395	0.0701	-1.5751	0.9533
	313.15	2.5757			-2.6273	
	328.15	3.5339			-3.6795	
	343.15	5.4460			-4.7318	
without BS	298.15	2.1931	16.4053	0.0603	-1.5978	0.9387
	313.15	2.4851			-2.5035	
	328.15	3.1749			-3.4093	
	343.15	4.7334			-4.3150	

The thermodynamic analysis shows that the extraction using p-cymene is random and irreversible ($\Delta S^0 > 0$), endothermic ($\Delta H^0 > 0$), and spontaneous ($\Delta G^0 < 0$). The results are according to what was found in other studies of vegetable oil extraction (Gasparetto et al., 2022b; Meziane and Kadi, 2008; Rodrigues et al., 2010).

5.4 CONCLUSIONS

The soybean oil extraction using p-cymene as a green solvent was investigated. The response surface methodology has correctly described the effects of temperature and solvent-to-solid mass ratio in the yield of soybean oil extraction at the equilibrium. For the soybean oil extracted at different temperatures, it was obtained its fatty acid profile and FTIR spectra, observing that the oil has high oxidative stability and is rich in polyunsaturated fatty acids. The SMM has shown to be the best model to describe this type of solid-liquid extraction. The bootstrap method was capable of reducing the bias of the estimators concerning the analysis of the likelihood confidence interval, the temperature dependence of C_∞ , and the thermodynamic assessment. Further, the better solubilization of the triacylglycerols by p-cymene was correctly described by the infinite dilution activity coefficient obtained through the COSMO-SAC theory. The results show that soybean oil extraction using p-cymene is a

good option for the replacement of hexane in the industry because of its superior extraction yield at 328.15 K.

CONFLICT OF INTERESTS

None.

ACKNOWLEDGMENT

The authors are grateful for the financial support and scholarships of the Human Resources Program of the National Agency for Petroleum, Natural Gas and Biofuels – PRH-ANP through the Human Resources Training Program for Petroleum and Biofuels Processing (PRH 52.1). The authors also acknowledge the soy-crushing company Granol for donating the soybean flakes.

REFERENCES

- M.H. Abdellah, C.A. Scholes, L. Liu, S.E. Kentish. Efficient Degumming of Crude Canola Oil Using Ultrafiltration Membranes and Bio-Derived Solvents. *Innovative Food Science & Emerging Technologies*, 59 (2020) 102274. <https://doi.org/10.1016/j.ifset.2019.102274>
- M.H. Abdellah, L. Liu, C.A. Scholes, B.D. Freeman, S.E. Kentish. Organic Solvent Nanofiltration of Binary Vegetable Oil/Terpene Mixtures: Experiments and Modelling. *Journal of Membrane Science*, 573 (2019) 694–703. <https://doi.org/10.1016/j.memsci.2018.12.026>
- T. Aktar, E. Adal. Determining the Arrhenius Kinetics of Avocado Oil: Oxidative Stability under Rancimat Test Conditions. *Foods*, 8 (2019) 236. <https://doi.org/10.3390/foods8070236>
- M.M. Batista, R. Guirardello, M.A. Krähenbühl. Determination of the Hansen Solubility Parameters of Vegetable Oils, Biodiesel, Diesel, and Biodiesel-Diesel Blends. *Journal of the American Oil Chemists' Society*, 92 (2014) 95–109. <https://doi.org/10.1007/s11746-014-2575-2>
- A. Benazzouz, L. Moity, C. Pierlot, M. Sergent, V. Molinier, J.-M. Aubry. Selection of a Greener Set of Solvents Evenly Spread in the Hansen Space by Space-Filling Design. *Industrial & Engineering Chemistry Research*, 52 (2013) 16585–16597. <https://doi.org/10.1021/ie402410w>
- S. Bertouche, V. Tomao, A. Hellal, C. Boutekedjiret, F. Chemat. First Approach on Edible Oil Determination in Oilseeds Products Using Alpha-Pinene. *Journal of Essential Oil Research*, 25 (2013) 439–443. <https://doi.org/10.1080/10412905.2013.782473>

T. Brouwer, B. Schuur. Model Performances Evaluated for Infinite Dilution Activity Coefficients Prediction at 298.15 K. *Industrial & Engineering Chemistry Research*, 58 (2019) 8903–8914. <https://doi.org/10.1021/acs.iecr.9b00727>

R.H. Byrd, J.C. Gilbert, J. Nocedal. A Trust Region Method Based on Interior Point Techniques for Nonlinear Programming. *Mathematical Programming*, 89 (2000) 149–185.

R.H. Byrd, M.E. Hribar, J. Nocedal. An Interior Point Algorithm for Large-Scale Nonlinear Programming. *SIAM Journal on Optimization*, 9 (1999) 877–900.

M.M. Cascant, C. Breil, S. Garrigues, M. de la Guardia, A.S. Fabiano-Tixier, F. Chemat. A Green Analytical Chemistry Approach for Lipid Extraction: Computation Methods in the Selection of Green Solvents as Alternative to Hexane. *Analytical and Bioanalytical Chemistry*, 409 (2017) 3527–3539. <https://doi.org/10.1007/s00216-017-0323-9>

C.-H. Chan, R. Yusoff, G.-C. Ngoh. Modeling and kinetics study of conventional and assisted batch solvent extraction. *Chemical Engineering Research and Design*, 92 (2014) 1169–1186. <https://doi.org/10.1016/j.cherd.2013.10.001>

X. Chen, Y. Luo, B. Qi, Y. Wan. Simultaneous extraction of oil and soy isoflavones from soy sauce residue using ultrasonic-assisted two-phase solvent extraction technology. *Separation and Purification Technology*, 128 (2014) 72–79. <https://doi.org/10.1016/j.seppur.2014.03.014>

M.-H. Cheng, K.A. Rosentrater. Economic Feasibility Analysis of Soybean Oil Production by Hexane Extraction. *Industrial Crops and Products*, 108 (2017) 775–785. <https://doi.org/10.1016/j.indcrop.2017.07.036>

M.-H. Cheng, J.J.K. Sekhon, K.A. Rosentrater, T. Wang, S. Jung, L.A. Johnson. Environmental Impact Assessment of Soybean Oil Production: Extruding-Expelling Process, Hexane Extraction and Aqueous Extraction. *Food and Bioproducts Processing*, 108 (2018) 58–68. <https://doi.org/10.1016/j.fbp.2018.01.001>

M.-H. Cheng, K.A. Rosentrater. Techno-Economic Analysis of Extruding-Expelling of Soybeans to Produce Oil and Meal. *Agriculture*, 9 (2019) 87. <https://doi.org/10.3390/agriculture9050087>

O. Claux, V. Rapinel, P. Goupy, N. Patouillard, M.A. Vian, L. Jacques, F. Chemat. Dry and Aqueous 2-Methyloxolane as Green Solvents for Simultaneous Production of Soybean Oil and Defatted Meal. *ACS Sustainable Chemistry & Engineering*, 9 (2021) 7211–7223. <https://doi.org/10.1021/acssuschemeng.0c09252>

T.F. Coleman, Y. Li. An Interior, Trust Region Approach for Nonlinear Minimization Subject to Bounds. *SIAM Journal on Optimization*, 6 (1996) 418–445.

T.F. Coleman, Y. Li. On the Convergence of Reflective Newton Methods for Large-Scale Nonlinear Minimization Subject to Bounds. *Mathematical Programming*, 67 (1994) 189–224.

A. Comerlato, F.A. Voll, A.L. Daga, É. Fontana. Mass Transfer in Soybean Oil Extraction Using Ethanol/Isopropyl Alcohol Mixtures. *International Journal of Heat and Mass Transfer*, 165 (2021) 120630. <https://doi.org/10.1016/j.ijheatmasstransfer.2020.120630>

B. Coto, I. Suárez, M.J. Tenorio, S. Nieto, N. Alvarez, J.L. Peña. Oil acidity reduction by extraction with imidazolium ionic liquids: Experimental, COSMO description and reutilization study. *Separation and Purification Technology*, 254 (2021) 117529. <https://doi.org/10.1016/j.seppur.2020.117529>

J.L.A. Dagostin, D. Carpiné, M.L. Corazza. Extraction of Soybean Oil Using Ethanol and Mixtures with Alkyl Esters (Biodiesel) as Co-Solvent: Kinetics and Thermodynamics. *Industrial Crops and Products*, 74 (2015) 69–75. <https://doi.org/10.1016/j.indcrop.2015.04.054>

J.L.A. Dagostin, D. Carpiné, P.R.S dos Santos, M.L. Corazza. Liquid-Liquid Equilibrium and Kinetics of Ethanolic Extraction of Soybean Oil Using Ethyl Acetate as Co-Solvent. *Brazilian Journal of Chemical Engineering*, 35 (2018) 415–428. <https://doi.org/10.1590/0104-6632.20180352s20160175>

A.C. Davison, D.V. Hinkley. *Bootstrap Methods and Their Application*. Cambridge University Press, 1997.

B. Efron, R.J. Tibshirani. *An Introduction to the Bootstrap*. CRC Press, 1994.

F. Ferrarini, G.B. Flôres, A.R. Muniz, R.P. de Soares. An Open and Extensible Sigma-Profile Database for COSMO-Based Models. *AIChE Journal*, 64 (2018) 3443–3455. <https://doi.org/10.1002/aic.16194>

H. Gasparetto, F. Castilhos, N.P.G. Salau. Recent advances in green soybean oil extraction: A review. *Journal of Molecular Liquids*, 361 (2022a) 119684. <https://doi.org/10.1016/j.molliq.2022.119684>

H. Gasparetto, A.L.B. Nunes, F. Castilhos, N.P.G. Salau. Soybean oil extraction using ethyl acetate and 1-butanol: from solvent selection to thermodynamic assessment, *Journal of Industrial and Engineering Chemistry*, (2022b). <https://doi.org/10.1016/j.jiec.2022.06.020>

R.P. Gerber, R.P. Soares. Assessing the Reliability of Predictive Activity Coefficient Models for Molecules Consisting of Several Functional Groups. *Brazilian Journal of Chemical Engineering*, 30 (2013) 1–11. <https://doi.org/10.1590/s0104-66322013000100002>

R.P. Gerber, R. P. Soares. Prediction of Infinite-Dilution Activity Coefficients Using UNIFAC and COSMO-SAC Variants. *Industrial & Engineering Chemistry Research*, 49 (2010) 7488–7496. <https://doi.org/10.1021/ie901947m>

J.A. Gerde, E.G. Hammond, L.A. Johnson, C. Su, T. Wang, P.J. White. Soybean Oil. *Bailey's Industrial Oil and Fat Products*, (2020) 1–68. <https://doi.org/10.1002/047167849x.bio041.pub2>

P.E. Gill, W. Murray, M.H. Wright. *Practical Optimization*, London, Academic Press, 1981.

S.P. Han. Globally Convergent Method for Nonlinear Programming. *Journal of Optimization Theory and Applications*, 22 (1977) 297.

C.M. Hansen. Hansen Solubility Parameters a User's Handbook. CRC Press, Taylor & Francis Group, 2018.

L. Hartman, R.C. Lago. Rapid preparation of fatty acid methyl esters from lipids. *Lab Pract.* 22 (1973) 475-494.

J.A. Ibemesi, J.C. Attah. Temperature Effects on the Extraction of Rubber and Melon Seed Oils. *Journal of the American Oil Chemists' Society*, 67 (1990) 443–445. <https://doi.org/10.1007/bf02638958>

O.A.Q. Jimenez, V.V. Lemos, E.A.C. Batista, M.P. Rolemberg, R.C. Basso. Hansen Solubility Parameters and Thermodynamic Modeling for LLE Description during Glycerol-Settling in Ester Production from Coconut Oil. *Fuel*, 241 (2019) 725–732. <https://doi.org/10.1016/j.fuel.2018.12.029>

J. Kennedy, R. Eberhart. Particle Swarm Optimization. *Proceedings of the IEEE International Conference on Neural Networks*. Perth, Australia, (1995) 1942–1945.

S.K. Kim, S. Brand, H.-S. Lee, Y. Kim, J. Kim. Production of Renewable Diesel by Hydrotreatment of Soybean Oil: Effect of Reaction Parameters. *Chemical Engineering Journal*, 228 (2013) 114–123. <https://doi.org/10.1016/j.cej.2013.04.095>

M.D. Kostić, N.M. Joković, O.S. Stamenković, K.M. Rajković, P.S. Milić, V.B. Veljković. The Kinetics and Thermodynamics of Hempseed Oil Extraction by n-Hexane. *Industrial Crops and Products*, 52 (2014) 679–686. <https://doi.org/10.1016/j.indcrop.2013.11.045>

J.C. Lagarias, J.A. Reeds, M.H. Wright, P.E. Wright. Convergence Properties of the Nelder-Mead Simplex Method in Low Dimensions. *SIAM Journal of Optimization*. 9 (1998) 112–147.

K. Levenberg. A Method for the Solution of Certain Problems in Least-Squares. *Quarterly Applied Mathematics* 2 (1944) 164–168.

Y. Li, F. Fine, A.-S. Fabiano-Tixier, M. Abert-Vian, P. Carre, X. Pages, F. Chemat. Evaluation of Alternative Solvents for Improvement of Oil Extraction from Rapeseeds. *Comptes Rendus Chimie*, 17 (2014) 242–251. <https://doi.org/10.1016/j.crci.2013.09.002>

Z. Li, K.H. Smith, G.W. Stevens. The Use of Environmentally Sustainable Bio-Derived Solvents in Solvent Extraction Applications - A Review. *Chinese Journal of Chemical Engineering*, 24 (2016) 215–220. <https://doi.org/10.1016/j.cjche.2015.07.021>

S. Lin, S.I. Sandler. A Priori Phase Equilibrium Prediction from a Segment Contribution Solvation Model. *Industrial & Engineering Chemistry Research*, 41 (2001) 899-913. <https://doi.org/10.1021/ie001047w>

D. Marquardt. An Algorithm for Least-squares Estimation of Nonlinear Parameters. *SIAM Journal Applied Mathematics*, 11 (1963) 431–441.

B.T.F. de Mello, I.J. Iwassa, R.P. Cuco, V.A.S. Garcia, C. da Silva. Methyl Acetate as Solvent in Pressurized Liquid Extraction of Crambe Seed Oil. *The Journal of Supercritical Fluids*, 145 (2019) 66–73. <https://doi.org/10.1016/j.supflu.2018.11.024>

S. Meziane, H. Kadi. Kinetics and Thermodynamics of Oil Extraction from Olive Cake. *Journal of the American Oil Chemists' Society*, 85 (2008) 391–396. <https://doi.org/10.1007/s11746-008-1205-2>

E. Mezura-Montes, C.A. Coello. Constraint-handling in nature-inspired numerical optimization: Past, present and future. *Swarm and Evolutionary Computation*. (2011) 173–194.

S.T. Mgoma, M. Basitere, V.V. Mshayisa. Kinetics and Thermodynamics of Oil Extraction from South African Hass Avocados Using Hexane as a Solvent. *South African Journal of Chemical Engineering*, 37 (2021) 244–251. <https://doi.org/10.1016/j.sajce.2021.06.007>

L. Mitrea, B.-E. Teleky, L.-F. Leopold, S.-A. Nemes, D. Plamada, F.V. Dulf, I.-D., Pop, D.C. Vodnar. The Physicochemical Properties of Five Vegetable Oils Exposed at High Temperature for a Short-Time-Interval. *Journal of Food Composition and Analysis*, 106 (2022) 104305. <https://doi.org/10.1016/j.jfca.2021.104305>

MOPAC2009, James J. P. Stewart, *Stewart Computational Chemistry*, (2008). <http://OpenMOPAC.net>

J.J. Moré. The Levenberg-Marquardt Algorithm: Implementation and Theory. *Numerical Analysis*, ed. G. A. Watson, *Lecture Notes in Mathematics* 630, Springer Verlag, (1977) 105–116.

J.J. Moré, B.S. Garbow, K.E. Hillstom. *User Guide for MINPACK 1*. Argonne National Laboratory, (1980) 80–74.

M. Naik, V. Natarajan, A. Rawson, J. Rangarajan, L. Manickam. Extraction Kinetics and Quality Evaluation of Oil Extracted from Bitter Gourd (*Momardica Charantia* L.) Seeds Using Emergent Technologies. *LWT*, 140 (2021) 110714. <https://doi.org/10.1016/j.lwt.2020.110714>

D.J. Nicolin, D.F. Rossoni, L.M.M. Jorge. Study of Uncertainty in the Fitting of Diffusivity of Fick's Second Law of Diffusion with the Use of Bootstrap Method. *Journal of Food Engineering*, 184 (2016) 63–68. <https://doi.org/10.1016/j.jfoodeng.2016.03.024>

A.L.B. Nunes, F. Castilhos. Chemical Interesterification of Soybean Oil and Methyl Acetate to FAME Using CaO as Catalyst. *Fuel*, 267 (2020) 117264. <https://doi.org/10.1016/j.fuel.2020.117264>

R. Oliveira, V. Oliveira, K.K. Aracava, C.E.C. Rodrigues. Effects of the Extraction Conditions on the Yield and Composition of Rice Bran Oil Extracted with Ethanol - A Response Surface Approach. *Food and Bioproducts Processing*, 90 (2012) 22–31. <https://doi.org/10.1016/j.fbp.2011.01.004>

G.V. Olivieri, J.V. de Quadros Jr, R. Giudici. Epoxidation Reaction of Soybean Oil: Experimental Study and Comprehensive Kinetic Modeling. *Industrial & Engineering Chemistry Research*, 59 (2020) 18808–18823. <https://doi.org/10.1021/acs.iecr.0c03847>

C. Pacheco, C. Palla, G.H. Crapiste, M.E. Carrín. Simultaneous Quantification of FFA, MAG, DAG, and TAG in Enzymatically Modified Vegetable Oils and Fats. *Food Analytical Methods*, 7 (2014) 2013-2022. <https://doi.org/10.1007/s12161-014-9830-x>

S.A. Pasiás, N.K. Barakos, N.G. Papayannakos. Catalytic Effect of Free Fatty Acids on Cotton Seed Oil Thermal Transesterification. *Industrial & Engineering Chemistry Research*, 48 (2009) 4266-4273. <https://doi.org/10.1021/ie801365k>

M.E. Pedersen. *Good Parameters for Particle Swarm Optimization*. Luxembourg: Hvas Laboratories, 2010.

L. Phan, H. Brown, J. White, A. Hodgson, P.G. Jessop. Soybean Oil Extraction and Separation Using Switchable or Expanded Solvents. *Green Chem.*, 11 (2009) 53–59. <https://doi.org/10.1039/b810423a>

S. Pinzi, P. Rounce, J.M. Herreros, A. Tsolakis, M.P. Dorado. The Effect of Biodiesel Fatty Acid Composition on Combustion and Diesel Engine Exhaust Emissions. *Fuel*, 104 (2013) 170–182. <https://doi.org/10.1016/j.fuel.2012.08.056>

J.N. Pritikin, L.M. Rappaport, M.C. Neale. Likelihood-Based Confidence Intervals for a Parameter with an Upper or Lower Bound. *Structural Equation Modeling: A Multidisciplinary Journal*. 24 (2017) 395-401. <https://doi.org/10.1080/10705511.2016.1275969>

E. Potrich, S.C. Miyoshi, P.F.S. Machado, F.F. Furlan, M.P.A. Ribeiro, P.W. Tardioli, R.L.C. Giordano, A.J.G. Cruz, R.C. Giordano. Replacing Hexane by Ethanol for Soybean Oil Extraction: Modeling, Simulation, and Techno-Economic-Environmental Analysis. *Journal of Cleaner Production*, 244 (2020) 118660. <https://doi.org/10.1016/j.jclepro.2019.118660>

M.J.D. Powell. A Fast Algorithm for Nonlinearly Constrained Optimization Calculations. *Numerical Analysis*, ed. G. A. Watson, Lecture Notes in Mathematics, Springer-Verlag, 1978a.

M.J.D. Powell. A Fortran Subroutine for Solving Systems of Nonlinear Algebraic Equations. *Numerical Methods for Nonlinear Algebraic Equations*, P. Rabinowitz, 1970.

M.J.D. Powell. The Convergence of Variable Metric Methods for Nonlinearly Constrained Optimization Calculations. *Nonlinear Programming 3* (O. L. Mangasarian, R. R. Meyer, and S. M. Robinson, eds.), Academic Press, 1978b.

N. Quiñones-Islas, O.G. Meza-Márquez, G. Osorio-Revilla, T. Gallardo-Velazquez. Detection of Adulterants in Avocado Oil by Mid-FTIR Spectroscopy and Multivariate Analysis. *Food Research International*, 51 (2013) 148–154. <https://doi.org/10.1016/j.foodres.2012.11.037>

R Core Team (2021). *R: A language and environment for statistical computing*. R Foundation for Statistical Computing, Vienna, Austria. <https://www.R-project.org/>

A. Rai, B. Mohanty, R. Bhargava. Modeling and response surface analysis of supercritical extraction of watermelon seed oil using carbon dioxide. *Separation and Purification Technology*, 141 (2015) 354-365. <https://doi.org/10.1016/j.seppur.2014.12.016>

- J.S. Ribeiro, D. Celante, L.N. Brondani, D.O. Trojahn, C. Silva, F. Castilhos. Synthesis of methyl esters and triacetin from macaw oil (*Acrocomia aculeata*) and methyl acetate over γ -alumina, *Industrial Crops & Products*, 124 (2018) 84-90. <https://doi.org/10.1016/j.indcrop.2018.07.062>
- C.E.C. Rodrigues, K.K. Aracava, F.N. Abreu. Thermodynamic and Statistical Analysis of Soybean Oil Extraction Process Using Renewable Solvent. *International Journal of Food Science & Technology*, 45 (2010) 2407–2414. <https://doi.org/10.1111/j.1365-2621.2010.02417.x>
- C.E.C. Rodrigues, C.B. Gonçalves, E.C. Marcon, E.A.C. Batista, A.J.A. Meirelles. Deacidification of rice bran oil by liquid-liquid extraction using renewable solvent. *Separation and Purification Technology*, 132 (2014) 84-92. <https://doi.org/10.1016/j.seppur.2014.05.009>
- G.M. Rodrigues, L. Cardozo-Filho, C. da Silva. Pressurized Liquid Extraction of Oil from Soybean Seeds. *The Canadian Journal of Chemical Engineering*, 95 (2017) 2383–2389. <https://doi.org/10.1002/cjce.22922>
- A. Rohman, M.A.B. Ghazali, A. Windarsih, Irnawati, S. Riyanto, F.M. Yusof, S. Mustafa. Comprehensive Review on Application of FTIR Spectroscopy Coupled with Chemometrics for Authentication Analysis of Fats and Oils in the Food Products. *Molecules*. 25 (2020) 5485. <https://doi.org/10.3390/molecules25225485>
- R. Saeed, S. Naz. Effect of Heating on the Oxidative Stability of Corn Oil and Soybean Oil. *Grasas y Aceites*, 70 (2019) 303. <https://doi.org/10.3989/gya.0698181>
- K.A. Santos, C.M. de Aguiar, E.A. da Silva, C. da Silva. Evaluation of Favela Seed Oil Extraction with Alternative Solvents and Pressurized-Liquid Ethanol. *The Journal of Supercritical Fluids*, 169 (2021) 105125. <https://doi.org/10.1016/j.supflu.2020.105125>
- S.B. dos Santos, M.A. Martins, A.L. Caneschi, P.R.M. Aguiar, J.S.R. Coimbra. Kinetics and Thermodynamics of Oil Extraction from *Jatropha curcas* L. using Ethanol as a Solvent. *International Journal of Chemical Engineering*, 2015 (2015) 1–9. <https://doi.org/10.1155/2015/871236>
- M.S.M. Sarip, N.A. Morad, Y. Yamashita, T. Tsuji, M.A.C. Yunus, M.K.A. Aziz, H.L. Lam. Crude palm oil (CPO) extraction using hot compressed water (HCW). *Separation and Purification Technology*, 169 (2016) 103-112. <https://doi.org/10.1016/j.seppur.2016.06.001>
- M.M. Sawada, L.L. Venâncio, T.A. Toda, C.E.C. Rodrigues. Effects of Different Alcoholic Extraction Conditions on Soybean Oil Yield, Fatty Acid Composition and Protein Solubility of Defatted Meal. *Food Research International*, 62 (2014) 662–670. <https://doi.org/10.1016/j.foodres.2014.04.039>
- A. Sharma, S.K. Khare, M.N. Gupta. Three Phase Partitioning for Extraction of Oil from Soybean. *Bioresource Technology*, 85 (2002) 327–329. [https://doi.org/10.1016/s0960-8524\(02\)00138-4](https://doi.org/10.1016/s0960-8524(02)00138-4)
- A.-G. Sicaire, M. Vian, F. Fine, F. Joffre, P. Carré, S. Tostain, F. Chemat. Alternative Bio-Based Solvents for Extraction of Fat and Oils: Solubility Prediction, Global Yield, Extraction

Kinetics, Chemical Composition and Cost of Manufacturing. *International Journal of Molecular Sciences*, 16 (2015) 8430–8453. <https://doi.org/10.3390/ijms16048430>

G.C. So, D.G. Macdonald. Kinetics of Oil Extraction from Canola (Rapeseed). *The Canadian Journal of Chemical Engineering*, 64 (1986) 80–86. <https://doi.org/10.1002/cjce.5450640112>

R.P. Soares. The Combinatorial Term for COSMO-Based Activity Coefficient Models. *Industrial & Engineering Chemistry Research*, 50 (2011) 3060–3063. <https://doi.org/10.1021/ie102087p>

Y. Srivastava, A.D. Semwal. A Study on Monitoring of Frying Performance and Oxidative Stability of Virgin Coconut Oil (VCO) during Continuous/Prolonged Deep Fat Frying Process Using Chemical and FTIR Spectroscopy. *Journal of Food Science and Technology*, 52 (2013) 984–991. <https://doi.org/10.1007/s13197-013-1078-8>

C.D. Tanzi, M.A. Vian, F. Chemat. New Procedure for Extraction of Algal Lipids from Wet Biomass: A Green Clean and Scalable Process. *Bioresource Technology*, 134 (2013) 271–275. <https://doi.org/10.1016/j.biortech.2013.01.168>

C.D. Tanzi, M.A. Vian, C. Ginies, M. Elmaataoui, F. Chemat. Terpenes as Green Solvents for Extraction of Oil from Microalgae. *Molecules*, 17 (2012) 8196–8205. <https://doi.org/10.3390/molecules17078196>

T.A. Toda, M.M. Sawada, C.E.C. Rodrigues. Kinetics of Soybean Oil Extraction Using Ethanol as Solvent: Experimental Data and Modeling. *Food and Bioprocess Technology*, 98 (2016) 1–10. <https://doi.org/10.1016/j.fbp.2015.12.003>

K. Tomita, S. Machmudah, Wahyudiono, R. Fukuzato, H. Kanda, A.T. Quitain, M. Sasaki, M. Goto. Extraction of rice bran oil by supercritical carbon dioxide and solubility consideration. *Separation and Purification Technology*, 125 (2014) 319–325. <https://doi.org/10.1016/j.seppur.2014.02.008>

R. Valand, S. Tanna, G. Lawson, L. Bengtström. A review of Fourier Transform Infrared (FTIR) spectroscopy used in food adulteration and authenticity investigations. *Food Additives & Contaminants: Part A*. 37 (2020) 19–38. <https://doi.org/10.1080/19440049.2019.1675909>

D.L. Vineyard, W.W. Ingwersen. A Comparison of Major Petroleum Life Cycle Models. *Clean Technologies and Environmental Policy*, 19 (2016) 735–747. <https://doi.org/10.1007/s10098-016-1260-6>

F.R.Voort, A. Ghetler, D.L. García-González, Y.D. Li. Perspectives on Quantitative Mid-FTIR Spectroscopy in Relation to Edible Oil and Lubricant Analysis: Evolution and Integration of Analytical Methodologies. *Food Analytical Methods*, 1 (2008) 153–163. <https://doi.org/10.1007/s12161-008-9031-6>

R.A.Waltz, J.L. Morales, J. Nocedal, D. Orban. An interior algorithm for nonlinear optimization that combines line search and trust region steps. *Mathematical Programming*, 107 (2006) 391–408. <https://doi.org/10.1007/s10107-004-0560-5>

H. Wu, M.C. Neale. Adjusted Confidence Intervals for a Bounded Parameter. *Behavior Genetics*, 42 (2012) 886–898. <https://doi.org/10.1007/s10519-012-9560-z>

E. Zahir, R. Saeed, M.A. Hameed, A. Yousuf. Study of Physicochemical Properties of Edible Oil and Evaluation of Frying Oil Quality by Fourier Transform-Infrared (FT-IR) Spectroscopy. *Arabian Journal of Chemistry*, 10 (2017) S3870-S3876. <https://doi.org/10.1016/j.arabjc.2014.05.025>

6 A NOVEL APPLICATION OF THE FRACTIONAL-ORDER MODEL TO GREEN SOYBEAN OIL EXTRACTION

Henrique Gasparetto, Fernanda de Castilhos, Nina Paula Gonçalves Salau

Chemical Engineering Department, Federal University of Santa Maria, Brazil

ABSTRACT

The fractional-order calculus was applied to soybean oil extraction using different solvents at different temperatures. The fractional model was derived from the regular power law first-order model using the Caputo fractional derivative and the Mittag-Leffler function. The fractional model (FOKM) and first-order model (FOM) were compared using the fitted coefficient of determination, the Akaike information criterion, and Fisher's exact test. The FOKM achieved the best statistical metrics with R_{adj}^2 over 0.9841 compared to 0.9043 for FOM. The AIC for FOKM was higher in almost all cases, and Fisher's exact test showed that FOM is not statistically similar to FOKM. Both models presented the residues normality by the Shapiro-Wilk normality test. A higher correlation between the parameters was found for the FOKM. However, it must be emphasized that the fractional model produced statistically significant improvements when fitting the data.

Keywords: Modeling; kinetic; green solvents; soybean oil; fractional model.

NOMENCLATURE

AIC - Akaike information criterion

B – Sensitivity matrix of models responses

C_i - Observed values [g/g]

\hat{C}_i - Predicted values [g/g]

\overline{C}_i - Mean of observed values [g/g]

C_∞ - Solute concentration at the equilibrium [g/g]

FOM - First-order model

k – Extraction rate constant [min^{-1}]

m – Order of the power law equation

n - Number of observations

p - Number of parameters of the model

R^2 - Coefficient of determination

R_{adj}^2 - Adjusted coefficient of determination

RMSE - Root-mean-square error

S – Objective function

v – Elements of the covariance matrix

V_θ – Covariance matrix

χ^2 - Chi-square distribution

ρ – Parameters correlation

θ – Parameters vector

Subscripts

1 - model with a lower number of parameters

2 - model with a higher number of parameters

6.1 INTRODUCTION

According to Anastas and Warner (2000) [1], green chemistry seeks to reduce waste, mitigate risks and toxic effects of chemicals, make chemical synthesis less harmful to humans and the environment, and use renewable resources. Besides, it is desired to reduce the stoichiometry number of reagents used, improve yields, use chemicals that do not produce smog and contribute to ozone layer depletion, improve energy efficiency, and use products

and reactants that degrade after use. Real-time monitoring shall be adopted to avoid pollution and minimize the environmental problems due to explosions, fires, and emissions. Against this background, the application of green solvents to solid-liquid extractions has grown exponentially. Green solvents are specially intended for food applications for being, most of the time, less hazardous for humans due to the natural origin of their components. Besides, several companies such as Sanofi, Pfizer, and GlaxoSmithKline have recommended green solvents [2,3].

Many authors have studied vegetable oil extraction [4,5,6,7] with the intention of replacing nonrenewable solvents. The study of soybean oil extraction using green solvents has become a great concern for scientists after hexane, the most industrially used solvent, has been included in the list of carcinogenic, reprotoxic, and mutagenic substances [8,9,10].

The modeling of soybean oil extraction includes the use of power law models [11], the So and Macdonald model [12,13], and the mass transfer-based kinetic models [10,11,13,14]. However, the fractional calculus has risen in popularity [15] due to its capability to capture characteristics not covered by models based on conventional calculus [16,17] once it considers integrals and derivatives of arbitrary order [18,19,20]. Many studies have shown the potential use of fractional-order models for many applications, such as optimization of cationic dye adsorption [21], adsorption of methane and nitrogen on MOFs [22], nutrients, bacteria and bioproducts modeling in bioprocess [23], PID controllers [24], diffusion-reaction problems [25], soybean drying [15,17,26], and rice hydration [18]. The modeling of drying processes obtained better statistical results with fractional-order models when compared to the Lewis and the Page model [15,17,26], and significant improvements concerning the Omoto model were observed when those models were applied to the rice hydration [18].

In this work, a fractional-order model derived from the first-order power law equation was assessed in comparison to the regular first-order kinetic model to describe the kinetics of soybean oil extraction in a variety of solvents and temperatures. The novelty of this study relies on the first use of fractional-order modeling to predict soybean oil extraction. Indeed, this approach has never been conducted to describe the kinetic of vegetable oil extractions. Thus, an in-depth statistical analysis of applying this model was evaluated through statistical parameters and tests for 35 systems of solvents and temperatures.

6.2 MATERIALS AND METHODS

6.2.1 Experimental data

Scientific literature and laboratory data were collected in this study. The literature data were collected considering different solvents (anhydrous and hydrous ethanol, ethanol with alkyl ester, ethanol with ethyl acetate, anhydrous and hydrous 2-MeTHF, and n-hexane) at different temperatures (from 298 to 333 K) as well as at extraction time intervals ranging from 0 to 90 minutes. Such literature data sets can be found in the following works: Dagostin et al. (2015) [11], Toda et al. (2016) [13], Dagostin et al. (2018) [14], and Claux et al. (2021) [10].

Furthermore, laboratory data were obtained according to the following methodology: the oil of soybean flakes (gently donated by the soy-crushing company Granol from Cachoeira do Sul, Brazil) was extracted with ethyl acetate (Sigma Aldrich, purity 99.8%, CAS N° 141-78-6), 1-butanol (Neon, purity 99%, CAS 71-36-3), and p-cymene (Sigma Aldrich, 99%, CAS N° 99-87-6) at the solvent/solid ratios of 1:7 for ethyl acetate and 1-butanol and 1:4 for p-cymene, the lower ratio for p-cymene was used. The time the extractions were 1, 2, 4, 8, 10, 15, 30, 60, and 90 minutes. The soybean oil extraction with the three solvents occurred at the following temperatures: 298.15 K, 313.15 K, and 328.15 K. Besides, the soybean oil extraction was also evaluated with the p-cymene at the temperature of 343 K due to the higher boiling point of this solvent. The boiling point of the solvents is 350.15 K for ethyl acetate, 391.15 K for 1-butanol, and 450.15 K for p-cymene [3]. The yield of the soybean oil extraction was determined gravimetrically concerning the mass of the soybean flakes (Eq. 1). More about the experimental procedure and others are described in detail in the cited reference [27]. All the data were obtained at least in triplicate.

$$\text{Yield (g/g)} = \frac{\text{Mass of soybean oil extracted (g)}}{\text{Mass of soybean flakes (g)}} \quad (1)$$

It may be highlighted that most of the scientific literature and laboratory data used in this work concern the use of green solvents in soybean extraction: anhydrous and hydrous ethanol, ethanol with alkyl ester (biodiesel), ethanol with ethyl acetate, anhydrous and hydrous 2-MeTHF, ethyl acetate, 1-butanol, and p-cymene. The non-renewable solvent n-hexane was also modeled using fractional calculus because it is the worldwide industrial solvent to extract soybean oil.

6.2.2 Kinetic Modeling and Parameter Estimation

Power law models have been extensively used to describe solid-liquid extraction processes [11,28,29]. A generalized mass balance for the fluid phase can be written as

$$\frac{dC}{dt} = k(C_{\infty} - C)^m \quad (2)$$

where C is the concentration of an extracted solute in each time (g/g), C_{∞} is the concentration of a solute at the equilibrium (g/g), k is the extraction rate constant (min^{-1}), and m is the order of the power law equation.

The first-order model (FOM) is obtained when $m = 1$ and has an analytical solution described by Eq. 3 when the concentration of a solute at the beginning of the extraction is zero, $C(0) = 0$.

$$C = C_{\infty} (1 - e^{-kt}) \quad (3)$$

However, the first-order model can better fit the data when using arbitrary order equations for the derivative term, as can be seen in Eq. 4.

$$\frac{d^{\alpha}C}{dt^{\alpha}} = k(C_{\infty} - C) \quad (4)$$

where α is the fractional order of the derivative, and it is between 0 and 1.

Eq. 4 can be solved using the Laplace transform, and the left term is obtained through Eq. 5 when [26].

$$L\left\{\frac{d^{\alpha}C}{dt^{\alpha}}\right\} = s^{\alpha}C(s) - s^{\alpha-1}C(0) \quad (5)$$

In general, $C(0) = 0$ for soybean oil extraction. The right term of Eq. 4 can be resolved using the regular properties of the Laplace transform; thus, Eq. 6 is obtained.

$$C(s) = C_{\infty} \left[\frac{k}{s(s^{\alpha} + k)} \right] \quad (6)$$

The most used approaches of fractional equations are based on the definitions of Caputo, Riemann-Liouville, and Grünwald-Letnikov [19]. The Caputo derivative was chosen in this work because it is the most widely used technique to solve fractional-order equations [15,17,18]. From the inverse Laplace transformation given by Eq. 7, it is possible to solve Eq. 6 to find the solution to the arbitrary order equation. It is used $p = 1$, obtaining a Caputo fractional derivative [15].

$$L^{-1} \left\{ \frac{k}{s(s^\alpha + k)} \right\} = 1 - E_\alpha \left[-k \left(\frac{t^p}{p} \right)^\alpha \right] \quad (7)$$

Applying the inverse Laplace transformation, the analytical solution of the fractional-order kinetic model (FOKM) can be attained.

$$C = C_\infty \left[1 - E_\alpha (-kt^\alpha) \right] \quad (8)$$

where E_α is the Mittag-Leffler function. The solution of Eq. 8 is obtained using the gamma function and Taylor series (Eq. 9).

$$C = C_\infty \left[1 - \sum_{i=0}^{\infty} \frac{(-kt^\alpha)^i}{\Gamma(\alpha i + 1)} \right] \quad (9)$$

The models were fitted by nonlinear regression using the built-in function *particleswarm* [30,31,32] hybridized with the deterministic algorithm *fmincon* to improve the error minimization in the software MatLab®. The objective function used was the sum of square errors (Eq. 10).

$$S(\theta) = \sum_{i=1}^n (C_i - \hat{C}_i)^2 \quad (10)$$

where S is the objective function with respect to the parameter vector θ , n is the total number of experiments, C_i is the experimental yield of extraction, and \hat{C}_i is the yield of extraction calculated by the model.

6.2.3 Statistical Evaluation

The correlation (ρ) between the parameters is proportional to the non-diagonal

elements of the covariance matrix (V_θ) defined by Eq. 11.

$$V_\theta = s^2 (B_i^T B_i)^{-1} \quad (11)$$

with

$$B_i = \begin{bmatrix} \frac{\partial C_{1,i}}{\partial \theta_1} & \dots & \frac{\partial C_{p,i}}{\partial \theta_1} \\ \vdots & \ddots & \vdots \\ \frac{\partial C_{n,i}}{\partial \theta_1} & \dots & \frac{\partial C_{n,i}}{\partial \theta_p} \end{bmatrix} \quad (12)$$

and

$$s^2 = \frac{S(\hat{\theta})}{n-p} \quad (13)$$

where $\hat{\theta}$ denotes the estimate of the point of minimum and p is the number of parameters of the model.

The correlation between parameters is obtained by Eq. 14.

$$\rho_{ij} = \frac{v_{ij}}{\sqrt{v_{ii} v_{jj}}} \quad (14)$$

where $\rho_{ij} \in [-1,1]$ increases in absolute values as the correlation between the parameters increases, and v_{ii} , v_{jj} , and v_{ij} are the ii , jj and ij elements of the covariance matrix.

The correlation between C_∞ and k is represented by Eq. 15 for the regular first-order model. The correlation between C_∞ and k for the fractional-order kinetic model is also obtained by Eq. 15. Eqs. 16 and 17 represent the correlation of C_∞ with α and k with α , respectively.

$$\rho_{C_\infty k} = \frac{\sum_{i=1}^{NE} \left(\frac{\partial C_i}{\partial C_\infty} \frac{\partial C_i}{\partial k} \right)}{\sqrt{\sum_{i=1}^{NE} \left(\frac{\partial C_i}{\partial C_\infty} \right)^2 \sum_{i=1}^{NE} \left(\frac{\partial C_i}{\partial k} \right)^2}} \quad (15)$$

$$\rho_{C_\infty\alpha} = \frac{\sum_{i=1}^{NE} -\left(\frac{\partial C_i}{\partial C_\infty} \frac{\partial C_i}{\partial \alpha}\right)}{\sqrt{\sum_{i=1}^{NE} \left(\frac{\partial C_i}{\partial C_\infty}\right)^2 \sum_{i=1}^{NE} \left(\frac{\partial C_i}{\partial \alpha}\right)^2}} \quad (16)$$

$$\rho_{k\alpha} = \frac{\sum_{i=1}^{NE} -\left(\frac{\partial C_i}{\partial k} \frac{\partial C_i}{\partial \alpha}\right)}{\sqrt{\sum_{i=1}^{NE} \left(\frac{\partial C_i}{\partial k}\right)^2 \sum_{i=1}^{NE} \left(\frac{\partial C_i}{\partial \alpha}\right)^2}} \quad (17)$$

More details about the calculation of the correlation between the parameters can be found in Schwaab and Pinto (2007) [33], Schwaab and Pinto (2008) [34], and Schwaab et al. (2008) [35].

The calculation of the coefficient of determination (R^2), chi-square distribution (χ^2), and root mean square error ($RMSE$) was used to assess the goodness of the fittings of the experimental data with the models. The adjusted coefficient of determination (R_{adj}^2) and the Akaike information criterion (AIC) were used for comparing the models.

$$R^2 = 1 - \frac{\sum_{i=1}^n (C_i - \hat{C}_i)^2}{\sum_{i=1}^n (C_i - \bar{C}_i)^2} \quad (19)$$

$$\chi^2 = \sum_{i=1}^n \frac{(C_i - \hat{C}_i)^2}{C_i} \quad (20)$$

$$RMSE = \sqrt{\frac{1}{n} \sum_{i=1}^n (C_i - \hat{C}_i)^2} \quad (21)$$

$$AIC = 2p + n \times \ln \left(\frac{\sum_{i=1}^n (C_i - \hat{C}_i)}{n} \right) \quad (22)$$

$$R_{adj}^2 = 1 - \frac{(n-1)(1-R^2)}{(n-p-1)} \quad (23)$$

Fisher's exact test was performed to verify if the first-order model can be statistically equal to the FOKM. The F calculated (given by Eq. 24) is compared with the F_{crit} obtained

from Fisher's distribution for 95% of confidence.

$$F = \frac{\left(\frac{S_1 - S_2}{p_2 - p_1} \right)}{\left(\frac{S_2}{n - p_2} \right)} \quad (24)$$

where subscript 1 refers to the model with a lower number of parameters and subscript 2 to the model with a higher number of parameters.

Finally, the Shapiro-Wilk test for the non-normality of the residues was performed in the open-source software R studio [37] using the built-in function *shapiro.test* for the residues to observe if the residues of the models are normally distributed.

6.3 RESULTS AND DISCUSSION

The parameters obtained for the regular first-order model are presented in Table 6.1, and the parameters obtained for the fractional-order kinetic model are presented in Table 6.2.

Table 6. 1 - Parameters obtained for the first-order model and their statistical metrics for different solvents and temperatures.

System	T (K)	C_{∞} (g/g)	k (min^{-1})	S	R^2	χ^2	RMSE	Reference of data
Ethanol anhydrous	298	0.1441	0.2929	4.76×10^{-4}	0.9813	0.0056	0.0073	[11]
	313	0.2023	0.2153	1.92×10^{-3}	0.9644	0.0183	0.0146	
	328	0.2457	0.1615	1.09×10^{-3}	0.9863	0.0074	0.0110	
Ethanol 96%	298	0.0587	0.3696	1.51×10^{-4}	0.9609	0.0034	0.0041	
Ethanol with 5% of biodiesel	298	0.1612	0.2383	9.02×10^{-4}	0.9731	0.0102	0.0100	
	313	0.2176	0.1775	2.13×10^{-3}	0.9684	0.0222	0.0154	
	328	0.2473	0.1690	1.12×10^{-3}	0.9879	0.0124	0.0112	
Ethanol with 10% of biodiesel	298	0.1848	0.1379	1.59×10^{-3}	0.9676	0.0191	0.0133	
	313	0.2324	0.1683	2.21×10^{-3}	0.9687	0.0232	0.0166	
	328	0.2503	0.2138	1.03×10^{-3}	0.9883	0.0104	0.0107	
Ethanol anhydrous	313	0.1440	0.1771	7.60×10^{-4}	0.9637	0.0055	0.0074	[13]
	323	0.1758	0.1445	1.16×10^{-3}	0.9638	0.0080	0.0091	
	333	0.1925	0.1456	1.42×10^{-3}	0.9626	0.0067	0.0051	
Ethanol 94.02%	313	0.0622	0.2431	1.55×10^{-5}	0.9958	2.63×10^{-4}	0.0011	
	323	0.0879	0.3054	1.76×10^{-4}	0.9761	0.0021	0.0035	
	333	0.1205	0.2230	4.97×10^{-4}	0.9648	0.0047	0.0060	
Ethanol with 5% of ethyl acetate	298	0.1699	0.1865	1.96×10^{-3}	0.9495	0.0223	0.0148	[14]
	313	0.2238	0.1852	2.26×10^{-3}	0.9572	0.0224	0.0158	
	328	0.2427	0.2385	1.01×10^{-4}	0.9860	0.0061	0.0106	
Ethanol with 10% of ethyl acetate	298	0.1956	0.1602	3.31×10^{-3}	0.9384	0.0359	0.0192	
	313	0.2362	0.2231	4.23×10^{-3}	0.9421	0.0354	0.0217	
	328	0.2415	0.2995	1.79×10^{-3}	0.9741	0.0109	0.0141	
n-Hexane	328	0.1604	0.1131	3.15×10^{-4}	0.9925	0.0026	0.0049	[10]
2-MeTHF	328	0.1746	0.0989	2.22×10^{-4}	0.9961	0.0144	0.0041	
2-MeTHF 95.5%	328	0.1827	0.0725	3.07×10^{-4}	0.9952	0.0297	0.0049	
Ethyl acetate	298	0.1694	0.1253	2.94×10^{-3}	0.9324	0.0408	0.0171	This work
	313	0.1776	0.2400	3.04×10^{-3}	0.9255	0.0290	0.0174	
	328	0.1855	0.3146	2.13×10^{-3}	0.9487	0.0161	0.0146	
1-Butanol	298	0.1316	0.0603	1.16×10^{-3}	0.9575	0.0275	0.0108	
	313	0.1463	0.0690	1.92×10^{-3}	0.9421	0.0120	0.0139	
	328	0.1800	0.0686	1.16×10^{-3}	0.9792	0.0250	0.0108	
P-cymene	298	0.1823	0.2021	1.84×10^{-3}	0.9599	0.0197	0.0136	
	313	0.1871	0.2871	1.77×10^{-3}	0.9600	0.0167	0.0133	
	328	0.1965	0.2714	2.58×10^{-3}	0.9474	0.0224	0.0161	
	343	0.2112	0.4104	2.56×10^{-3}	0.9493	0.0167	0.0160	

Considering the parameters obtained for the first-order model using the same solvent (absolute or with co-solvents), the temperature dependence of C_{∞} could be observed. This is imperative to evaluate the thermodynamic parameters of standard enthalpy change, standard entropy change, and standard Gibbs free energy change of the extraction since the partition coefficient between solid and liquid phases is usually calculated after this parameter estimation step [11]. The extraction rate constant (k) neither increases nor decreases with temperature.

Table 6. 2 - Parameters obtained for the fractional-order kinetic model and its statistical metrics for different solvents and temperatures.

System	T (K)	C_{∞} (g/g)	k ($min^{-\alpha}$)	α	S	R^2	χ^2	RMSE	Reference of data
Ethanol anhydrous	298	0.1561	0.3502	0.7693	1.48×10^{-5}	0.9993	1.20×10^{-4}	0.0013	[11]
	313	0.2354	0.2904	0.6689	5.62×10^{-5}	0.9987	4.46×10^{-4}	0.0025	
	328	0.2646	0.2004	0.8202	2.38×10^{-4}	0.9968	0.0025	0.0051	
Ethanol 96%	298	0.0675	0.4199	0.6414	5.39×10^{-6}	0.9985	1.09×10^{-4}	7.74×10^{-4}	
Ethanol with 5% of biodiesel	298	0.1811	0.3048	0.7166	1.91×10^{-5}	0.9993	2.01×10^{-4}	0.0015	
	313	0.2514	0.2548	0.6838	1.51×10^{-4}	0.9979	0.0011	0.0041	
	328	0.2661	0.2190	0.8053	1.48×10^{-4}	0.9979	5.77×10^{-4}	0.0018	
Ethanol with 10% of biodiesel	298	0.2259	0.2006	0.6552	3.91×10^{-5}	0.9990	3.23×10^{-4}	0.0021	
	313	0.2683	0.2489	0.6720	6.31×10^{-5}	0.9988	4.76×10^{-4}	0.0028	
	328	0.2644	0.2607	0.8347	3.05×10^{-4}	0.9958	0.0021	0.0058	
Ethanol anhydrous	313	0.1749	0.3671	0.5556	2.41×10^{-3}	0.9884	0.0017	0.0041	[13]
	323	0.2154	0.2864	0.5896	2.08×10^{-4}	0.9934	0.0012	0.0039	
	333	0.2459	0.2877	0.5527	2.43×10^{-4}	0.9936	0.0014	0.0042	
Ethanol 94.02%	313	0.0636	0.3070	0.8912	7.33×10^{-6}	0.9980	1.17×10^{-4}	7.23×10^{-4}	
	323	0.1435	0.6424	0.2148	3.00×10^{-5}	0.9959	3.39×10^{-4}	0.0015	
	333	0.1545	0.5638	0.4171	6.58×10^{-5}	0.9953	6.20×10^{-4}	0.0022	
Ethanol with 5% of ethyl acetate	298	0.2093	0.2668	0.6126	1.23×10^{-4}	0.9962	9.45×10^{-4}	0.0037	[14]
	313	0.2609	0.2618	0.6725	1.04×10^{-4}	0.9982	8.71×10^{-4}	0.0034	
	328	0.2556	0.2721	0.8516	3.92×10^{-4}	0.9945	0.0054	0.0066	
Ethanol with 10% of ethyl acetate	298	0.2663	0.2398	0.5391	2.07×10^{-4}	0.9950	0.0013	0.0048	
	313	0.2883	0.3208	0.5931	5.96×10^{-4}	0.9901	0.0040	0.0081	
	328	0.2629	0.3537	0.7620	3.92×10^{-4}	0.9940	0.0019	0.0066	
n-Hexane	328	0.1681	0.1329	0.8951	1.62×10^{-4}	0.9963	0.0036	0.0035	[10]
2-MeTHF	328	0.1764	0.1029	0.9769	2.13×10^{-4}	0.9964	0.0169	0.0041	
2-MeTHF 95.5%	328	0.1843	0.0747	0.9832	3.02×10^{-4}	0.9954	0.0333	0.0048	
Ethyl acetate	298	0.2744	0.1826	0.4773	1.40×10^{-4}	0.9954	0.0011	0.0037	This work
	313	0.2347	0.3266	0.5304	8.59×10^{-5}	0.9975	6.51×10^{-4}	0.0029	
	328	0.2206	0.3869	0.6281	9.14×10^{-5}	0.9976	6.64×10^{-4}	0.0030	
1-Butanol	298	0.5945	0.0349	0.4533	2.83×10^{-5}	0.9985	7.31×10^{-4}	0.0017	
	313	0.8022	0.0322	0.4078	8.17×10^{-5}	0.9964	0.0013	0.0029	
	328	0.2543	0.0974	0.6487	1.99×10^{-4}	0.9946	0.0029	0.0045	
P-cymene	298	0.2158	0.2844	0.6529	6.34×10^{-5}	0.9983	4.59×10^{-4}	0.0025	
	313	0.2146	0.3756	0.6686	1.08×10^{-4}	0.9972	0.0010	0.0033	
	328	0.2323	0.3633	0.6309	1.74×10^{-4}	0.9959	0.0014	0.0042	
	343	0.2467	0.4909	0.6228	6.89×10^{-5}	0.9986	3.93×10^{-4}	0.0026	

For FOKM the C_∞ parameter tends to increase with the increase in temperature; however, some random behavior can be observed. Furthermore, the same happens for k , although the non-dependence of this parameter on temperature is observed in the works of Dagostin et al. (2015) [11], Toda et al. (2016) [13], and Dagostin et al. (2018) [14].

It can be seen from Tables 6.1 and 6.2 that the FOKM has the best fitting to the data than the non-fractional model. Besides a better R^2 , the FOKM is related to lower χ^2 , and $RMSE$ for most systems of solvent and temperatures.

Table 6.3 compares the models through the R_{adj}^2 and the AIC for each model. The correlation among the parameters for each model is also presented. Therefore, the F calculated and the F_{crit} from Fisher's distribution are presented with 95% of confidence.

Table 6. 3 - Statistical comparison of the models for different solvents and temperatures.

(to be continued)

System	T (K)	FOM			FOKM			Comparison		Reference of data
		R_{adj}^2	AIC	ρ	R_{adj}^2	AIC	ρ	F	F_{crit}	
Ethanol anhydrous	298	0.9751	-84.63	-0.5096 ^a	0.9989	-113.85	-0.6939 ^a ; -0.8901 ^b ; -0.7694 ^c	186.84	5.99	[11]
	313	0.9525	-72.05	-0.5570 ^a	0.9980	-101.84	-0.8063 ^a ; -0.9513 ^b ; -0.8300 ^c	199.25	5.99	
	328	0.9817	-77.12	-0.5916 ^a	0.9949	-88.88	-0.7203 ^a ; -0.8946 ^b ; -0.8361 ^c	21.68	5.99	
Ethanol 96%	298	0.9479	-94.93	-0.4744 ^a	0.9977	-122.15	-0.7764 ^a ; -0.9431 ^b ; -0.7928 ^c	148.19	5.99	
Ethanol with 5% of biodiesel	298	0.9641	-78.87	-0.5421 ^a	0.9989	-111.55	-0.7592 ^a ; -0.9277 ^b ; -0.8095 ^c	276.65	5.99	
	313	0.9579	-71.12	-0.5814 ^a	0.9954	-92.97	-0.8101 ^a ; -0.9519 ^b ; -0.8404 ^c	78.94	5.99	
	328	0.9839	-76.87	-0.5868 ^a	0.9967	-93.17	-0.7226 ^a ; -0.8977 ^b ; -0.8281 ^c	40.00	5.99	
Ethanol with 10% of biodiesel	298	0.9568	-73.77	-0.6064 ^a	0.9984	-105.12	-0.8624 ^a ; -0.9718 ^b ; -0.8703 ^c	238.14	5.99	
	313	0.9562	-61.54	-0.6303 ^a	0.9979	-88.00	-0.8059 ^a ; -0.9479 ^b ; -0.8375 ^c	170.28	6.61	
	328	0.9844	-77.65	-0.5579 ^a	0.9933	-86.64	-0.6741 ^a ; -0.8653 ^b ; -0.7927 ^c	14.32	5.99	
Ethanol anhydrous	313	0.9571	-133.49	-0.4674 ^a	0.9849	-147.57	-0.9342 ^a ; -0.9927 ^b ; -0.9615 ^c	23.69	4.84	[13]
	323	0.9573	-127.51	-0.5232 ^a	0.9914	-149.65	-0.9324 ^a ; -0.9920 ^b ; -0.9603 ^c	50.71	4.84	
	333	0.9595	-124.71	-0.5210 ^a	0.9917	-147.44	-0.9488 ^a ; -0.9955 ^b ; -0.9649 ^c	53.37	4.84	
Ethanol 94.02%	313	0.9950	-187.96	-0.3971 ^a	0.9974	-196.47	-0.5602 ^a ; -0.8291 ^b ; -0.8814 ^c	12.31	4.84	
	323	0.9717	-154.01	-0.3581 ^a	0.9947	-176.61	-0.2447 ^a ; -0.9029 ^b ; -0.6196 ^c	9.95	4.84	
	333	0.9584	-139.43	-0.4142 ^a	0.9939	-166.53	-0.1442 ^a ; -0.9764 ^b ; -0.3504 ^c	10.41	4.84	
Ethanol with 5% of ethyl acetate	298	0.9326	-71.88	-0.5756 ^a	0.9939	-94.82	-0.8611 ^a ; -0.9715 ^b ; -0.8540 ^c	89.66	5.99	[14]
	313	0.9572	-70.60	-0.5765 ^a	0.9970	-96.35	-0.8161 ^a ; -0.9548 ^b ; -0.8404 ^c	125.65	5.99	
	328	0.9814	-77.90	-0.5420 ^a	0.9913	-84.38	-0.6534 ^a ; -0.8505 ^b ; -0.7787 ^c	9.39	5.99	
Ethanol with 10% of ethyl acetate	298	0.9179	-67.16	-0.5924 ^a	0.9920	-90.10	-0.9186 ^a ; -0.9826 ^b ; -0.8801 ^c	89.83	5.99	
	313	0.9228	-64.96	-0.5519 ^a	0.9841	-80.60	-0.8550 ^a ; -0.9701 ^b ; -0.8417 ^c	36.58	5.99	
	328	0.9655	-72.69	-0.5061 ^a	0.9903	-84.38	-0.6938 ^a ; -0.8942 ^b ; -0.7709 ^c	21.43	5.99	
n-Hexane	328	0.9910	-134.15	-0.5996 ^a	0.9951	-140.83	-0.7059 ^a ; -0.8963 ^b ; -0.8730 ^c	9.46	4.96	[10]
2-MeTHF	328	0.9953	-138.71	-0.6281 ^a	0.9952	-137.26	-0.6511 ^a ; -0.8544 ^b ; -0.8755 ^c	0.43	4.96	
2-MeTHF 95.5%	328	0.9942	-134.51	-0.6963 ^a	0.9939	-132.71	-0.7131 ^a ; -0.8909 ^b ; -0.9025 ^c	0.16	4.96	

^aBetween C_∞ and k ; ^bBetween C_∞ and α ; ^cBetween k and α .

Table 6. 4 - Statistical comparison of the models for different solvents and temperatures.

(conclusion)

System	T (K)	FOM			FOKM			Comparison		Reference of data
		R_{adj}^2	AIC	ρ	R_{adj}^2	AIC	ρ	F	F_{crit}	
Ethyl acetate	298	0.9131	-77.32	-0.6465 ^a	0.9931	-105.74	-0.9627 ^a ; -0.9821 ^b ; -0.9078 ^c	140.03	5.19	This work
	313	0.9043	-76.98	-0.5936 ^a	0.9963	-110.65	-0.9021 ^a ; -0.9800 ^b ; -0.8682 ^c	241.07	5.19	
	328	0.9340	-80.56	-0.5471 ^a	0.9964	-110.03	-0.8228 ^a ; -0.9561 ^b ; -0.8347 ^c	155.88	5.19	
1-Butanol	298	0.9453	-86.63	-0.7066 ^a	0.9977	-121.74	-0.9982 ^a ; -0.9719 ^b ; -0.9566 ^c	279.59	5.19	
	313	0.9255	-81.57	-0.6871 ^a	0.9946	-111.15	-0.9989 ^a ; -0.9667 ^b ; -0.9545 ^c	157.57	5.19	
	328	0.9733	-86.62	-0.6879 ^a	0.9918	-102.25	-0.9418 ^a ; -0.9896 ^b ; -0.9190 ^c	33.99	5.19	
P-cymene	298	0.9484	-82.02	-0.6150 ^a	0.9975	-113.68	-0.8344 ^a ; -0.9593 ^b ; -0.8541 ^c	195.90	5.19	
	313	0.9485	-82.37	-0.5641 ^a	0.9958	-108.40	-0.7953 ^a ; -0.9423 ^b ; -0.8261 ^c	109.10	5.19	
	328	0.9324	-78.64	-0.5741 ^a	0.9939	-103.57	-0.8267 ^a ; -0.9572 ^b ; -0.8391 ^c	96.63	5.19	
	343	0.9348	-78.71	-0.4970 ^a	0.9979	-112.99	-0.7964 ^a ; -0.9471 ^b ; -0.8144 ^c	7.78	5.19	

^aBetween C_∞ and k ; ^bBetween C_∞ and α ; ^cBetween k and α .

There are only 2 out of 35 cases where the R_{adj}^2 and AIC are higher for the regular first-order model than the FOKM, and F calculated is lower than F_{crit} . In the other cases, the R_{adj}^2 is higher, and AIC is lower. The F calculated it is higher than the F_{crit} for 33 cases, proving that the model with fewer parameters (regular first-order) is not statistically similar to the model with more parameters (FOKM). These results suggest that the inclusion of the order of the equation as a third parameter is related to improvements in model fitting.

It can be seen that the correlation between the parameters is higher for the FOKM than for FOM. This model has to be used with caution once the correlation among the parameters can be high, despite the correlations of parameters of complex nonlinear functions tending to be high, as seen for the Arrhenius equation's parameters [33]. In this context, it shall be highlighted that the FOKM presented better statistical results regarding the lower χ^2 and $RMSE$ and better results over the statistical Fisher's exact test. The simulation of the models with the experimental data is presented in Figs. 6.1 to 6.11.

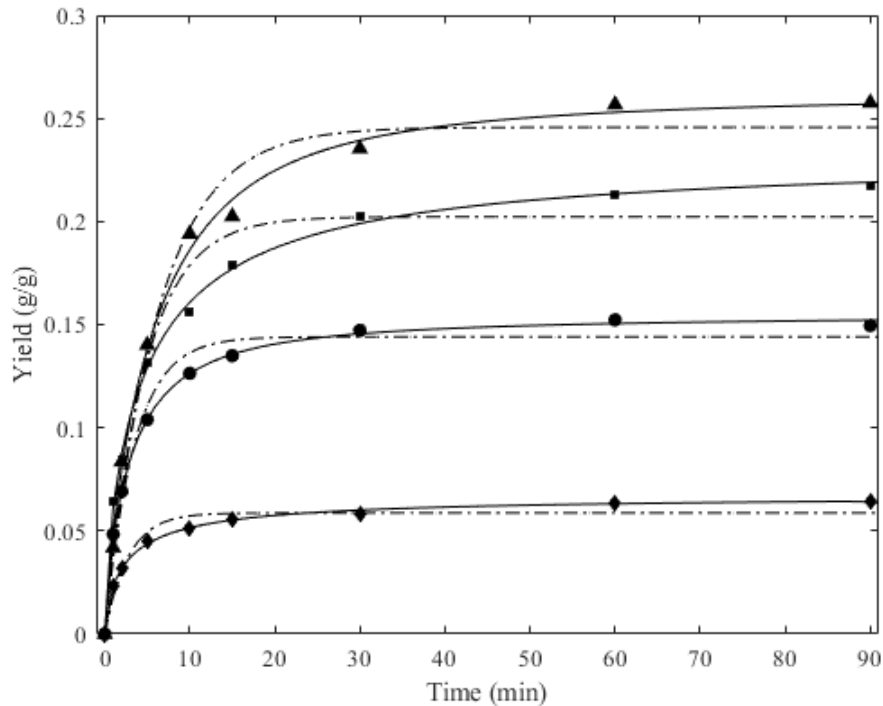


Figure 6. 1 - Experimental and predicted yields of extraction for FOKM (continuous line) and FOM (dash-dotted) at (●) 298 K, (■) 313 K, and (▲) 328 K using ethanol anhydrous and (◆) ethanol 96% at 298 K [11].

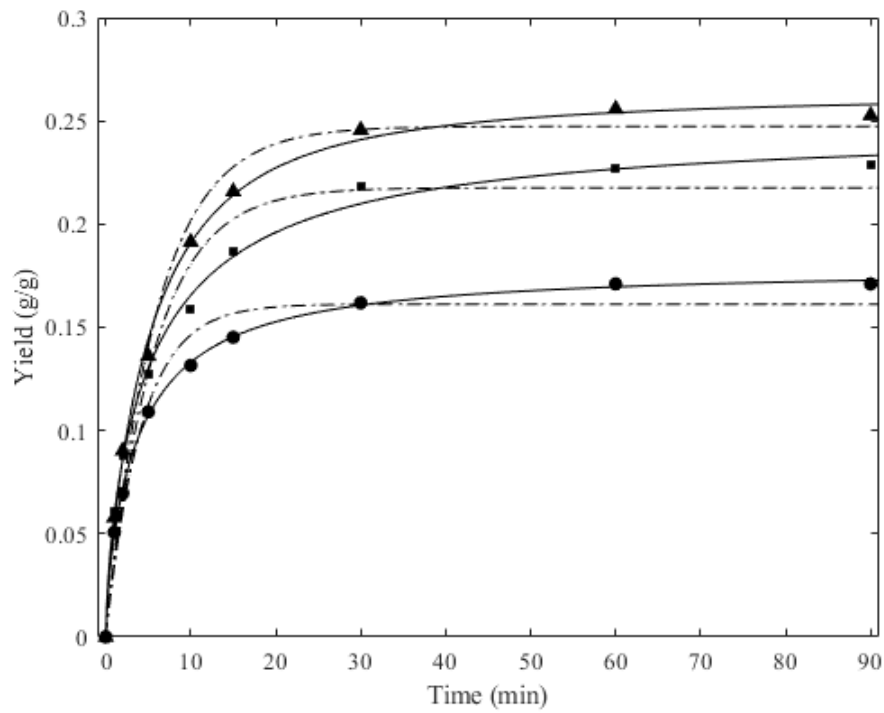


Figure 6. 2 - Experimental and predicted yields of extraction for FOKM (continuous line) and FOM (dash-dotted) at (●) 298 K, (■) 313 K, and (▲) 328 K using ethanol with 5% of biodiesel [11].

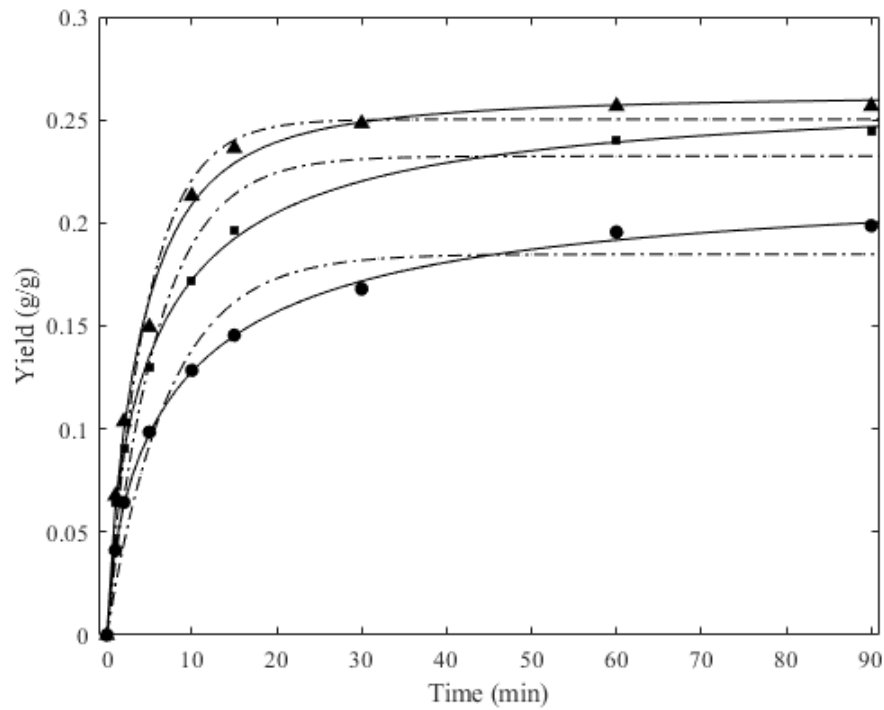


Figure 6. 3 - Experimental and predicted yields of extraction for FOKM (continuous line) and FOM (dash-dotted) at (●) 298 K, (■) 313 K, and (▲) 328 K using ethanol with 10% of biodiesel [11].

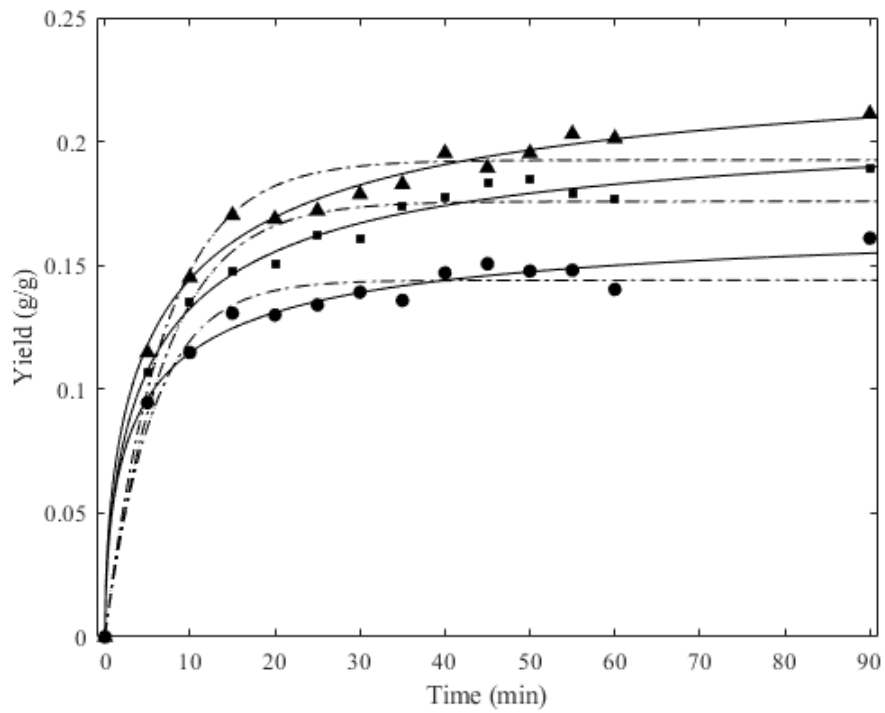


Figure 6. 4 - Experimental and predicted yields of extraction for FOKM (continuous line) and FOM (dash-dotted) at (●) 313 K, (■) 323 K, and (▲) 333 K using ethanol anhydrous [13].

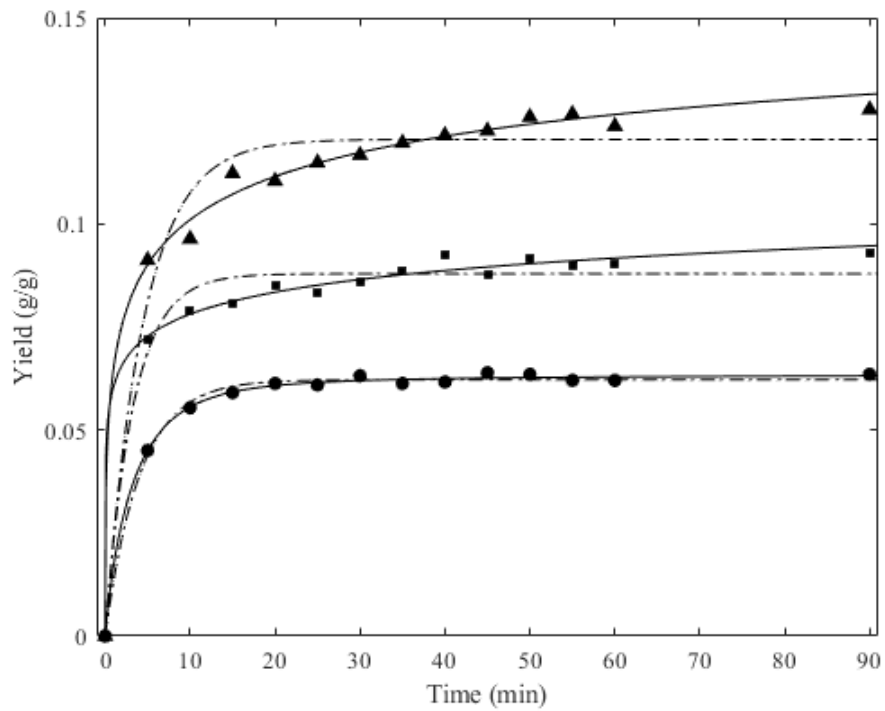


Figure 6. 5 - Experimental and predicted yields of extraction for FOKM (continuous line) and FOM (dash-dotted) at (●) 313 K, (■) 323 K, and (▲) 333 K using ethanol 94.02% [13].

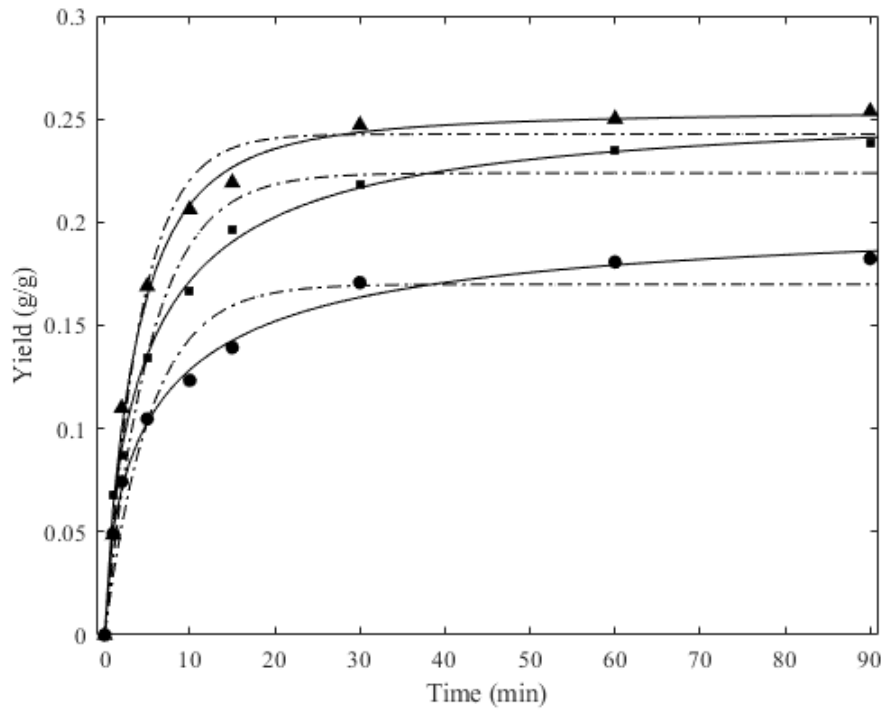


Figure 6. 6 - Experimental and predicted yields of extraction for FOKM (continuous line) and FOM (dash-dotted) at (●) 298 K, (■) 313 K, and (▲) 328 K using ethanol with 5% of ethyl acetate [14].

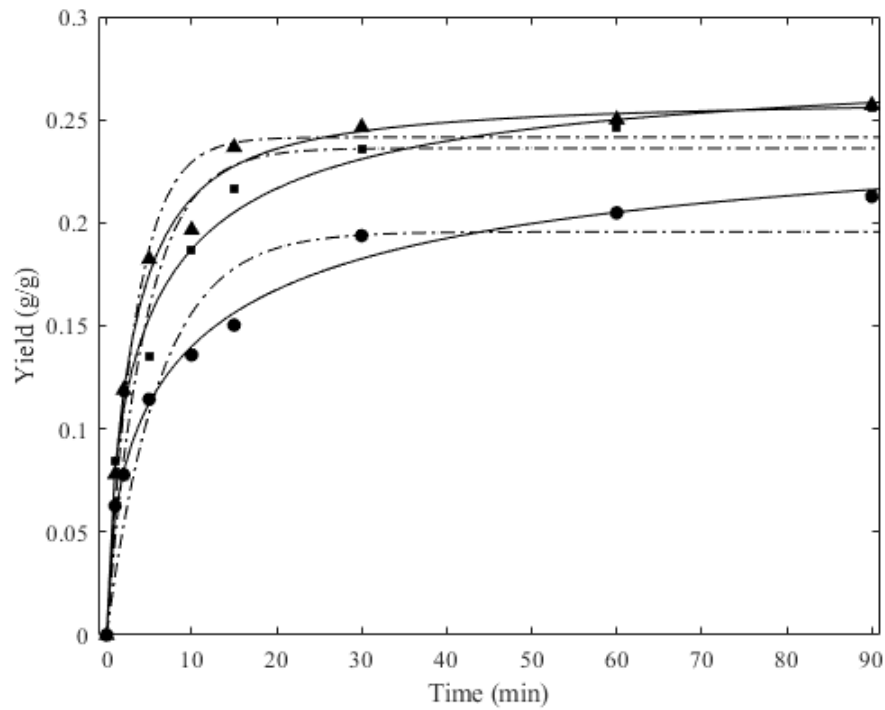


Figure 6. 7 - Experimental and predicted yields of extraction for FOKM (continuous line) and FOM (dash-dotted) at (●) 298 K, (■) 313 K, and (▲) 328 K using ethanol with 10% of ethyl acetate [14].

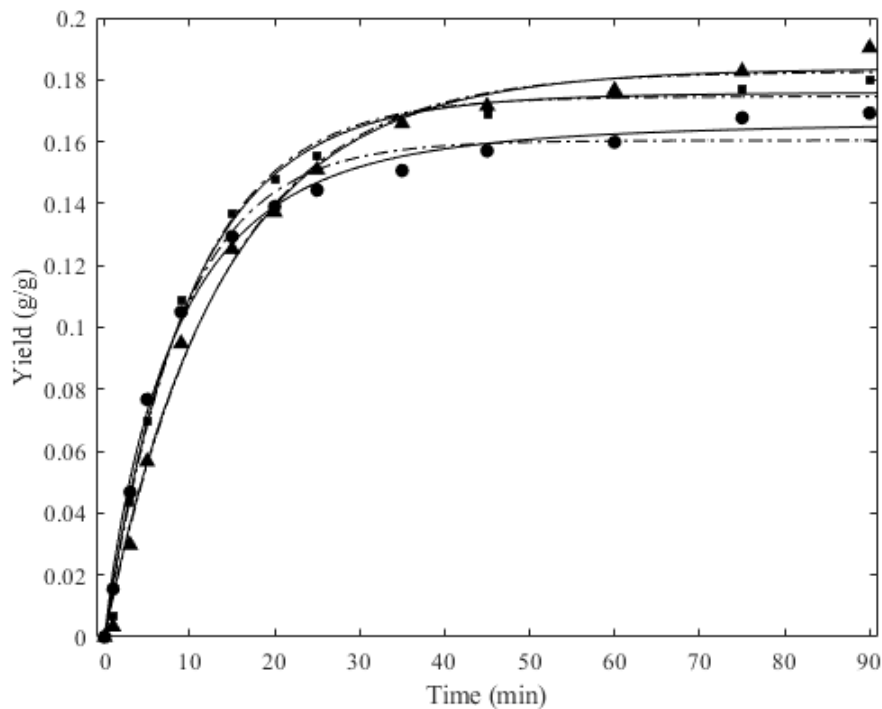


Figure 6. 8 - Experimental and predicted yields of extraction for FOKM (continuous line) and FOM (dash-dotted) at 328 K for (●) n-hexane (■) 2-MeTHF, and (▲) 2-MeTHF 95.5% [10].

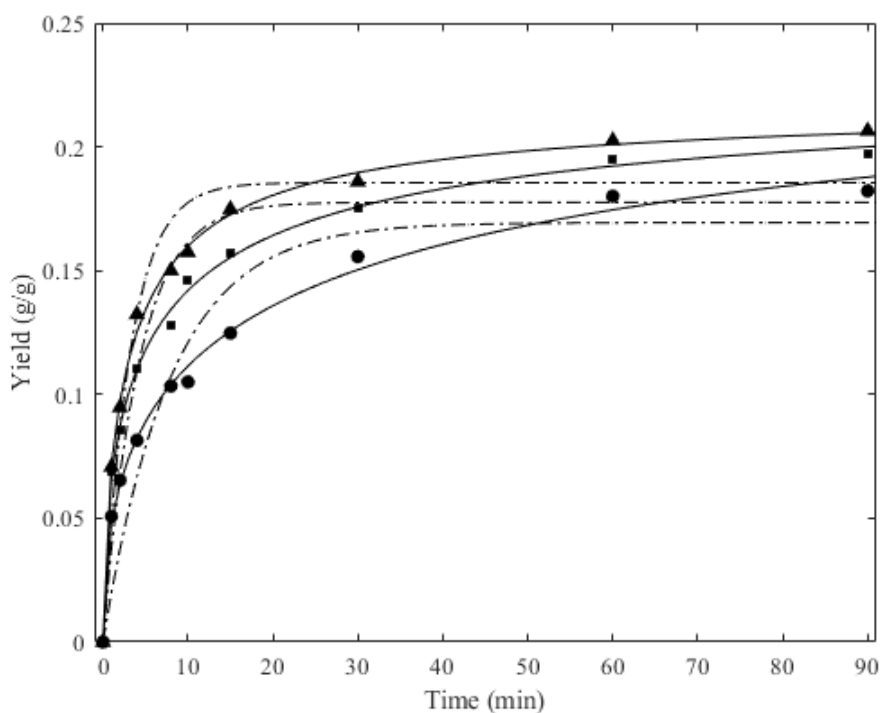


Figure 6. 9 - Experimental and predicted yields of extraction for FOKM (continuous line) and FOM (dash-dotted) at (●) 298 K, (■) 313 K, and (▲) 328 K using ethyl acetate (This work).

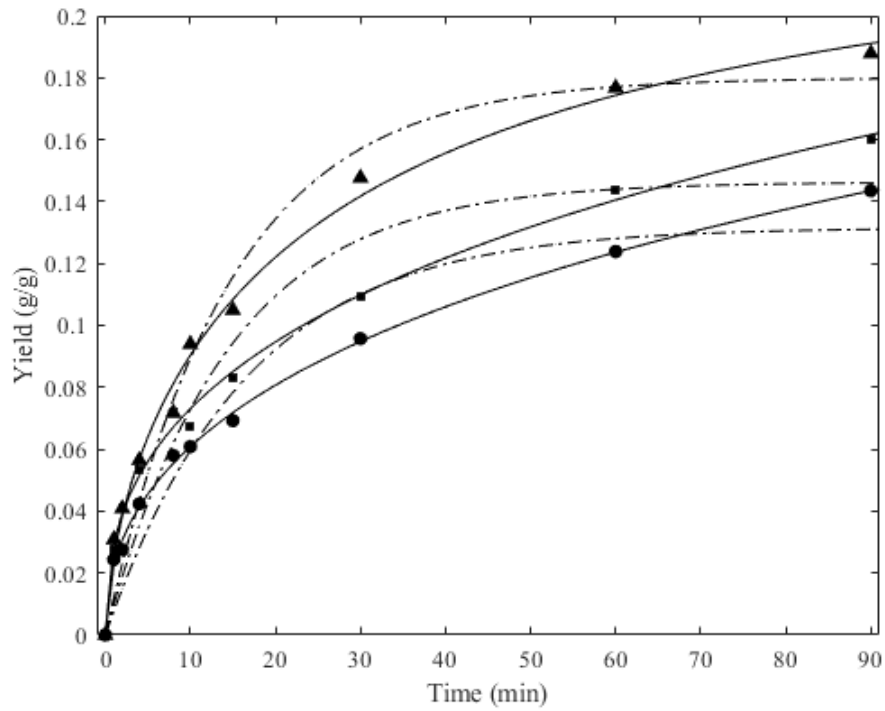


Figure 6.10 - Experimental and predicted yields of extraction for FOKM (continuous line) and FOM (dash-dotted) at (●) 298 K, (■) 313 K, and (▲) 328 K using 1-butanol (This work).

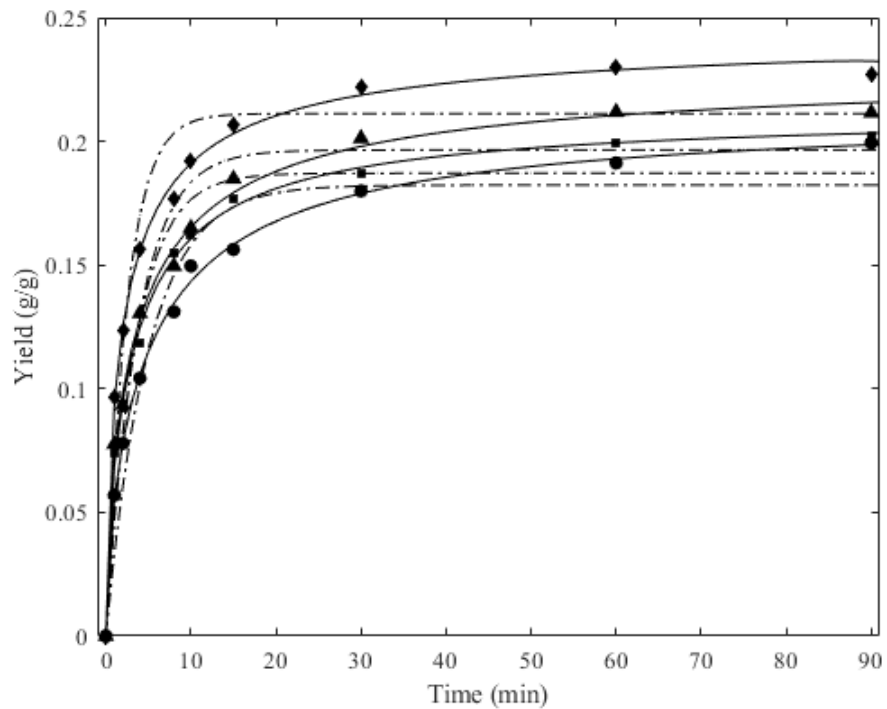


Figure 6.11 - Experimental and predicted yields of extraction for FOKM (continuous line) and FOM (dash-dotted) at (●) 298 K, (■) 313 K, (▲) 328 K, and (◆) 443 K using p-cymene (This work).

Currently, industrial soybean oil extraction is performed with an isomeric mixture of n-hexane [3]. Although this study focused on green solvents applied in soybean oil extraction, Fig. 6.8 shows the application of n-hexane compared to 2-MeTHF. Interestingly, soybean oil extraction using 2-MeTHF is higher than using the petroleum-derived solvent. Soybean oil extraction is even higher when using hydrous 2-MeTHF. The extraction yield shall not be higher when using an alternative solvent. However, the higher extraction yield observed for some green solvents might make their use even more attractive.

The p-value for the Shapiro-Wilk test is presented in Table 6.4 for FOM and FOKM. On the contrary to what was found by Nicolin et al. (2017a) [18], the non-normality of the residues was rejected for both of the models once the p-values found for the Shapiro-Wilk test were higher than 0.05 for 95% of confidence.

Table 6. 5 - Shapiro-Wilk normality test applied for both models.

System	T (K)	p -value		Reference of data	
		FOM	FOKM		
Ethanol anhydrous	298	0.5009	0.6147	[11]	
	313	0.7740	0.6115		
	328	0.6181	0.4191		
Ethanol 96%	298	0.4199	0.7599		
	Ethanol with 5% of biodiesel	298	0.6754		0.1828
		313	0.6972		0.7496
Ethanol with 10% of biodiesel	328	0.4491	0.1004		
	298	0.3251	0.8324		
	313	0.5932	0.8472		
Ethanol anhydrous	328	0.8700	0.1074	[13]	
	313	0.5021	0.2123		
	323	0.8510	0.5607		
Ethanol 94.02%	333	0.8399	0.0947		
	313	0.1633	0.2875		
	323	0.6136	0.2269		
Ethanol with 5% of ethyl acetate	333	0.9860	0.4168	[14]	
	298	0.2228	0.7843		
	313	0.9764	0.5967		
Ethanol with 10% of ethyl acetate	328	0.8101	0.7800		
	298	0.8525	0.3106		
	313	0.5702	0.2580		
n-Hexane	328	0.0517	0.2026	[10]	
	328	0.2643	0.2729		
	328	0.8665	0.5428		
2-MeTHF	328	0.8599	0.7239		
	2-MeTHF 95.5%	328	0.8599		0.7239
	Ethyl acetate	298	0.6303		0.4409
313		0.5828	0.5590		
328		0.3203	0.2286		
1-Butanol	298	0.4622	0.2347		
	313	0.5718	0.9695		
	328	0.5805	0.4518		
p-cymene	298	0.7167	0.2105		
	313	0.4820	0.9972		
	328	0.9440	0.5511		
	343	0.9191	0.1059		

The FOKM has a significant statistical improvement for almost all the systems evaluated in this work. The estimated concentration of soybean oil at the equilibrium (C_{∞}) is the yield of oil extraction that could be achieved in an infinite time for each temperature, which is extremely important to obtain the thermodynamic parameters of the van't Hoff equation [7,11,37]. In this context, it can be seen from the simulations that the FOM does not reach the equilibrium in agreement with the experimental points, proving that the estimated concentration of soybean oil at the equilibrium is probably thermodynamically inaccurate.

6.4 CONCLUSIONS

The kinetic of soybean oil extraction was evaluated using data from the literature and experimentally through the regular first-order and fractional-order kinetic models. The systems evaluated included the renewable solvents anhydrous and hydrous ethanol, ethanol with alkyl esters, ethanol with ethyl acetate, anhydrous and hydrous 2-MeTHF, ethyl acetate, 1-butanol, and p-cymene, at different temperatures (298.15 to 434.15 K) and at extraction times ranging from 0 to 90 minutes. The application of n-hexane was modeled for comparison purposes. This novel approach for modeling the kinetic of soybean oil extraction shows that the fractional model has a considerable improvement in the statistical performance over the analysis of the R_{adj}^2 , the *AIC*, and Fisher's exact test. For both models, the normality of the residues is guaranteed through the Shapiro-Wilk normality test. The correlation between the parameters was found to be higher for the FOM than for the FOKM. However, it should attract attention that a statistically better performance in fitting the experimental data made its application advantageous for soybean oil extraction.

CONFLICT OF INTERESTS

The authors report no declaration of interest.

ACKNOWLEDGMENT

The authors are grateful for the financial support and scholarships of the Human Resources Program of the National Agency for Petroleum, Natural Gas and Biofuels – PRH-ANP through the Human Resources Training Program for Petroleum and Biofuels Processing (PRH 52.1). The authors also acknowledge the soy-crushing company Granol for donating the soybean flakes.

REFERENCES

- [1] P.T. Anastas; J.C. Warner, Green Chemistry: Theory and Practice. Oxford University Press, USA, 2000.
- [2] F. Chemat, M.A. Vian, H.K. Ravi, B. Khadhraoui, S. Hilali, S. Perino, A.-S.F. Tixier. Review of Alternative Solvents fro Green Extraction of Food and Natural Products: Panorama, Principles, Applications and Prospects. *Molecules*, 24 (2019) 3007. <https://doi.org/10.3390/molecules24163007>

- [3] H. Gasparetto, F. Castilhos, N.P.G. Salau. Recent advances in green soybean oil extraction: A review. *Journal of Molecular Liquids*, 361 (2022a) 119684. <https://doi.org/10.1016/j.molliq.2022.119684>
- [4] M.C. Capellini, V. Giacomini, M.S. Cuevas, C.E.C. Rodrigues. Rice Bran Oil Extraction Using Alcoholic Solvents: Physicochemical Characterization of Oil and Protein Fraction Functionality. *Industrial Crops and Products*, 104 (2017) 133–143. <https://doi.org/10.1016/j.indcrop.2017.04.017>
- [5] M.C. Ferreira, D. Gonçalves, L.C.B.A. Bessa, C.E.C. Rodrigues, A.J.A. Meirelles, E.A.C. Batista. Soybean Oil Extraction with Ethanol from Multiple-Batch Assays to Reproduce a Continuous, Countercurrent, and Multistage Equipment. *Chemical Engineering and Processing - Process Intensification*, 170 (2022) 108659. <https://doi.org/10.1016/j.cep.2021.108659>
- [6] S. Meziane, H. Kadi. Kinetics and Thermodynamics of Oil Extraction from Olive Cake. *Journal of the American Oil Chemists' Society*, 85 (2008) 391–396. <https://doi.org/10.1007/s11746-008-1205-2>
- [7] S.B. dos Santos, M.A. Martins, A.L. Caneschi, P.R.M. Aguilar, J.S.R. Coimbra. Kinetics and Thermodynamics of Oil Extraction from *Jatropha Curcas* L. Using Ethanol as a Solvent. *International Journal of Chemical Engineering*, 2015 (2015) 1–9. <https://doi.org/10.1155/2015/871236>
- [8] M.H. Abdellah, L. Liu, C.A. Scholes, B.D. Freeman, S.E. Kentish. Organic Solvent Nanofiltration of Binary Vegetable Oil/Terpene Mixtures: Experiments and Modelling. *Journal of Membrane Science*, 573 (2019) 694–703. <https://doi.org/10.1016/j.memsci.2018.12.026>
- [9] A. Benazzouz, L. Moity, C. Pierlot, M. Sergent, V. Molinier, J.-M. Aubry. Selection of a Greener Set of Solvents Evenly Spread in the Hansen Space by Space-Filling Design. *Industrial & Engineering Chemistry Research*, 52 (2013) 16585–16597. <https://doi.org/10.1021/ie402410w>
- [10] O. Claux, V. Rapinel, P. Goupy, N. Patouillard, M.A. Vian, L. Jacques, F. Chemat. Dry and Aqueous 2-Methyloxolane as Green Solvents for Simultaneous Production of Soybean Oil and Defatted Meal. *ACS Sustainable Chemistry & Engineering*, 9 (2021) 7211–7223. <https://doi.org/10.1021/acssuschemeng.0c09252>
- [11] J.L.A. Dagostin, D. Carpiné, M.L. Corazza. Extraction of Soybean Oil Using Ethanol and Mixtures with Alkyl Esters (Biodiesel) as Co-Solvent: Kinetics and Thermodynamics. *Industrial Crops and Products*, 74 (2015) 69–75. <https://doi.org/10.1016/j.indcrop.2015.04.054>
- [12] C.E.C. Rodrigues, N.M. Longo, C.C. Silva, K.K. Aracava, B.R. Garavazo. Ethanolic extraction of soybean oil: oil solubility equilibria and kinetic studies. *Chemical Engineering Transactions*, 24 (2011). <https://doi.org/10.3303/CET1124136>

- [13] T.A. Toda, M.M. Sawada, C.E.C. Rodrigues. Kinetics of Soybean Oil Extraction Using Ethanol as Solvent: Experimental Data and Modeling. *Food and Bioproducts Processing*, 98 (2016) 1–10. <https://doi.org/10.1016/j.fbp.2015.12.003>
- [14] J.L.A. Dagostin, D. Carpiné, P.R.S. dos Santos, M.L. Corazza. Liquid-Liquid Equilibrium and Kinetics of Ethanolic Extraction of Soybean Oil Using Ethyl Acetate as Co-Solvent. *Brazilian Journal of Chemical Engineering*, 35 (2018) 415–428. <https://doi.org/10.1590/0104-6632.20180352s20160175>
- [15] R. Ozarslan, E. Bas. Kinetic Model for Drying in Frame of Generalized Fractional Derivatives. *Fractal and Fractional*, 4 (2020) 17. <https://doi.org/10.3390/fractalfract4020017>
- [16] J.A.T. Machado, A.M.S.F. Galhano, J.J. Trujillo. On development of fractional calculus during the last fifty years. *Scientometrics*, 98 (2014) 577–582. <https://doi.org/10.1007/s11192-013-1032-6>
- [17] D.J. Nicolin, R.O. Defendi, D.F. Rossoni, L.M.M. Jorge. Mathematical Modeling of Soybean Drying by a Fractional-Order Kinetic Model. *Journal of Food Process Engineering*, 41 (2017b). <https://doi.org/10.1111/jfpe.12655>
- [18] D.J. Nicolin, T.C.V. Balbinoti, R.M.M. Jorge, L.M.M. Jorge. Generalization of a Lumped Parameters Model Using Fractional Derivatives Applied to Rice Hydration. *Journal of Food Process Engineering*, 41 (2017a). <https://doi.org/10.1111/jfpe.12641>
- [19] K.B. Oldham, J. Spanier. *The Fractional Calculus*. Academic Press, 1974.
- [20] I. Podlubny. *Fractional differential equations*. Academic Press, 1999.
- [21] A.A. Babaei, A. Khataee, E. Ahmadpour, M. Sheydaei, B. Kakavandi, Z. Alaei. Optimization of Cationic Dye Adsorption on Activated Spent Tea: Equilibrium, Kinetics, Thermodynamic and Artificial Neural Network Modeling. *Korean Journal of Chemical Engineering*, 33 (2015) 1352–1361. <https://doi.org/10.1007/s11814-014-0334-6>
- [22] D. Ursueguía, E. Díaz, S. Ordóñez. Adsorption of Methane and Nitrogen on Basolite MOFs: Equilibrium and Kinetic Studies. *Microporous and Mesoporous Materials*, 298 (2020) 110048. <https://doi.org/10.1016/j.micromeso.2020.110048>
- [23] I. Bazhlekova, E. Bazhlekova. Fractional Derivative Modeling of Bioreaction-Diffusion Processes. *Thermophysical Basis of Energy Technologies (TBET 2020) AIP Conference Proceedings*, 2021. <https://doi.org/10.1063/5.0041611>
- [24] G.L. Grandi, J.O. Trierweiler. Tuning of Fractional Order PID Controllers Based on the Frequency Response Approximation Method. *IFAC-PapersOnLine*, 52 (2019) 982–987. <https://doi.org/10.1016/j.ifacol.2019.06.190>
- [25] J.E. Macías-Díaz, A. Gallegos. Design and Numerical Analysis of a Logarithmic Scheme for Nonlinear Fractional Diffusion–Reaction Equations. *Journal of Computational and Applied Mathematics*, 404 (2022) 113118. <https://doi.org/10.1016/j.cam.2020.113118>

- [26] G.S. Matias, C.A. Bissaro, L.M.M. Jorge, D.F. Rossoni. The Fractional Calculus in Studies on Drying: A New Kinetic Semi-Empirical Model for Drying. *Journal of Food Process Engineering*, 42 (2018). <https://doi.org/10.1111/jfpe.12955>
- [27] H. Gasparetto, A.L.B. Nunes, F. Castilhos, N.P.G. Salau. Soybean oil extraction using ethyl acetate and 1-butanol: from solvent selection to thermodynamic assessment, *Journal of Industrial and Engineering Chemistry*, 113 (2022b) 450-460. <https://doi.org/10.1016/j.jiec.2022.06.020>
- [28] H.C. Man, M.H. Hamzah, H. Jamaludin, Z.Z. Abidin. Preliminary Study: Kinetics of Oil Extraction from Citronella Grass by Ohmic Heated Hydro Distillation. *APCBEE Procedia*, 3 (2012) 124–128. <https://doi.org/10.1016/j.apcbee.2012.06.057>
- [29] S. Sayyar, Z.Z. Abidin, R. Yunus, A. Muhammad. Extraction of Oil from Jatropha Seeds-Optimization and Kinetics. *American Journal of Applied Sciences*, 6 (2009) 1390–1395. <https://doi.org/10.3844/ajassp.2009.1390.1395>
- [30] J. Kennedy, R. Eberhart. Particle Swarm Optimization. *Proceedings of ICNN'95 - International Conference on Neural Networks*, 1995. <https://doi.org/10.1109/icnn.1995.488968>
- [31] E. Mezura-Montes, C.A.C. Coello. Constraint-Handling in Nature-Inspired Numerical Optimization: Past, Present and Future. *Swarm and Evolutionary Computation*, 1 (2011) 173–194. <https://doi.org/10.1016/j.swevo.2011.10.001>
- [32] M.E. Pedersen. *Good Parameters for Particle Swarm Optimization*. Luxembourg: Hvas Laboratories, 2010.
- [33] M. Schwaab, J.C. Pinto. Optimum reference for reparameterization of the Arrhenius equation. Part 1: Problems involving one kinetic constant. *Chemical Engineering Science*, 62 (2007) 2750-2764. <https://doi.org/10.1016/j.ces.2007.02.020>
- [34] M. Schwaab, J.C. Pinto. Optimum reparameterization of power functions models. *Chemical Engineering Science*, 63 (2008) 4631-4635. <https://doi.org/10.1016/j.ces.2008.07.005>
- [35] M. Schwaab, E.C. Biscaia Jr, J.L. Monteiro, J.C. Pinto. Nonlinear Parameter Estimation through Particle Swarm Optimization. *Chemical Engineering Science*, 63 (2008) 1542–1552. <https://doi.org/10.1016/j.ces.2007.11.024>
- [36] R Core Team. *R: A language and environment for statistical computing*. R Foundation for Statistical Computing, Vienna, Austria (2022). <https://www.R-project.org/>
- [37] C.M. Agu, A.C. Agulanna. Kinetics and Thermodynamics of Oil Extracted from Amaranth. *Nutritional Value of Amaranth*, 2020. <https://doi.org/10.5772/intechopen.88344>

7 DISCUSSÃO DOS RESULTADOS

A fim de organizar as contribuições para o estado da arte sobre a extração de óleo de soja utilizando solventes verdes é necessário realizar uma discussão geral dos resultados.

De maneira geral, o solvente p-cimeno obteve melhor resultado que o hexano a 55 °C na extração de óleo de soja, enquanto o acetato de etila e o 1-butanol obtiveram rendimentos inferiores a mesma temperatura. Do melhor para o pior solvente verde apresentam-se: p-cimeno, 1-butanol e acetato de etila, enquanto as concentrações no equilíbrio a 55 °C estimada para cada solvente foram 0,2466 g/g DM, 0,2170 g/g DM e 0,2079 g/g DM, respectivamente, pelo modelo de So e Macdonald. Para o n-hexano, o valor estimado foi de 0,2356 g/g DM.

Os solventes acetato de etila, 1-butanol e p-cimeno também apresentaram rendimentos de extração superiores à aplicação de etanol anidro, evidência de que seu uso pode não ser muito vantajoso, além de contribuir na promoção da matriz energética renovável brasileira. De fato, além de baixos rendimentos de extração e miscibilidade incompleta com o óleo de soja, o uso de etanol anidro pode acarretar em acúmulo de água no solvente devido à umidade natural da matéria-prima. Por conseguinte, a aplicação de etanol hidratado resulta em mais dois pontos negativos: supressão do rendimento da extração e aumento da quantidade de ácidos graxos livres no produto final devido hidrólise dos glicerídeos. Desta forma, esta dissertação apresentou os solventes verdes como alternativas viáveis ao etanol, sendo possível destacar que o acetato de etila, o 1-butanol e o p-cimeno não são miscíveis com água e/ou apresentam baixíssima solubilidade.

O p-cimeno caracterizou-se como o melhor solvente sob ponto de vista técnico, todavia, a substituição direta do hexano pode não ser viável devido ao seu alto ponto de ebulição (cerca de 177 °C) e baixa pressão de vapor (200 Pa). Para este, a recuperação do solvente por destilação e evaporação pode não ser apropriada, sendo recomendado processos de separação por membrana.

Não menos importante, apesar do 1-butanol possuir maior afinidade com os triacilgliceróis que o acetato de etila, o primeiro artigo mostrou que a taxa inicial de extração é menor para o álcool devido a sua maior viscosidade. Portanto, a substituição direta do hexano pode ser facilitada ao utilizar o acetato de etila, pois este também possui menor ponto de ebulição (77 °C) e maior pressão de vapor (12.425 Pa).

Genericamente, o coeficiente de atividade em diluição infinita obtido pela teoria COSMO-SAC (MOPAC) obteve a melhor previsão sobre o potencial de solvatação do 1-butanol, acetato de etila, p-cimeno, etanol e hexano em relação aos parâmetros de solubilidade

de Hansen. A análise dos perfis sigma indica que pequenas cargas positivas induzidas em conjunto com uma maior quantidade de segmentos neutros na molécula de solvente podem ser responsáveis pelo melhor desempenho de solvatação do p-cimeno, resultando em um balanço de energias mais favorável.

A metodologia de superfície de resposta foi capaz de descrever a influência da temperatura e razão solvente-sólido na extração de óleo de soja utilizando acetato de etila, 1-butanol e p-cimeno. A ANOVA simplificada avaliou a significância dos parâmetros e indicou a necessidade de redução da ordem dos modelos estatísticos. A um nível de confiança de 95%, pelos testes exato de Fisher, Shapiro-Wilk para normalidade e Breusch-Pagan para heterocedasticidade, os modelos finais foram considerados estatisticamente significantes.

Em comparação com os modelos de ordem de potência e o modelo cinético de transferência de massa, o modelo de So e Macdonald obteve a melhor performance estatística no segundo artigo que compõe esta dissertação. Neste sentido, é possível depreender que neste tipo de extração sólido-líquido estão presentes dois mecanismos principais: (i) dissolução rápida do óleo presente na superfície das partículas e (ii) extração lenta controlada pela difusão interna do soluto dentro dos bolsões e capilares fibrosos das lâminas de soja. Por conseguinte, a reamostragem *bootstrap* foi capaz de reduzir o viés dos estimadores do modelo de So e Macdonald, aumentando a correlação entre K e T para a equação de van't Hoff, bem como, entre C_∞ e T , e corrigindo o intervalo de máxima verossimilhança dos parâmetros estimados.

Ademais, o modelo cinético de transferência de massa obteve bons ajustes para o caso a se desconsiderar a resistência externa ao efeito do transporte de massa. De fato, todos os solventes possuem bons potenciais de solvatação, sendo possível assumir que a transferência do soluto da superfície da partícula para a fase fluida ocorre de maneira instantânea. O coeficiente de difusão efetiva a 55 °C foi estimado em $1,63 \times 10^{-10}$ m²/s para o acetato de etila, $3,63 \times 10^{-11}$ m²/s para o 1-butanol e $2,11 \times 10^{-10}$ m²/s para o p-cimeno, provando que este possui relação direta com a viscosidade do solvente assim como descrito por Boucher et al. (1942), uma vez que $\mu_{1\text{-butanol}} > \mu_{\text{p-cimene}} > \mu_{\text{acetato de etila}}$.

A análise termodinâmica indicou processos irreversíveis, endotérmicos e espontâneos para todas as extrações utilizando solventes verdes e os altos coeficientes de determinação acusam a qualidade dos resultados experimentais.

O espectro do FTIR mostrou que o óleo extraído apresenta composição típica de óleos vegetais, caracterizado principalmente pelos picos de transmitância em 2925 e 2855 cm⁻¹, evidenciados pela presença de ácidos graxos poli-insaturados, 1746 cm⁻¹, resultado da ligação

dos ácidos graxos com a molécula de glicerol, em 1466, 1378 e 1164 cm^{-1} , os quais caracterizam-se como a impressão digital deste tipo de gordura apolar. A análise do perfil dos ácidos graxos mostrou uma composição típica de ácidos palmíticos, esteáricos, oleicos, linoleicos e linolênicos. Para o óleo extraído utilizando p-cimeno maior é a quantidade de ácidos graxos livres em temperaturas brandas, ainda assim, a porcentagem relativa de FFA é menor que 3%.

O modelo cinético de primeira ordem de derivada fracionária ajustado utilizando mínimos quadrados não lineares e enxame de partículas refinado pelo algoritmo de ponto interior obteve melhores resultados estatísticos para $RMSE$, χ^2 e R^2 que o respectivo modelo de derivada de ordem inteira. Apesar de apresentar parâmetros mais correlacionados entre si, o teste exato de Fisher e o critério de informação Akaike mostraram que a inserção de um parâmetro não compromete o desempenho estatístico do modelo de derivada fracionária.

8 CONCLUSÕES E SUGESTÕES DE TRABALHOS FUTUROS

8.1 CONCLUSÕES

Em geral, esta dissertação mostrou que a aplicação de solventes verdes na extração de óleo de soja é tecnicamente viável. O solvente p-cimeno obteve resultados superiores à aplicação de n-hexano a 55 °C, enquanto a substituição direta do solvente de origem fóssil pode ser facilitada pelo uso de acetato de etila devido a sua tendência de melhor facilidade de recuperação. O acetato de etila, o 1-butanol e o p-cimeno também obtiveram rendimentos de extração superiores à aplicação de etanol anidro. A teoria COSMO-SAC mostrou-se capaz de prever o potencial de solvatação do acetato de etila, 1-butanol, p-cimeno, etanol e n-hexano em comparação com os parâmetros de solubilidade de Hansen. A análise termodinâmica das extrações mostrou processos endotérmicos, irreversíveis e espontâneos. O modelo de derivada fracionária generalizado obteve melhores resultados através de uma análise estatística aprofundada em comparação ao modelo de ordem de potência de primeira ordem.

8.2 SUGESTÕES DE TRABALHOS FUTUROS

Como sugestão de trabalhos futuros é possível citar:

1. Avaliar a cinética, termodinâmica e de transferência de massa na extração de óleo de soja sobre a utilização de outros sistemas de solventes: d-limoneno, 2-metiltetrahydrofurano, α e β -pineno; ciclopentil metil éter na forma hidratada; acetona, 1-butanol, p-cimeno e ciclopentil metil éter como cossolventes junto ao etanol; solventes eutéticos profundos como cossolventes; e misturas azeotrópicas com desvio positivo da lei de Raoult;
2. Estudar o equilíbrio líquido-líquido em sistemas contendo cossolventes e a partição de óleo entre as fases solvente verde e água;
3. Estudar a extração utilizando solventes verdes em leito-fixo e realizar a modelagem do processo considerando e desconsiderando a resistência externa à transferência de massa;
4. Aplicar o cálculo fracionário em modelos fenomenológicos;
5. Realizar a análise econômica da aplicação de diferentes solventes verdes na extração de óleo de soja.

REFERÊNCIAS

- ABDELLAH, M. H. et al. Organic solvent nanofiltration of binary vegetable oil/terpene mixtures: Experiments and modelling. **Journal of Membrane Science**, v. 573, p. 694–703, 2019.
- ABRAHAM, G. et al. Water accumulation in the alcohol extraction of cottonseed. **Journal of the American Oil Chemists' Society**, v. 70, p. 207–208, 1993.
- ANASTAS, P. T.; WARNER, J. C. **Green Chemistry: Theory and Practice**. Oxford University Press, USA, 2000.
- ANTONIASSI, R. et al. **Otimização do Método Hartman e Lago de Preparação de Ésteres Metílicos de Ácidos Graxos**. Embrapa Agroindústria de Alimentos, 2018.
- ANWAR, F. et al. Variations of quality characteristics among oils of different soybean varieties. **Journal of King Saud University - Science**, v. 28, p. 332–338, 2016.
- AOCS, 1998. Official Methods and Recommended Practices of the American Oil Chemists' Society, **AOCS Press**, Champaign, USA.
- BENAZZOUZ, A. et al. Selection of a Greener Set of Solvents Evenly Spread in the Hansen Space by Space-Filling Design. **Industrial & Engineering Chemistry Research**, v. 52, p. 16585–16597, 2013.
- BERGMAN, T. L. et al. **Fundamentos de Transferência de Calor E de Massa**. LTC, 2014.
- BERTOUCHE, S. et al. First approach on edible oil determination in oilseeds products using alpha-pinene. **Journal of Essential Oil Research**, v. 25, p. 439–443, 2013.
- BERTSEKAS, D.; NEDIC, A.; OZDAGLAR, A. **Convex Analysis and Optimization**. Athena Scientific, 2003.
- BLAKE, B. Solubility Rules: Three Suggestions for Improved Understanding. **Journal of Chemical Education**, v. 80, p. 1348, 2003.
- BOYD, S.; BOYD, S. P.; VANDENBERGHE, L. **Convex Optimization**. Cambridge University Press, 2004.
- BOUCHER, D. F.; BRIER, J. C.; OSBURN, J. O. Extraction of oil from a porous solid. **Transactions of the American Institute of Chemical Engineers**, v. 38, p. 967-993, 1942.
- BREIMAN, L. **Classification and Regression Trees**. Routledge, 2017.
- BROUWER, T.; SCHUUR, B. Model Performances Evaluated for Infinite Dilution Activity Coefficients Prediction at 298.15 K. **Industrial & Engineering Chemistry Research**, v. 58, p. 8903–8914, 2019.

CERUTTI, M. L. M. N.; DE SOUZA, A. A. U.; DE SOUZA, S. M. de A. G. U. Solvent extraction of vegetable oils: Numerical and experimental study. **Food and Bioproducts Processing**, v. 90, p. 199–204, 2012.

CHAN, C.-H.; YUSOFF, R.; NGOH, G.-C. Modeling and kinetics study of conventional and assisted batch solvent extraction. **Chemical Engineering Research and Design**, v. 92, p. 1169–1186, 2014.

CHEN, X. et al. Lipase-mediated methanolysis of soybean oils for biodiesel production. **Journal of Chemical Technology & Biotechnology**, v. 83, p. 71–76, 2007.

CLAUX, O. et al. Dry and Aqueous 2-Methyloxolane as Green Solvents for Simultaneous Production of Soybean Oil and Defatted Meal. **ACS Sustainable Chemistry & Engineering**, v. 9, p. 7211–7223, 2021.

COLEMAN, T. F.; LI, Y. An Interior Trust Region Approach for Nonlinear Minimization Subject to Bounds. **SIAM Journal on Optimization**, v. 6, p. 418–445, 1996.

COLEMAN, T. F.; LI, Y. On the convergence of interior-reflective Newton methods for nonlinear minimization subject to bounds. **Mathematical Programming**, v. 67, p. 189–224, 1994.

COLOMBO, K. et al. Production of biodiesel from Soybean Oil and Methanol, catalyzed by calcium oxide in a recycle reactor. **South African Journal of Chemical Engineering**, v. 28, p. 19–25, 2019.

COMERLATTO, A. dos S. **Estudo da Influência de Misturas entre Etanol e Isopropanol na Transferência de Massa na Extração de Óleo de Soja**. 2020. Dissertação - Universidade Federal do Paraná, 2020.

COMERLATTO, A. et al. Mass transfer in soybean oil extraction using ethanol/isopropyl alcohol mixtures. **International Journal of Heat and Mass Transfer**, v. 165, p. 120630, 2021.

CONN, A. R.; GOULD, N. I. M.; TOINT, Ph. L. **Trust Region Methods**. SIAM, 2000.

CRANK, J.; CRANK, E. P. J. **The Mathematics of Diffusion**. Oxford University Press, 1979.

UNITED STATES DEPARTMENT OF AGRICULTURE (USDA). **Crop explorer for major crop regions**. 2020. Disponível em: https://ipad.fas.usda.gov/cropexplorer/cropview/commodityView.aspx?cropid=2222000&sel_year=2020&startrow=1. Acesso em: 1 jun. 2022.

DA SILVA, C. A. S. et al. Mutual Solubility for Systems Composed of Vegetable Oil + Ethanol + Water at Different Temperatures. **Journal of Chemical & Engineering Data**, v. 55, p. 440–447, 2009.

DAGOSTIN, J. L. A. et al. Liquid-liquid equilibrium and kinetics of ethanolic extraction of soybean oil using ethyl acetate as co-solvent. **Brazilian Journal of Chemical Engineering**, v. 35, p. 415–428, 2018.

DAGOSTIN, J. L. A.; CARPINÉ, D.; CORAZZA, M. L. Extraction of soybean oil using ethanol and mixtures with alkyl esters (biodiesel) as co-solvent: Kinetics and thermodynamics. **Industrial Crops and Products**, v. 74, p. 69–75, 2015.

DAVISON, A. C.; HINKLEY, D. V. **Bootstrap Methods and Their Application**. Cambridge University Press, 1997.

DIJKSTRA, A. J. Soybean Oil. In: **ENCYCLOPEDIA OF FOOD AND HEALTH**. Elsevier, 2016. p. 58–63.

DRAPER, N. R.; SMITH, H. **Applied Regression Analysis**. John Wiley & Sons, 2014.

EISEN, L.; MARANO, N.; GLAZIER, S. Activity-Based Approach for Teaching Aqueous Solubility, Energy, and Entropy. **Journal of Chemical Education**, v. 91, p. 484–491, 2014.

ERICKSON, D. R. **Handbook of Soy Oil Processing and Utilization**. Amer Oil Chemists Society, 1980.

ERICKSON, D. R. **Practical Handbook of Soybean Processing and Utilization**. Elsevier, 2015.

FERREIRA, M. C. et al. Soybean oil extraction with ethanol from multiple-batch assays to reproduce a continuous, countercurrent, and multistage equipment. **Chemical Engineering and Processing - Process Intensification**, v. 170, p. 108659, 2022.

FOLLEGATTI-ROMERO, L. A. et al. Mutual Solubility of Pseudobinary Systems Containing Vegetable Oils and Anhydrous Ethanol from (298.15 to 333.15) K. **Journal of Chemical & Engineering Data**, v. 55, p. 2750–2756, 2010.

FRANCO, D. et al. Ethanolic extraction of Rosa rubiginosa soluble substances: Oil solubility equilibria and kinetic studies. **Journal of Food Engineering**, v. 79, p. 150–157, 2007.

GANDHI, A. P. et al. Studies on alternative solvents for the extraction of oil-I soybean. **International Journal of Food Science and Technology**, v. 38, p. 369–375, 2003.

GASPARETTO, H.; DE CASTILHOS, F.; PAULA GONÇALVES SALAU, N. Recent advances in green soybean oil extraction: A review. **Journal of Molecular Liquids**, v. 361, p. 119684, 2022.

GERDE, J. A. et al. Soybean Oil. **Bailey's Industrial Oil and Fat Products**, , p. 1–68, 2020.

HAMMOND, E. G.; GLATZ, B. A. Biotechnology applied to fats and oils. In: **Developments in food biotechnology**. New York: John Wiley & Sons, p. 173–217, 1989.

HANSEN, C. M. **Hansen Solubility Parameters: A User's Handbook**. CRC Press, 2007.

HARTMAN, L.; LAGO, R. C. A. Rapid preparation of fatty acid methyl esters from lipids. **Laboratory Practice**, v. 22, p. 475–476, 1973.

HAYYAN, A. et al. Application of deep eutectic solvent as novel co-solvent for oil extraction from flaxseed using sonoenergy. **Industrial Crops and Products**, v. 176, p. 114242, 2022.

HRON, R. J.; KOLTUN, S. P.; GRACI, A. V. Biorenewable Solvents for Vegetable oil extraction. **Journal of the American Oil Chemists' Society**, v. 59, p. 674A-684A, 1982.

HUI, Y. H. **Bailey's Industrial Oil and Fat Products, Edible Oil and Fat Products: Processing Technology**. Wiley-Interscience, 1996.

JIMENEZ, O. A. Q. et al. Hansen solubility parameters and thermodynamic modeling for LLE description during glycerol-settling in ester production from coconut oil. **Fuel**, v. 241, p. 725–732, 2019.

JOKIĆ, S. et al. Supercritical CO₂ extraction of soybean oil: process optimisation and triacylglycerol composition. **International Journal of Food Science & Technology**, v. 45, p. 1939–1946, 2010.

JOHNSON, L. A.; LUCAS, E. W. Comparison of alternative solvents for oils extraction. **Journal of the American Oil Chemists' Society**, v. 60, p. 229-242, 1983.

JUN-QING, Q. Studies on method for aqueous extraction of soybean oil. **Journal of Zhejiang University - SCIENCE A**, v. 2, p. 209–213, 2001.

KARNOFSKY, G. The theory of solvent extraction. **Journal of the American Oil Chemists Society**, v. 26, p. 564-569, 1949.

KHANESAR, M. A.; TESHNEHLAB, M.; SHOOREHDELI, M. A. A novel binary particle swarm optimization. In: **2007 Mediterranean Conference on Control & Automation**. IEEE, 2007.

KENNEDY, J.; EBERHART, R. Particle swarm optimization. In: **Proceedings of ICNN'95 - International Conference on Neural Networks**. IEEE, 1995.

KIM, S. K. et al. Production of renewable diesel by hydrotreatment of soybean oil: Effect of reaction parameters. **Chemical Engineering Journal**, v. 228, p. 114–123, 2013.

KONG, W. et al. An energy-friendly alternative in the large-scale production of soybean oil. **Journal of Environmental Management**, v. 230, p. 234–244, 2019.

KOSTIĆ, M. D. et al. The kinetics and thermodynamics of hempseed oil extraction by n-hexane. **Industrial Crops and Products**, v. 52, p. 679–686, 2014.

LAGARIAS, J. C. et al. Convergence Properties of the Nelder-Mead Simplex Method in Low Dimensions. **SIAM Journal on Optimization**, v. 9, p. 112–147, 1998.

LI, Y. et al. Evaluation of alternative solvents for improvement of oil extraction from rapeseeds. **Comptes Rendus Chimie**, v. 17, p. 242–251, 2014.

LI, Z.; SMITH, K. H.; STEVENS, G. W. The use of environmentally sustainable bio-derived solvents in solvent extraction applications - A review. **Chinese Journal of Chemical Engineering**, v. 24, p. 215–220, 2016.

LIN S.; SANDLER, S. I. A Priori Phase Equilibrium Prediction from a Segment Contribution Solvation Model. **Industrial & Engineering Chemistry Research**, v. 41, p. 899-913, 2001.

LIU, K. **Soybeans: Chemistry, Technology, and Utilization**. Springer, 2012.

LIU, X. et al. Transesterification of soybean oil to biodiesel using SrO as a solid base catalyst. **Catalysis Communications**, v. 8, p. 1107–1111, 2007.

MISTAKIDIS, E. S.; STAVROULAKIS, G. E. **Nonconvex Optimization in Mechanics: Algorithms, Heuristics and Engineering Applications by the F.E.M.** Springer Science & Business Media, 2013.

MITREA, L. et al. The physicochemical properties of five vegetable oils exposed at high temperature for a short-time-interval. **Journal of Food Composition and Analysis**, v. 106, p. 104305, 2022.

MIYASAKA, S. **A Soja no Brasil**. Campinas: ITAL, 1981.

MORETTIN, P. A.; BUSSAB, W. O. **ESTATÍSTICA BÁSICA**. Saraiva Educação S.A., 2017.

NAVARRO, M. L. M. **Estudo da Transferência de Massa no Processo de Extração com Solventes de Óleos Vegetais em Coluna de Leito Fixo**. 2002. Dissertação - Universidade Federal de Santa Catarina, 2002.

NDLELA, S. C. et al. Aqueous Extraction of Oil and Protein from Soybeans with Subcritical Water. **Journal of the American Oil Chemists' Society**, v. 89, p. 1145–1153, 2012.

NICOLIN, D. J.; ROSSONI, D. F.; JORGE, L. M. M. Study of uncertainty in the fitting of diffusivity of Fick's Second Law of Diffusion with the use of Bootstrap Method. **Journal of Food Engineering**, v. 184, p. 63–68, 2016.

OLIVIERI, G. V.; DE QUADROS, J. V.; GIUDICI, R. Epoxidation Reaction of Soybean Oil: Experimental Study and Comprehensive Kinetic Modeling. **Industrial & Engineering Chemistry Research**, v. 59, p. 18808–18823, 2020.

PATRICELLI, A.; ASSOGNA, A.; CASALAINA, A.; EMMI, A.; SODINI, G. Fattori che influenzano l'estrazione dei lipidi da semi decorticati di girasole. **La Rivista Italiana Delle Sostanze Grasse**, v. 56, p. 136-142, 1979.

PERKINS, E. G. Composition of Soybeans and Soybean Products. In: **Practical handbook of soybean processing and utilization**. USA: AOCS Press, p. 9–28, 1995.

PEÇANHA, R. P. **Sistemas particulados # Operações unitárias envolvendo partículas e fluidos**. Elsevier, 2014.

PHAN, L. et al. Soybean oil extraction and separation using switchable or expanded solvents. **Green Chemistry**, v. 11, p. 53–59, 2009.

POTRICH, E. et al. Replacing hexane by ethanol for soybean oil extraction: Modeling, simulation, and techno-economic-environmental analysis. **Journal of Cleaner Production**, v. 244, p. 118660, 2020.

PRAMPARO, M.; GREGORY, S.; MATTEA, M. Immersion vs. percolation in the extraction of oil from oleaginous seeds. **Journal of the American Oil Chemists' Society**, v. 79, p. 955–960, 2002.

QIN, P.; WANG, T.; LUO, Y. A review on plant-based proteins from soybean: Health benefits and soy product development. **Journal of Agriculture and Food Research**, v. 7, p. 100265, 2022.

QUIÑONES-ISLAS, N. et al. Detection of adulterants in avocado oil by Mid-FTIR spectroscopy and multivariate analysis. **Food Research International**, v. 51, p. 148–154, 2013.

R Core Team (2022). R: A language and environment for statistical computing. **R Foundation for Statistical Computing**, Vienna, Austria. URL <https://www.R-project.org/>.

RIBEIRO, J. S.; CELANTE, D.; BRONDANI, L. N.; TROJAHN, D. O.; SILVA, C.; CASTILHOS, F. Synthesis of methyl esters and triacetin from macaw oil (*Acrocomia aculeata*) and methyl acetate over γ -alumina. **Industrial Crops & Products**, v. 124, p. 84–90, 2018.

RODRIGUES, C. E. C.; ARACAVAL, K. K.; ABREU, F. N. Thermodynamic and statistical analysis of soybean oil extraction process using renewable solvent. **International Journal of Food Science & Technology**, v. 45, p. 2407–2414, 2010.

RODRIGUES, G. M.; CARDOZO-FILHO, L.; DA SILVA, C. Pressurized liquid extraction of oil from soybean seeds. **The Canadian Journal of Chemical Engineering**, v. 95, p. 2383–2389, 2017.

SAEED, R.; NAZ, S. Effect of heating on the oxidative stability of corn oil and soybean oil. **Grasas y Aceites**, v. 70, p. 303, 2019.

SANTOS, S. B. dos et al. Kinetics and Thermodynamics of Oil Extraction from *Jatropha curcas* L. Using Ethanol as a Solvent. **International Journal of Chemical Engineering**, v. 2015, p. 1–9, 2015.

SAWADA, M. M. et al. Effects of different alcoholic extraction conditions on soybean oil yield, fatty acid composition and protein solubility of defatted meal. **Food Research International**, v. 62, p. 662–670, 2014.

SCALDAFERRI, C. A.; PASA, V. M. D. Production of jet fuel and green diesel range biohydrocarbons by hydroprocessing of soybean oil over niobium phosphate catalyst. **Fuel**, v. 245, p. 458–466, 2019.

SCHWAAB, M. et al. Nonlinear parameter estimation through particle swarm optimization. **Chemical Engineering Science**, v. 63, p. 1542–1552, 2008.

SCHWAAB, M.; LEMOS, L. P.; PINTO, J. C. Optimum reference temperature for reparameterization of the Arrhenius equation. Part 2: Problems involving multiple reparameterizations. **Chemical Engineering Science**, v. 63, p. 2895–2906, 2008.

SCHWAAB, M.; PINTO, J. C. **Análise de Dados Experimentais: I. Fundamentos de Estatística e Estimação de Parâmetros**. Editora E-papers, 2007a.

SCHWAAB, M.; PINTO, J. C. Optimum reference temperature for reparameterization of the Arrhenius equation. Part 1: Problems involving one kinetic constant. **Chemical Engineering Science**, v. 62, p. 2750–2764, 2007b.

SCHWERTNER, A. E. **O método de Levenberg-Marquardt para problemas de otimização de menor valor ordenado**. 2019. Dissertação, 2019.

SHAHIDI, W. *Bailey's Industrial Oil and Fat Products*. **Wiley Blackwell**, v. 5, 2005.

SHARMA, A.; KHARE, S. K.; GUPTA, M. N. Three phase partitioning for extraction of oil from soybean. **Bioresource Technology**, v. 85, p. 327–329, 2002.

SICAIRE, A.-G. et al. Alternative Bio-Based Solvents for Extraction of Fat and Oils: Solubility Prediction, Global Yield, Extraction Kinetics, Chemical Composition and Cost of Manufacturing. **International Journal of Molecular Sciences**, v. 16, p. 8430–8453, 2015.

SILVEIRA, C. L. **Modelagem de processos enzimáticos e fermentativos usando otimização por enxame de partículas**. 2015. Dissertação – Universidade Federal de Santa Maria, 2015.

SO, G. C.; MACDONALD, D. G. Kinetics of oil extraction from canola (rapeseed). **The Canadian Journal of Chemical Engineering**, v. 64, p. 80–86, 1986.

SOUZA, P. R.; DOTTO, G. L.; SALAU, N. P. G. Detailed numerical solution of pore volume and surface diffusion model in adsorption systems. **Chemical Engineering Research and Design**, v. 122, p. 298–307, 2017.

SRIVASTAVA, Y.; SEMWAL, A. D. A study on monitoring of frying performance and oxidative stability of virgin coconut oil (VCO) during continuous/prolonged deep fat frying process using chemical and FTIR spectroscopy. **Journal of Food Science and Technology**, v. 52, p. 984–991, 2013.

TALEBIAN-KIAKALAEH, A.; AMIN, N. A. S. Kinetic Modeling, Thermodynamic, and Mass-Transfer Studies of Gas-Phase Glycerol Dehydration to Acrolein over Supported Silicotungstic Acid Catalyst. **Industrial & Engineering Chemistry Research**, v. 54, p. 8113–8121, 2015.

TANZI, C. D.; ABERT VIAN, M.; CHEMAT, F. New procedure for extraction of algal lipids from wet biomass: A green clean and scalable process. **Bioresource Technology**, v. 134, p. 271–275, 2013.

TANZI, C. D. et al. Terpenes as Green Solvents for Extraction of Oil from Microalgae. **Molecules**, v. 17, p. 8196–8205, 2012.

TODA, T. A.; SAWADA, M. M.; RODRIGUES, C. E. C. Kinetics of soybean oil extraction using ethanol as solvent: Experimental data and modeling. **Food and Bioproducts Processing**, v. 98, p. 1–10, 2016.

TOMITA, K. et al. Extraction of rice bran oil by supercritical carbon dioxide and solubility consideration. **Separation and Purification Technology**, v. 125, p. 319–325, 2014.

YAN, W. et al. Opportunities and Emerging Challenges of the Heterogeneous Metal-Based Catalysts for Vegetable Oil Epoxidation. **ACS Sustainable Chemistry & Engineering**, v. 10, p. 7426–7446, 2022.

YARA-VARÓN, E. et al. Is it possible to substitute hexane with green solvents for extraction of carotenoids? A theoretical *versus* experimental solubility study. **RSC Advances**, v. 6, p. 27750–27759, 2016.

YUAN, Y. A review of trust region algorithms for optimization. **In: Proceedings of the 4th International Congress on Industrial & Applied Mathematics**, p. 271–282, 2000.

YUAN, Y. Recent advances in trust region algorithms. **Mathematical Programming**, v. 151, p. 249–281, 2015.

ZAHIR, E. et al. Study of physicochemical properties of edible oil and evaluation of frying oil quality by Fourier Transform-Infrared (FT-IR) Spectroscopy. **Arabian Journal of Chemistry**, v. 10, p. S3870–S3876, 2017.

APÊNDICE A – CROMATOGRAMA

Figura A 1 - Cromatograma para determinação de FFA, MAG, DAG e TAG.

